Characterisation of peroxisome-organelle contacts and cooperation

Submitted by **Alexa Bishop** to the University of Exeter as a thesis for the degree of **Masters by Research in Biological Sciences** in September 2018

This thesis is available for Library use on the understanding that it is
copyright material and that no quotation from the thesis may be published without
proper acknowledgement.

I certify that all material in this thesis which is not my own work has
been identified and that any material that has previously been submitted and approved
for the award of a degree by this or any other University has been acknowledged.

(Signature)

……

Abstract:

Peroxisomes are organelles which are vital for human health and development. They represent dynamic subcellular compartments which play cooperative roles in essential cellular metabolic processes such as lipid metabolism and redox balance. For example, cooperation between peroxisomes and the endoplasmic reticulum (ER) is essential for the production of myelin lipids which are required for normal neurological function. We recently discovered that peroxisome-ER interaction is mediated by physical linkages in the form of membrane contact sites. These contact sites are mediated by the interaction of peroxisomal ACBD5 and ER-resident VAPB proteins. ACBD5-deficient patients have recently been identified who display retinal dystrophy, white matter disease and accumulation of very-long-chain fatty acids, which can only be degraded in peroxisomes. There is currently a need to develop simple and robust tools to allow efficient visualisation and quantification of these membrane contact sites to further their characterisation and investigate their function. Moreover, these should allow the dynamics of membrane contact sites under physiological conditions to be assessed. This study presents the optimisation of two systems to investigate peroxisome-ER interactions, the proximity ligation assay, Duolink® and a split fluorescent reporter system, split superfolder green fluorescent protein. These allow peroxisome-ER interactions to be visualised and measured *in situ* with a fluorescence-based readout when the organelles are in close proximity. These systems are powerful and modifiable and will help further characterise peroxisome-ER (or other organelle) membrane contacts and shed light on the interplay between peroxisomes and the ER.

Acknowledgements:

Firstly, I would like to express my gratitude to my supervisor Professor Michael Schrader for all of his valuable guidance and support throughout the duration of this project. I would also like to thank Tina Schrader for all of her technical assistance, particularly with the Duolink® experiments.

I would like to extend a huge thank you the entire Schrader group. In particular to Joe Costello, words cannot describe how valuable your support and encouragement were to me throughout this project. Without your constant guidance and, of course, your encyclopaedic knowledge of proteins, this project would not have been possible. Josiah Passmore, for not only being a great lab buddy and friend but also for the many milkshakes and teaching me your rather interesting methods of lab work. Your expert figure making and statistics knowledge was invaluable to me throughout the project and write up and your collaboration in creating the custom ImageJ macro was also very much appreciated. I also extend thanks to Suzan Kors for being a constant source of support and friendship and providing entertainment during 3 x 5 minute wash steps. I am also grateful to Maki Kamoshita for her collaboration with the Duolink® experiments.

I would like to thank all members of Lab 211, in particular, Connor Horton and Lauren Adams for their support and numerous laughs, and especially Beth Dean for being a constant ray of sunshine. I would also like to thank Ana Correia from Bioimaging for her help and guidance with imaging.

I would like to thank Henrietta Lacks for inspiring me to become a scientist and making studies like these possible.

I also extend my gratitude to my parents and my brothers for their continuous support and love. Particularly my mother whose unwavering support and encouragement carried me through this project.

Finally, I would like to thank Alex, you got me through this.

List of Contents:

List of figures:

List of tables:

List of abbreviations:

AADHAP-R - Acyl/alkyl-dihydroxyacetone phosphate reductase

ABC - ATP-binding cassette

AcB - Acyl-CoA binding

ACBD5 - Acyl-CoA-binding domain-containing protein 5

ADHAPS - Alkyl-dihydroxyacetone phosphate synthase

ALDP – Adrenoleukodystrophy protein

AMACR - 2-methylacyl-CoA racemase

coIP – Co-immunoprecipitation

DBP – D-bifunctional protein

ddFP - Dimerisation-dependent Fluorescent Protein

ddGFP – Dimerisation-dependent Green Fluorescent Protein

DHAP - Dihydroxyacetone phosphate

DHAPAT - Dihydroxyacetone phosphate acyltransferase

DHCA/THCA - Di- and trihydroxycholestanoic acid

EM – Electron microscopy

ER – Endoplasmic reticulum

FFAT - Two phenylalanines (FF) in an acidic tract

FIB-SEM - Focused Ion Beam Scanning Electron Microscopy

FRET - Fluorescence resonance energy transfer

GFP – Green Fluorescent Protein

HBSS - Hank's Balanced Salt Solution

LACS - Long-chain acyl-CoA synthetase

LD – Lipid droplet

MAM - Mitochondria-associated ER membranes

MCS – Membrane Contact Site

MSP - Major sperm protein

PBD – Peroxisome biogenesis disorder

PBS – Phosphate-buffered saline

PCR – Polymerase chain reaction

PLA – Proximity Ligation Assay

PMP – Peroxisomal Membrane Protein

RCA – Rolling circle amplification

RCDP - Rhizomelic chondrodysplasia punctata

RFP – Red Fluorescent Protein

ROS – Reactive oxygen species

SCPx - Sterol carrier protein X

SEM – Standard error of the mean

spGFP – Split Superfolder Green Fluorescent Protein

TMD-T – Transmembrane domain and tail

VAPA/B - Vesicle-associated membrane protein-associated protein A/B

VDAC - Voltage-dependent anion channel

VLCFA – Very long chain fatty acid

X-ALD - X-linked adrenoleukodystrophy

YFP- Yellow Fluorescent Protein

ZS – Zellweger syndrome

Chapter 1: General Introduction

The role of peroxisomes in health and disease and their cooperation with other subcellular compartments.

Eukaryotic cells are defined by their highly organised internal architecture. This is composed of a set of membrane-bound subcellular structures, known as organelles, which each play specialised roles. Organelles allow for normal functioning of the biological system through providing spatial and temporal separation of incompatible metabolic processes, allowing them to occur simultaneously. The interest in organelles and the roles they play continues to increase as new biological functions and molecular features are identified, revealing the role of these structures in both health and disease (Satori *et al.*, 2013). Moreover, recent studies have led to the understanding that organelles do not function exclusively as separate entities as once thought, rather they cooperate extensively, forming a so-called organelle interactome (Valm *et al.*, 2017).

The first observation of organelles was in 1682 by microscopist Antonie Van Leeuwenhoek who noted the presence of a nucleus in the red blood cells of fish species (Harris, 2000). However, the significance of this finding was not realised until 1833, when botanist Robert Brown rediscovered this structure and coined the term “nucleus”. This then resulted in the observation of this structure in many cell types before its function was uncovered (Chaffey, 2010). Following this, organelles continued to be observed in microscopy studies, starting with the discovery of mitochondria in the 1850s by Rudolph Albert von Kolliker (Ernster and Schatz, 1981). Since these initial observations, many more organelles were discovered and their functions continue to be elucidated.

One important organelle is the peroxisome, originally termed “microbody”. Peroxisomes were first discovered in 1954 by Johannes Rhodin whilst investigating mouse kidney cells through electron microscopy (EM) (Rhodin, 1954). Although first thought to have no independent function and regarded as “fossil organelles”, it is now widely understood that these organelles play essential roles in human health and disease. This insight was first provided following the isolation of peroxisomes from rat liver cells in 1966 by Christian De Duve and Pierre Baudhuin which led to the discovery that peroxisomes contained hydrogen peroxide-producing oxidases and a hydrogen peroxide-degrading enzyme, catalase (De Duve and Baudhuin, 1966). Furthermore, the development of a specific cytochemical staining for peroxisomes for light and electron microscopy, alkaline 3, 3′-diaminobenzidine (DAB) reaction which

stains catalase (Fahimi, 1968; Novikoff and Goldfischer, 1969), led to the discovery that peroxisomes are ubiquitous organelles amongst eukaryotic organisms (Hruban *et al.*, 1972).

Mammalian peroxisomes are 0.1-1 µm in size (Schrader and Fahimi, 2008) and are found in all eukaryotic cells with the highest abundance in cells of the liver and kidney (Vasko, 2016). They have a single membrane surrounding a granular matrix and they play a critical role in a variety of metabolic processes, such as fatty acid oxidation, ether-lipid biosynthesis, glyoxylate detoxification and the metabolism of reactive oxygen species (ROS) (Delille *et al.*, 2006). In response to the needs of the cell, peroxisomes can rapidly alter their number by growth and division and a specialised form of autophagy, called pexophagy. Defects in this process and in the metabolic processes within peroxisomes have been linked to the onset of severe neurodegenerative disorders (Costello and Schrader, 2018). Moreover, peroxisomes have recently been identified to physically tether to the endoplasmic reticulum (ER), another essential organelle, in order to perform some of its critical functions (Costello *et al.*, 2017a; Hua *et al.*, 2017).

1.1 Peroxisome biogenesis:

Peroxisome biogenesis includes the growth and division of pre-existing organelles, the synthesis of new organelles and the import of matrix proteins. In mammals, these processes require the coordinated activity of PEX proteins, or peroxins, encoded by their corresponding *PEX* genes (Braverman *et al.*, 2013). As peroxisomes do not contain any DNA, all peroxisomal proteins are encoded by nuclear DNA and are synthesised on free polyribosomes before being imported post-translationally (Lazarow and Fujiki, 1985). Peroxisomes require matrix proteins in order to carry out their numerous biochemical functions. Most matrix proteins in humans are imported into peroxisomes via a C-terminal PTS1 targeting signal. This was first identified due to the presence of this signal on luciferase of the firefly *Photinus pyralis.* Within this organism luciferase targets to peroxisomes where it initiates a bioluminescent reaction (Gould *et al.*, 1987; Keller *et al.*, 1987). Most peroxisomal matrix proteins have a C-terminal PTS1 signal and few have an N-terminal PST2 signal. Unlike other organelles, such as the ER or mitochondria, peroxisomes are able to import fully folded, co-factor-bound or oligomeric proteins through shuttling receptors (Léon *et al.,*

2006). Peroxisomal matrix proteins containing a PTS1 or PTS2 targeting signal are recognised by soluble receptors PEX5 and PEX7 respectively. These are found in the cytosol where they bind PTS1/2-containing proteins and guide them along the cytoskeleton to dock at the peroxisomal membrane by binding PEX13 and PEX14 (Braverman *et al.*, 2013). Following transport of these cargo proteins into the lumen of the peroxisome, the proteins are released and the PEX5/7 receptors are shuttled back into the cytosol (Hasan *et al.,* 2013) (Fig. 1.1). The process of translocation of folded proteins across the membrane and cargo release is not well understood. It has been postulated that a pinocytosis-like mechanism underlies this process (McNew and Goodman, 1996), however, this idea has been superseded by the “transient pore” model (Erdmann and Schliebs, 2005). This model suggests that a pore is dynamically formed by the import receptors to allow translocation and release of cargo although the exact mechanisms of this process remain to be fully elucidated.

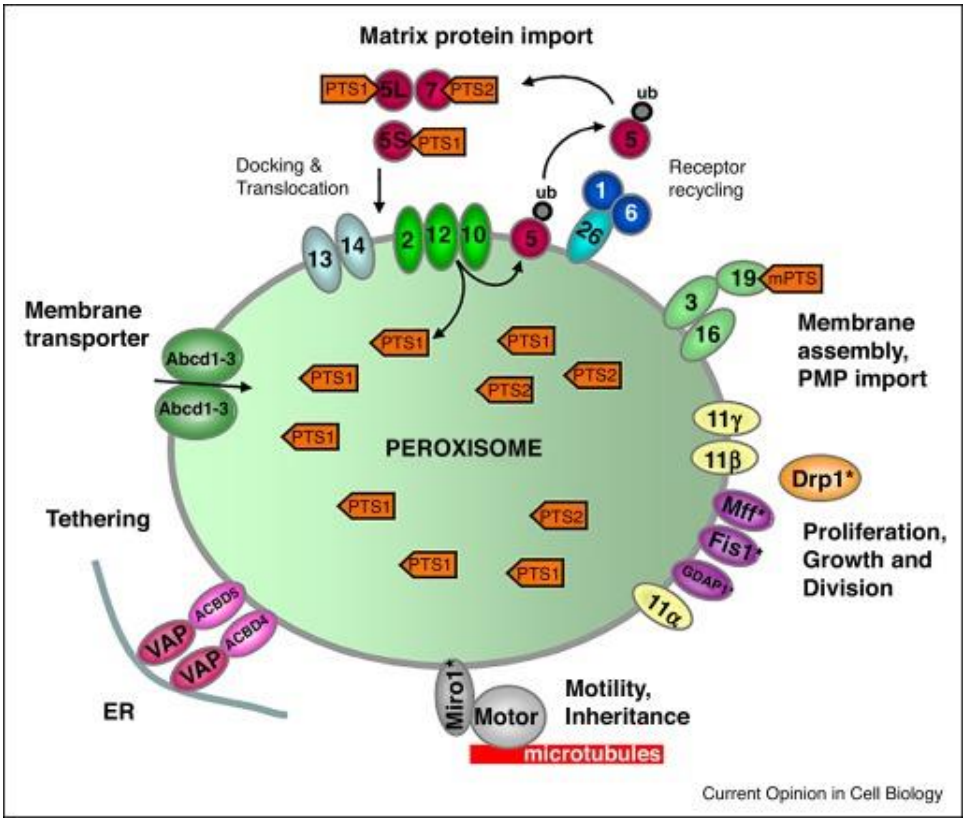

Fig. 1.1. Schematic overview of the molecular machineries involved in peroxisome biogenesis (From: Costello and Schrader, 2018)

The import of peroxisomal membrane proteins (PMPs) is not as well characterised. The import of PMPs depends on their internal membrane targeting sequences (mPTS) and requires the peroxins, PEX3 and PEX19 and

also PEX16 in mammals. The mPTS contains a PEX19 binding site and a membrane anchoring sequence (Van Ael and Fransen, 2006). PEX19 is thought to bind to the PMPs in the cytosol where it is then recruited by the peroxisome membrane receptor PEX3 (Fujiki *et al.*, 2006). The role of PEX16 is less well understood, but it is thought to function as a tethering factor for PEX3 (Honsho *et al.*, 2002; Fang *et al.*, 2004) (Fig. 1.1).

In order to adapt to suit the needs of the cell, it is essential that peroxisomes can increase or decrease their abundance. This requires dynamic processes such as biogenesis to increase their number and pexophagy to reduce their number (Costello and Schrader, 2018). This functional plasticity is essential, as indicated by the occurrence of peroxisome biogenesis disorders (PBDs) which are severe neurodegenerative disorders that manifest if there is a defect in any of these processes (Delille *et al.*, 2006). An increase in peroxisome proliferation is triggered by a member of the subfamily of ligand-dependent nuclear transcription factors, peroxisome proliferator-activated receptor α (PPARα). This is activated by lipid ligands such as fatty acids and synthetic peroxisome proliferators and regulates the expression of genes associated with peroxisomal fatty acid β-oxidation and peroxisome proliferation (Schrader *et al.*, 2013). The first model of peroxisome biogenesis was the “growth and division” model that was first proposed in 1985 (Lazarow and Fujiki, 1985). This suggested that peroxisomes divide and replicate autonomously like mitochondria and chloroplasts through the import of membrane and matrix proteins synthesised on free polyribosomes and inserted post-translationally into the pre-existing peroxisomes (Lazarow and Fujiki, 1985). This model also suggested that it was not possible for peroxisomes to form *de novo,* however, it is now widely accepted that peroxisome biogenesis can also occur *de novo* from interactions with neighbouring organelles. This new model was first initiated following a series of experiments involving mutations of peroxins PEX3, PEX16 and PEX19. These are required to maintain the peroxisomal membrane and their loss of function leads to a lack of peroxisomes (South and Gould, 1999; Hettema *et al.*, 2000; Heiland and Erdmann, 2005). Re-introduction of functional copies of these proteins led to *de novo* generation of peroxisomes, suggesting that peroxisomes must derive from another cellular compartment (Hoepfner *et al.*, 2005; Kragt *et al.*, 2005; Haan *et al.*, 2006; Kim *et al.*, 2006). Subsequently,

it was found that PEX3 originally localises to the ER prior to peroxisome formation (Hoepfner *et al.*, 2005; Haan *et al.*, 2006), indicating a role for the ER in this model of peroxisome biogenesis. The exact mechanisms for ER-derived peroxisome biogenesis have remained a source of controversy in the field. It was first suggested, following studies in the yeast *Saccharomyces cerevisiae,* that PEX3 first localises to the ER before attracting PEX19 to mark the site for insertion of other PMPs, initiating the formation of fully competent peroxisomes (Hoepfner *et al.*, 2005). Further studies showed that several other PMPs localise to the ER in *pex3* mutant cells (van der Zand *et al.*, 2010) and, following reintroduction of functional PEX3 proteins, incorporate into preperoxisomal vesicles which fuse to form peroxisomes (van der Zand *et al.*, 2012). However, this model was challenged following the finding that PEX3 is not required for the formation of preperoxisomal vesicles (Knoops *et al.*, 2014). Recent work has aided our understanding of this process, however, by showing that preperoxisomal vesicles originate at the ER in regions containing PEX30 and that their size and number is regulated by the actions of both PEX30 and PEX31, strengthening the argument for the role of the ER in peroxisome biogenesis (Joshi *et al.*, 2016).

It was recently identified that mitochondria also play a role in *de novo* peroxisome biogenesis (Sugiura *et al.*, 2017). This study investigated *de novo* peroxisome biogenesis using human fibroblast cell lines lacking PEX3 or PEX16. Following reintroduction of PEX3, it was found that this peroxin targeted mitochondria and exited in preperoxisomal vesicles. Conversely, PEX16 localised to the ER and was released in vesicles which fused with the mitochondria-derived pre-peroxisomes to form new peroxisomes (Sugiura *et al.*, 2017). This finding demonstrated a potential role for mitochondria in the *de novo* formation of peroxisomes, consistent with theories that peroxisomes have evolved from the mitochondria and corroborating the idea of a functional endomembrane system within eukaryotic cells (Bolte *et al.,* 2015; Gould *et al.*, 2016).

Despite the novel insights into the *de novo* biogenesis of peroxisomes, it is still widely accepted that peroxisome number is mainly controlled via growth and division of pre-existing organelles (Motley and Hettema, 2007). This pathway requires remodelling and expansion of the peroxisomal membrane which occurs

through the formation of tubular membrane extensions which constrict and divide into new peroxisomes (Schrader *et al.*, 2016). The peroxisomal protein PEX11β plays an integral role in this process. PEX11β deforms and elongates the peroxisomal membrane prior to fission (Delille *et al.*, 2010) and also aids in the assembly of the fission machinery. The fission machinery consists of the dynamin-like GTPase DRP1 and the membrane adaptors MFF and FIS1 (Schrader *et al.*, 2016). PEX11β also acts as a GTPase activating protein for DRP1, enabling the process of peroxisomal fission (Williams *et al.*, 2015) (Fig. 1.1). Many of these fission machinery proteins are also shared with mitochondria, which further substantiates the idea of the peroxisome-mitochondria connection (Schrader *et al.*, 2015). In addition, patients with a defect in PEX11β have also been identified. These patients display symptoms including neurological defects, progressive hearing loss, skeletal abnormalities and eye problems, however, all biochemical parameters commonly used for diagnosing peroxisomal disorders are normal (Ebberink *et al.*, 2012; Taylor *et al.*, 2017). This suggests that the symptoms observed are caused by a lack of control of peroxisome number in response to physiological cues, highlighting the importance of regulating peroxisome abundance (Costello and Schrader, 2018).

To maintain peroxisome homeostasis and ensure that peroxisomes can efficiently carry out their essential biochemical functions, peroxisomes also need to be degraded to regulate their number. Pexophagy is a specialised form of autophagy which allows for the selective degradation of peroxisomes (Yorimitsu and Klionsky, 2005). The molecular mechanisms underlying pexophagy have not been fully characterised, although, it is understood that pexophagy can be triggered by different mechanisms (Cho *et al.*, 2018). Firstly, pexophagy can be mediated by ubiquitination of PMPs. In this case, ubiquitin bound to PMPs is exposed to the cytoplasm and can be targeted by ubiquitin-binding autophagy adaptors, such as p62. This triggers targeting of peroxisomes to autophagosomes which fuse to lysosomes allowing degradation of peroxisomes (Kim *et al.*, 2008). Additionally, the protein NBR1 induces peroxisome clustering and targeting to lysosomes to induce pexophagy (Deosaran *et al.*, 2013). It has been speculated that 65% of all cases of PBDs are caused by the inability to prevent pexophagy, leading to a lack of

peroxisomes in the cell (Law *et al.*, 2017; Nazarko, 2017). This is because the AAA ATPase complex consisting of the peroxins PEX1, PEX6 and PEX26 which is mutated in many PBDs, prevents pexophagy (Law *et al.*, 2017). The accuracy of this speculation remains controversial in the field, suggesting further research into the importance of pexophagy in health and disease is still required.

1.2 Biochemical roles played by peroxisomes:

Peroxisomes play many important roles in human metabolism and are, accordingly, vital for human health and development. This is highlighted by the occurrence of severe diseases caused by a lack of peroxisomes (PBDs) or by deficiencies in essential peroxisomal metabolic enzymes (Wanders, 2004).

1.2.1 Fatty acid β-oxidation:

One of the main roles played by peroxisomes is fatty acid β-oxidation. The distinct difference between mitochondrial and peroxisomal fatty acid β-oxidation is that peroxisomes can only chain shorten fatty acids and cannot fully degrade them. In mitochondria, the β-oxidation pathway removes a two-carbon unit from the fatty acid in the form of an acetyl-CoA unit which can then be degraded in the Krebs cycle to CO_2, H_2O and ATP. However, peroxisomes lack a Krebs cycle so are unable to degrade the acetyl-CoA units. For this reason, peroxisomes transfer their β-oxidation products to the mitochondria for complete degradation (Wanders *et al.*, 2001a). Additionally, very long chain fatty acids (VLCFAs) (≥C22) can only be metabolised in peroxisomes. This includes hexacosanoic acid (C26:0), pristanic acid (obtained from dietary sources or as a product from the α-oxidation of phytanic acid) and di- and trihydroxycholestanoic acid (DHCA and THCA) which are intermediates in the formation of bile acids. Peroxisomal fatty acid β-oxidation also functions in the biosynthesis of polyunsaturated fatty acids, such as docosahexaenoic acid from linolenic acid in cooperation with the ER (Wanders, 2004).

1.2.2. Biosynthesis of ether-phospholipids:

Another essential role played by peroxisomes is the biosynthesis of ether-phospholipids. These are a special class of phospholipids that have an ether linkage at the sn-1 position of the glycerol backbone rather than an ester

linkage as in diacylglycerophospholipids. Certain ether-phospholipids are known as plasmalogens which are constituents of many tissues in the body, including brain myelin which is required for normal neurological function and also heart muscle, skeletal muscle and kidneys. In the peroxisomal biogenesis disorder rhizomelic chondrodysplasia punctata (RCDP), plasmalogen synthesis is severely impaired due to the lack of PTS2-mediated import of alkyl-dihydroxyacetone phosphate synthase (ADHAPS) caused by a mutation in the gene encoding the peroxisomal protein transporter, PEX7 (Brites *et al.*, 2004).

Plasmalogen biosynthesis starts in peroxisomes and involves the esterification of dihydroxyacetone phosphate (DHAP) with a long-chain acyl-CoA ester and is carried out by dihydroxyacetone phosphate acyltransferase (DHAPAT) (Hajra, 1997). The ether bond at the sn-1 position is introduced by the replacement of the sn-1 fatty acid with a long-chain fatty alcohol. This is catalysed by ADHAPS and produces alkyl-DHAP (Brown and Snyder, 1982; Singh *et al.*, 1993). Both DHAP and ADHAPS are strictly peroxisomal enzymes (Singh *et al.,* 1993). The ketone group at the sn-2 position of alkyl-DHAP is then reduced by acyl/alkyl-dihydroxyacetone phosphate reductase (AADHAP-R), which has a bimodal distribution in peroxisomes and the ER (Ghosh and Hajra, 1986; Datta *et al.*, 1990). This results in the formation of 1-alkyl-*sn*-glycero-3-phosphate which undergoes conversion into mature plasmalogens in the ER (Braverman and Moser, 2012).

1.2.3. Fatty acid α-oxidation:

Fatty acids which have a methyl group at the β-position cannot directly undergo β-oxidation. Instead, these fatty acids need to first be α-oxidised to remove their terminal carboxyl group as CO_2. One such fatty acid which requires metabolism in this way is phytanic acid. The α-oxidation of phytanic acid begins with its activation to phytanoyl-CoA, via the long-chain acyl-CoA synthetase (LACS) localised on the peroxisomal membrane. Following uptake into the peroxisomal matrix, phytanoyl-CoA undergoes hydroxylation and cleavage to pristanal and formyl-CoA. Pristanal is then converted into pristanic acid which undergoes three cycles of β-oxidation within the peroxisome before being fully oxidised in the mitochondria. Phytanic acid is known to accumulate in Refsum disease due to a defect in this process (Wanders *et al.,* 2001b).

1.2.4. Reactive oxygen species (ROS) metabolism:

Reactive oxygen species (ROS) are oxygen-derived radical species. They play an essential role in physiological conditions such as the mediation of cell signalling, host defence and ageing (Bonekamp *et al.*, 2009). However, their overproduction under conditions of oxidative stress can cause detrimental effects on the cell and has been linked to conditions such as cancer, neurodegeneration and atherosclerosis (Schrader and Fahimi, 2006). Peroxisomes have been identified as key players in ROS metabolism due to their ability to both generate and break down ROS. Essential cellular metabolic processes involving peroxisomes, such as fatty acid β-oxidation, are known to produce hydrogen peroxide (H_2O_2). H_2O_2 is often associated with ROS due to its potential to be easily converted into radical species, for example, into $^{\bullet}OH$ via Fenton-catalysed reduction. In addition, peroxisomes contain other ROS-producing oxidases (Bonekamp *et al.*, 2009). Interestingly, peroxisomes also contain several ROS-degrading enzymes, such as catalase, glutathione peroxidase, manganese superoxide dismutase, epoxide hydrolase and peroxiredoxin I, highlighting their important role in maintaining balance in cellular ROS levels (Schrader and Fahimi, 2006).

1.3 Role of peroxisomes in disease:

It has now become evident that peroxisomes are vital for human health and development. This is corroborated by the existence of several inherited peroxisomal diseases caused by defects in essential peroxisomal genes (Waterham *et al.,* 2016). These diseases often present with severe phenotypes and can affect the brain, spinal cord, eyes, ears, liver, kidney, adrenal cortex and skeletal system amongst other organs (Gould and Valle, 2000). Peroxisomal diseases generally fall into two categories; single enzyme deficiencies which may affect one specific peroxisomal function or metabolic pathway, and the peroxisome biogenesis disorders (PBDs) in which the affected protein is a peroxin (Waterham *et al.*, 2016). PBDs vary in severity, but they usually result in either impairment or completely inhibition of peroxisome function. In some cases, PBDs can lead to the formation of peroxisomal "ghosts" which are empty, non-functional peroxisomal membranes. This occurs as many peroxins are involved in protein import, so a defect in these proteins renders peroxisomes unable to take up peroxisomal matrix proteins from the

cytosol, resulting in peroxisomes being unable to carry out their essential biochemical functions. This ultimately leads to an accumulation of peroxisomal substrates, such as, VLCFAs, pristanic and phytanic acids, bile acid intermediates and pipecolic acid, which can be toxic to the cell. There is also a lack of essential peroxisomal-derived products such as plasmalogens which are required for normal neurological function (Delille *et al.,* 2006).

1.3.1. Peroxisome biogenesis disorders:

PBDs are autosomal-recessive diseases which consist of two broad clinical spectra; the Zellweger spectrum, which accounts for 80% of all occurrences of PBDs, and the rhizomelic chondrodysplasia punctata (RCDP) spectrum (Rosewich *et al.*, 2005). The most severe Zellweger spectrum class is Zellweger Syndrome, first described in 1964 by Bowen *et al* (Bowen *et al.*, 1964). It is a rare disease affecting 1:50,000 births and is characterised by an absence of peroxisomes (Goldfischer *et al.*, 1973). Affected patients usually present with neonatal hypotonia, craniofacial dysmorphy, hepatomegaly, renal cysts, adrenal atrophy and neurological abnormalities (Waterham *et al.,* 2016). These patients also show distinct biochemical parameters such as an increased level of VLCFAs, bile acid intermediates, pipecolic and phytanic acid in the blood. Patients with Zellweger syndrome usually do not survive past the first year of life. Most Zellweger spectrum disorders are caused by mutations in PEX1, an AAA ATPase involved in PTS1/2 protein import (Reuber *et al.*, 1997).

RCDP type 1 is clinically and genetically distinctive from the Zellweger syndrome spectrum and was first described in 1985 (Heymans *et al.*, 1985). This spectrum includes RCDP type 1, and also milder variants. RCDP type 1 is caused by mutations in the *PEX7* gene encoding the PEX7 cytosolic receptor. This disrupts the import of PTS2-containing proteins, such as, alkyldihydroxy-acetonephosphate synthase (ADHAPS) involved in the synthesis of plasmalogens. Patients present with shortening of the limbs, cataracts and psychomotor retardation (Rosewich *et al.,* 2005) and do not usually survive past the first decade of life (Wanders and Waterham, 2004).

1.3.2. Single peroxisomal enzyme deficiencies:

The single peroxisomal enzyme deficiencies differ from PBDs as the defect is not in a PEX gene. The clinical symptoms presented by affected patients result

from a deficiency in a peroxisomal enzyme involved in a specific anabolic or catabolic pathway (Aubourg and Wanders, 2013). The most common single peroxisomal enzyme deficiency is X-linked adrenoleukodystrophy (X-ALD) with an estimated incidence of 1:17,000 (Kemp *et al.,* 2012). X-ALD is caused by a mutation in the *ABCD1* gene which encodes an ATP-binding cassette (ABC) transporter protein of the peroxisomal membrane, called ABCD1 or ALDP, which plays a role in the uptake of VLCFAs (Mosser *et al.*, 1993).

In addition to X-ALD, there are also several other single peroxisomal enzyme deficiencies which affect peroxisomal fatty acid β-oxidation. These include: acyl-CoA-oxidase-1 (ACOX1) deficiency (Poll-the *et al.*, 1988) and D-bifunctional protein (DBP) deficiency (Suzuki *et al.*, 1997), both characterised by the accumulation of VLCFAs (Wanders and Waterham, 2006). Additionally, 2-methylacyl-CoA racemase (AMACR) deficiency (Ferdinandusse *et al.*, 2000) and sterol carrier protein X (SCPx) deficiency (Ferdinandusse *et al.*, 2006) have been identified which are both associated with an increase in the levels of phytanic and pristanic acid as well as DHCA and THCA, however, there is no accumulation of VLCFAs (Wanders and Waterham, 2006).

1.4 Membrane contact sites:

We now know that eukaryotic organelles do not operate as separate entities, rather they cooperate extensively in order to efficiently carry out their functions. This is made possible through vesicular trafficking pathways and membrane contact sites (MCS). MCSs are sites of close apposition between two or more organelles which allows the exchange of materials such as metabolites, lipids and proteins (Cohen *et al.*, 2018). The first indication that organelles may interact in this way was provided by early electron microscopy studies in which organelles were frequently found to be closely apposed to each other at defined foci (Bernhard and Rouiller, 1956; Porter and Palade, 1957; Copeland and Dalton, 1959; Rosenbluth, 1962; Gray, 1963). Subsequent studies on the triadic muscle junction between the ER and plasma membrane invaginations in skeletal muscle cells showed that these inter-organellar connections are mediated through interacting proteins which act as tethers to bridge the respective organelle membranes (Kawamoto *et al.*, 1986).

In recent years, it has become increasingly evident that most organelles interact in this way. Accordingly, the list of known proteins which are implicated in the formation or function of contact sites, is constantly expanding (Eisenberg-Bord *et al.*, 2016). These proteins can have various functions. Some act to physically tether the interacting organelles (Csordás *et al.*, 2006; Helle *et al.*, 2013), whilst others act as mediators of metabolite exchange, for example, in the non-vesicular exchange of small molecules (Prinz, 2014; Henne, 2016). Some proteins may even act to regulate the size and abundance of organelle contact sites in response to environmental and physiological cues (Kornmann *et al.*, 2011; Elbaz-Alon *et al.*, 2014; Henne *et al.*, 2015). It should be noted, however, that not all cases in which organelles are tethered in this way are considered true MCSs. In order to aid in the identification of bona fide MCSs, it has been suggested that interactions such as these must have the following four properties: (1) the tethered organelle membranes must be in close apposition, typically within 30 nm, (2) the membranes do not fuse, (3) specific proteins and/or lipids must be enriched at the MCS and (4) MCS formation must affect the function or composition of at least one of the tethered organelles (Prinz, 2014).

Improvements in microscopical and biochemical methods to study MCSs has significantly aided in their identification and advanced our understanding of their function. This has led to the recognition that MCSs can be implicated in several cellular processes. Perhaps the best studied function is the exchange of Ca^{2+} ions that occurs at several MCSs, including ER-plasma membrane, ER-endosome and ER-mitochondria contacts (Phillips and Voeltz, 2016). An example of this in mammalian cells is the interaction between the voltage-dependent anion channel (VDAC) on the outer mitochondrial membrane and the IP3 receptor on the ER which mediates Ca^{2+} homeostasis (Szabadkai *et al.*, 2006). In addition, almost all known MCSs have been identified to function in lipid transfer. For instance, the transfer of phospholipids occurs at ER-mitochondria MCSs (Phillips and Voeltz, 2016) and the transfer of fatty acids is known to occur at ER-lipid droplet and lipid droplet-mitochondria MCSs (Gatta and Levine, 2017). In some cases, MCSs may also play a role in organelle division, as is the case for mitochondria which divide when the ER wraps around mitochondrial constriction sites (Friedman *et al.*, 2011). Finally, MCSs

may also simply play a role in the arrangement of the cellular landscape, providing a dynamic, but controlled architecture to enable the correct targeting of molecules and optimise biosynthetic pathways (Shai *et al.*, 2016).

1.4.1. Peroxisome-organelle contact sites:

Like other organelles, peroxisomes also participate in inter-organelle cooperation. For decades, it has been observed in electron microscopy images from fungi, plants and mammals that peroxisomes are often found juxtaposed to other organelles, in particular the ER, plasma membrane, lipid droplets, chloroplasts and mitochondria (Herzog and Fahimi, 1976; Hicks and Fahimi, 1977; Fahimi and Yokota, 1981). These provided the first indication that peroxisomes may form MCSs with neighbouring organelles. In recent years, several peroxisome-organelle contact sites have been identified in yeast and mammals and we now have a greater idea of the role that they play in the cell.

1.4.2. Peroxisome-mitochondria contacts:

It has been long understood that mitochondria and peroxisomes maintain a close relationship. Despite different evolutionary origins, both organelles are morphologically and functionally similar (Schrader and Yoon, 2007). In recent years, it has been uncovered that this organelle relationship may be closer than originally proposed. Cooperation between these organelles includes fatty acid β-oxidation in which mitochondria fully degrade fatty acids which have been partially degraded in peroxisomes (Wanders *et al.*, 2001a) (see Section 1.2.1 for further detail). Additionally, both organelles share key proteins of their division machinery such as DRP1, FIS1 and MFF (Schrader *et al.,* 2012). Mitochondria and peroxisomes have also been shown to cooperate in maintaining redox balance in the cell (Fransen *et al.*, 2012) as well as cooperate in antiviral signalling and defence (Odendall and Kagan, 2013). Moreover, a vesicular trafficking pathway between peroxisomes and mitochondria has also been identified which could allow direct cargo exchange between both organelles (Neuspiel *et al.*, 2008). Recently, some peroxisome-mitochondria contact sites have been proposed in yeast. In 2015, a genome-wide localisation study of the peroxisomal protein PEX11 identified that this protein may interact and form a peroxisome-mitochondria tether with mitochondrial MDM34, a protein involved in the yeast mitochondria-ER tethering complex, ERMES

(Mattiazzi Ušaj *et al.*, 2015). In 2018, a new peroxisome-mitochondria contact site was uncovered in yeast. This contact site, named “PerMit” consists of two tethering proteins, peroxisomal PEX34 and mitochondrial FZO1 and has been demonstrated to play a role in fatty acid β-oxidation (Shai *et al.*, 2018). In mammals, the ACBD2/ECI2 protein, which has been reported to be shared between both peroxisomes and mitochondria, has been suggested to play a role in enabling contact between the two organelles, but this has not been extensively studied (Fan *et al.*, 2016). The observed proximity and extensive cooperation between the organelles, however, make the existence of a bona fide tethering complex likely. Furthermore, in the yeast *S. cerevisiae,* peroxisomes have been found adjacent to a mitochondrial niche in which the mitochondria-ER contact occurs (Cohen *et al.*, 2014). The proximity of these three organelles has led to the hypothesis that they may form a “tripartite” contact site, allowing bi-directional transfer of molecules between the organelles simultaneously (Shai *et al.,* 2016). More research in this area is needed to fully uncover the components and mechanisms involved in mammalian peroxisome-mitochondria contact sites and further investigate the possibility of a tripartite contact site.

1.4.3. Peroxisome-lipid droplets contacts:

Lipid droplets (LDs) are dynamic organelles found in eukaryotic cells. They contribute to many cellular functions and act as a store for neutral lipids such as triacylglycerol and cholesterol ester (Beller *et al.*, 2010). Early ultrastructural studies first suggested an interaction between LDs and peroxisomes (Novikoff *et al.*, 1980) and this has since been confirmed by live cell imaging (Schrader, 2001). It has been postulated that the peroxisome-LD interaction may link lipolysis mediated by LDs to peroxisomal fatty acid β-oxidation and that lipids generated by peroxisomes may move into LDs (Schrader *et al.*, 2013). In support of this, a study in the nematode *Caenorhabditis elegans* found that defects in peroxisomal fatty acid β-oxidation resulted in enlarged LDs (Zhang *et al.*, 2010). Additionally, changes in the size and number of LDs have been observed in peroxisome-deficient knock-out mice (Dirkx *et al.*, 2005). Despite these observations, a peroxisome-LD tether has yet to be identified. In *S. cerevisiae,* an interactome map of protein-protein interactions between peroxisomes and LDs was generated which revealed that the LD proteins

ERG6 and PET10 interact with several peroxisomal proteins (Pu *et al.*, 2011), however, whether these proteins constitute a genuine tether has not yet been determined.

1.4.4. Peroxisome-lysosome contacts:

Lysosomes are ubiquitous organelles best known for their role in the digestion of intracellular components such as autophagic organelles (Muffly, 2007). They also provide a major source for cellular cholesterol (Jin *et al.*, 2015). In 2015, the first peroxisome-lysosome contact site was discovered. The integral lysosomal membrane protein, synaptotagmin VII (Syt7) was shown to bind to the lipid $PI(4,5)P_2$ on the peroxisomal membrane. (Jin *et al.,* 2015). This contact is required for the transport of cholesterol from the lysosome to the plasma membrane (Chu *et al.*, 2015). Cholesterol accumulation in lysosomes has been observed in cells from patients suffering from the peroxisomal diseases X-ALD and Zellweger spectrum disorders, highlighting the importance of peroxisome-lysosome contact for cholesterol transport (Shai *et al.*, 2016).

1.4.5. Peroxisome-peroxisome contacts:

Peroxisomes have also been found to self-interact in transient and long term contacts in live cell studies (Bonekamp *et al.*, 2012) and in ultrastructural studies where the presence of small peroxisome groups with close apposition have been observed (Zaar *et al.*, 1984; Stier *et al.*, 1998). The physiological role for this interaction is not well understood, although it has been hypothesised that these interactions may provide a “signalling system” to the cell to monitor the state and distribution of peroxisomes to ensure that their population is stably maintained (Schrader *et al.*, 2013). Functionally, these contacts may be required for the exchange of metabolites, such as H_2O_2 or other ROS. The close interaction between the peroxisomes may allow efficient exchange of these species and minimise leakage (Shai *et al.,* 2016). Furthermore, peroxisomes moving along microtubules in the cell have been observed to interact with other peroxisomes (Schrader *et al.*, 2013). The exact mechanisms underlying peroxisomal self-interaction have yet to be uncovered.

1.4.6. Peroxisome-ER contacts:

By far the best studied peroxisome-organelle contact is that between peroxisomes and the ER. Early ultrastructural studies revealed that peroxisomes are found in close proximity to the ER and in some cases they are even wrapped in ER cisternae (Novikoff and Novikoff, 1972; Zaar *et al.,* 1987; Grabenbauer *et al.*, 2000). Originally, the close apposition of these two organelles was hypothesised to be involved in the formation of new peroxisomes (Novikoff and Shin, 1964), an idea which has subsequently been corroborated following elucidation of the role of the ER in *de novo* peroxisome biogenesis. As well as contributing to *de novo* formation of peroxisomes, the ER has also been found to play a role in the non-vesicular delivery of phospholipids to nascent peroxisomes to enable membrane growth when peroxisomes divide by growth and division (Raychaudhuri and Prinz, 2008; Hettema *et al.*, 2014).

In addition to contributing to the biogenesis of peroxisomes, the ER has also been implicated in several essential biochemical processes which occur in peroxisomes. An example of such is the biosynthesis of plasmalogens which is initiated in peroxisomes but requires further reactions in the ER for completion (Braverman and Moser, 2012) (see Section 1.2.2 for further detail). The production of polyunsaturated fatty acids, such as docosahexaenoic acid, also requires cooperation between the two organelles. Fatty acids produced in the ER are transferred to peroxisomes where they are partially degraded by fatty acid β-oxidation until a double bond is formed at position 4 of the carbon chain (Sprecher and Chen, 1999; Su *et al.*, 2001). At this point, they can then be transported back to the ER where they can be used for membrane lipid biosynthesis (Sprecher and Chen, 1999). Furthermore, bile acid synthesis also requires cooperation with the ER. The ER contains enzymes which are essential for the import of THCA, a bile acid precursor, into peroxisomes where it can be processed by β-oxidation (Mihalik *et al.*, 2002). Defects in any of these pathways have been linked to severe neurodegenerative disorders (Wanders and Poll-The, 2017), highlighting the importance of cooperation between these two organelles.

Despite our understanding of the importance of cooperation between these two organelles, we have only recently started to gain insight into the formation, structure and function of this association. In yeast, a peroxisome-ER contact site (EPCON) and a peroxisome-ER tether consisting of PEX3 and INP1

required for inheritance have been identified (David *et al.*, 2013; Knoblach *et al.*, 2013), but mammalian homologues remained undiscovered. In 2017, however, the first bona fide mammalian MCS between peroxisomes and the ER was discovered in parallel studies by two different groups (Costello *et al.*, 2017a; Hua *et al.*, 2017). It was identified that the peroxisomal membrane protein acyl-coenzyme A–binding domain protein 5 (ACBD5) is a binding partner for the ER protein vesicle-associated membrane protein-associated protein B (VAPB) (Fig. 1.2). The first suggestion that these proteins were involved in tethering the respective organelle membranes was made following a search for proteins which interact with known peroxisomal membrane proteins. Costello *et al* investigated ACBD5 as a protein of interest, whilst Hua *et al* investigated PEX16, a peroxin which has been identified to initially target to the ER before being trafficked to peroxisomes and is involved in peroxisome biogenesis (Kim *et al.*, 2006; Aranovich *et al.*, 2014; Hua *et al.*, 2015). Both studies identified ER proteins VAPA and VAPB as candidate interactors. VAP proteins are known to participate in contact sites and mediate protein interactions due to the presence of a major sperm protein (MSP) domain within their structure (Wyles and Ridgway, 2004). The MSP domain is a 7-beta strand globular domain (120-140 amino acids) which interacts with proteins that contain two phenylalanines (FF) in an acidic tract (FFAT) motif (Fig. 1.2). VAPA/B also contain a linker region (≤ 100 aa) which partly forms a coiled-coil, and a C-terminal transmembrane tail anchor that targets the ER (Murphy and Levine, 2016). VAPB has also been implicated in the neurodegenerative disorder, amyotrophic lateral sclerosis (ALS) which is caused by a proline-to-serine mutation in the protein at position 56 (P56S) (Nishimura *et al.*, 2004). ACBD5 was predicted to have a FFAT-like motif, further validating its potential as an interacting partner for VAPB (Murphy and Levine, 2016) (Fig 1.2). FFAT motifs have a core of six defined elements across a stretch of seven residues E^{1}-F^{2}-F^{3}-D^{4}-A^{5}-x-E^{7} (using the single letter amino acid code, where x is any amino acid) (Loewen *et al.*, 2003) and can bind to the MSP domain in VAPA/B proteins with a micromolar dissociation constant (Murphy and Levine, 2016). In addition, ACBD5 consists of an N-terminal acyl-CoA binding (AcB) domain and a C-terminal transmembrane tail anchor which targets to the peroxisomal membrane (Costello *et al.*, 2017a) (Fig. 1.2).

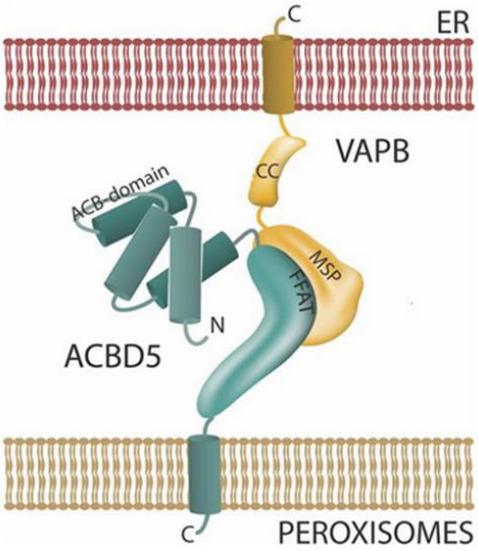

Fig. 1.2. Schematic model of the ACBD5–VAPB interaction (From: Costello *et al.*, 2017a).

Collectively, these studies proved that the interactions between these proteins constitute a genuine tether. Hua *et al* showed that VAP proteins were enriched in puncta which are localised in close proximity to peroxisomes using structured illumination superresolution microscopy. Both studies showed that VAPA/B and ACBD5 specifically mediate the organelle interactions through demonstrating that loss of each protein individually, particularly loss of ACBD5, leads to a disruption in peroxisome-ER interaction. Furthermore, it was found that this protein interaction occurs specifically through the FFAT-like motif of ACBD5 as mutations in the FFAT-like motif disrupted binding between the two proteins, whilst mutations in other domains had no effect on binding. Additionally, Costello *et al* demonstrated that overexpression of both proteins significantly increased the number of peroxisomes in close contact with the ER (<15 nm distance). It was also shown that interaction between these proteins is required for functional activity of the two organelles. A depletion in ACBD5 leads to a loss of tethering to the ER and subsequently increased peroxisome motility. Moreover, depletion of one of the tethering components also reduces peroxisomal membrane expansion, suggesting that the peroxisome-ER connection is required for the transfer of membrane lipids for peroxisomal growth and division. Finally, Hua *et al* also demonstrated that this connection may be implicated in lipid synthesis. A depletion in VAPA/B or ACBD5 led to an overall reduction in plasmalogen and cholesterol levels in the cell, suggesting that this tether also functions in cooperative biochemical pathways.

Following these studies, it was subsequently found that another tail-anchored peroxisomal membrane protein ACBD4, can also bind to VAPB and tether peroxisomes to the ER (Costello *et al.*, 2017b). ACBD4 is also a member of the ACBD family and shares 58% sequence identity with ACBD5. Accordingly, ACBD4 also contains an N-terminal acyl-CoA binding domain and is predicted to contain a coiled-coil domain and FFAT-like motif. Using pull down studies and mass spectrometry, VAPA and VAPB were identified as potential interactors. Subsequent immunoprecipitation experiments confirmed the interaction between ACBD4 and VAPB, proving the existence of another peroxisome-ER tether (Costello *et al.*, 2017b).

1.4.7. The role of ACBD5 in health and disease:

The exact function of ACBD5 has yet to be fully elucidated, however, it has recently been implicated in disease. In 2013, an exome sequencing study of patients with retinal dystrophy revealed ACBD5 as a novel candidate disease gene. Three siblings were identified with a homozygous splice site mutation in ACBD5 resulting in loss of function and syndromic retinal dystrophy (Abu-Safieh *et al.*, 2013). This study, however, did not assess the physiological and functional consequences of the mutation. Additionally, a patient has been identified with a loss of function mutation in ACBD5 resulting in progressive leukodystrophy, cleft palate, ataxia and retinal dystrophy. This patient also presented with elevated levels of VLCFAs in the plasma, indicating defective fatty acid β-oxidation presumably due to insufficient uptake of VLCFAs into peroxisomes. This led to the suggestion that ACBD5 may function as a membrane-bound receptor for very-long-chain fatty acyl-CoAs (VLCFA-CoAs) (Ferdinandusse *et al.*, 2017). It was postulated that the exposed AcB domain of ACBD5 attaches to VLCFAs in the cytosol and brings them to the VLCFA transporter ABCD1 on the peroxisomal membrane. This, in turn, transfers the VLCFAs into peroxisomes where they can be degraded by fatty acid β-oxidation (Ferdinandusse *et al.*, 2017). The ability of ACBD5 to interact with ABC transporters remains questionable, however, as a recent study showed that ACBD5 fails to interact with an ABCD1 homologue, ABCD2 (Geillon *et al.*, 2017). ACBD5 was also suggested to play a role in pexophagy based on sequence similarity with the ATG37 protein of the yeast *Pichia pastoris*, which performs this function (Nazarko *et al.*, 2014). However, subsequent studies

using an ACBD5 knock-out cell line and an established pexophagy assay failed to reveal a role for ACBD5 in this process (Ferdinandusse *et al.*, 2017). It appears as if diseases associated with loss of ACBD5 are linked to a loss in its physiological functions, however, it has still not been established whether a reduction in peroxisome-ER contact, which would likely occur with loss of ACBD5, plays any role in the symptoms observed.

1.4.8. The need for multiple tethers:

The existence of more than one tether between peroxisomes and the ER is consistent with findings from studies on other inter-organelle contacts. For example, it has been reported that ER-mitochondria interactions are mediated by multiples tethers which are linked to different functions (Naon and Scorrano, 2014). However, the requirement for multiple peroxisome-ER tethers has yet to be understood.

As ACBD4 has been shown to be functionally similar to ACBD5 in terms of mediating peroxisome-ER tethering, it would be tempting to speculate that loss of ACBD5 could be complemented by ACBD4. However, this seems unlikely based on the severe consequences associated with a loss of function of ACBD5 in patients (Abu-Safieh *et al.*, 2013; Ferdinandusse *et al.*, 2017). This is also corroborated by the finding in the ACBD5-VAPB interaction study by Costello *et al* where knockdown of ACBD5 in HepG2 cells significantly reduces peroxisome-ER contacts (Costello *et al.*, 2017a). ACBD4 is also reported to be expressed in these cells (Yang *et al.*, 2016), so if it was capable of complementing the function of ACBD5, this significant reduction would not have occurred. This suggests that ACBD4 and ACBD5 may have distinct physiological functions separate from mediating tethering between peroxisomes and the ER, leading to the requirement of both proteins. It has also been hypothesised that ACBD5 may act as the major tether for peroxisome-ER contacts, whereas ACBD4 may play a role in more specialised peroxisome-ER contacts (Costello *et al.*, 2017b). Our current understanding of contact sites in peroxisomes and in other organelles suggests that it would be likely that there are other proteins which act as tethers for peroxisome-ER associations. However, to date, the available tools for deciphering novel contact site proteins are lacking. For this reason, it has become essential to devise new methods to

identify the proteins involved in order to fully elucidate the function of this organelle cooperation.

1.5 Visualising contact sites:

Our extensive findings in the field of inter-organelle contacts and our increased understanding of the relevance of this phenomenon in both health and disease have paved the way for a new, exciting area of organelle research. However, many questions remain unanswered. It is currently unclear whether we have identified all of the existing inter-organelle contact sites. The observed proximity and established physiological cooperation between most organelles suggest we have only touched the surface. Additionally, the coordination and regulation behind the formation of contact sites has yet to be elucidated. Moreover, the function of many known contact sites has still not been fully characterised. These questions have led to a drive to establish simple, yet robust methods to aid in the discovery of novel contact sites and further our understanding of existing sites. Our understanding of these sites depends on the quality and availability of the tools we have to study them. To this end, the number of tools created and optimised for this use has increased in recent years.

In order to first identify organelles which are in close proximity, microscopy methods are required. The size of contact sites is generally within the range of 10-40 nm which is well below the diffraction limit of conventional light microscopy (Eisenberg-Bord *et al.*, 2016). Consequently, imaging these sites requires more specialised microscopy methods such as electron microscopy (EM). EM provides a much higher resolution (Dresser, 2001) and much higher magnification (between x10 and x1,000,000) than light microscopy (Goldberg and Fiserova, 2010) which allows for efficient imaging of close contact between organelles. In order to further characterise the morphology of contact sites, electron cryo-tomography (cryo-ET) has been used increasingly. This method allows thin samples to be imaged in three-dimension in a nearly native state to ~4 nm resolution (Tocheva *et al.*, 2010). Importantly, this method was used to investigate mitochondria-ER contacts sites. Analysis with cryo-ET revealed that ER tubules tightly wrap around mitochondria, indicating the important role for these contact sites in mitochondrial division (Friedman *et al.*, 2011; Murley *et al.*, 2013). Furthermore, cryo-ET has also been used to directly visualise tether structures between two organelle membranes *in situ.* In fractionated rat liver

cells, structures with no molecular identification which connect the mitochondrial outer membrane to the ER have been observed (Csordás *et al.*, 2006). Additionally, more advanced EM techniques such as Focused Ion Beam Scanning EM (FIB-SEM) have been employed. FIB-SEM uses a focused ion beam to collect an image whilst simultaneously milling the specimen surface (Cohen *et al.,* 2018). This has been used to visualise contacts between the ER and other organelles, including mitochondria, peroxisomes and the plasma membrane in neurons (Wu *et al.*, 2017). Despite the unparalleled spatial resolution offered by these microscopy techniques, their advantages are offset by the requirement for samples to be fixed. As we know that contact site formation can often be dynamic and transient, a method to visualise contacts in live cells and in real-time is required to fully understand these structures (Cohen *et al.*, 2018). In addition, ultrastructural imaging methods are often time-consuming and required specialised equipment and expertise, rendering them an expensive method which may not be accessible for all research groups (Choudhary and Priyanka, 2017).

To enable dynamic, real-time analysis of contact sites with molecular specificity, the use of genetically encoded fluorescent fusion proteins is often employed (Cohen *et al.*, 2018). When fused to a protein of interest, for example, a protein known to localise to contact sites, the resulting fluorescence can be observed using fluorescence microscopy at the resolution of standard light microscopy. During fluorescence microscopy, the protein of interest is fused to a fluorescent protein, such as green fluorescent protein (GFP) or red fluorescent protein (RFP), which contains a fluorophore. If the fused protein is a contact site protein, this could provide indication of number of contact sites present. Moreover, when this technique is employed in live cell imaging, the dynamic nature of the protein and related contact site can also be assessed.

Similarly, immunofluorescent methods are often utilised. These methods capitalise on the wide range of monoclonal antibodies available which are specific to a protein of interest and can only be conducted in fixed cell samples. Indirect immunofluorescence is most commonly used which allows the localisation and abundance of a protein to be determined and can be applied to assess known contact site proteins. Immunofluorescent methods, generally, are much less laborious and time consuming than fluorescent fusion protein-based

methods as they do not require the complex process of molecular cloning and transformation into cells (Celler *et al.*, 2016), however, their requirement to be carried out in fixed cells limits their application in the study of protein dynamics.

Increasingly, methods optimised for the study of protein-protein interactions have been applied to the study of organelle contact sites. An example of this is the use of proximity ligation assays (PLA), also known as “Duolink®”. This system relies on the targeting of two primary antibodies to two proteins which are hypothesised to be in close proximity. The output of this system is a fluorescent signal which can be visualised by fluorescence microscopy (Gullberg and Andersson, 2010). This system and its use in the study of contact sites is described in detail in Section 3.1.

Another method of this type is bimolecular fluorescence complementation (BiFC). This method has offered a more sophisticated approach to studying contact sites. BiFC consists of a split fluorescent protein technology such as split Venus, dimerisation-dependent GFP and split superfolder GFP. In these systems, two non-fluorescent portions of a fluorescent protein are fused to abundant membrane proteins or known tethering proteins on two interacting organelles. When the two halves of fluorescent protein are brought in close proximity, through contact of the respective organelle membranes, fluorescence is restored and can be used as a measure of organelle contact (Harmon *et al.*, 2017). These systems have allowed for the study of the dynamics of contact site formation in live cells (Alford *et al.*, 2012a) and can also be employed in fixed cells to assess changes in contact sites following alterations in physiological cellular conditions (Cieri *et al.*, 2018). For this reason, these systems have been used extensively in contact site studies and are described in detail in Section 4.1.

Fluorescence resonance energy transfer (FRET) is a similar method to BiFC and is also commonly used in the study of contact sites. FRET is a molecular imaging technique in which a donor fluorophore fused to one protein transfers energy to an acceptor fluorophore fused to another protein. If these proteins are in close proximity (≤10 nm distance), fluorescence will be produced indicating contact between the organelles (Cohen *et al.*, 2018). This can be performed by attaching fluorophores to known membrane proteins on the organelles of interest, meaning that the knowledge of specific tethering proteins is not

required. This method has been previously used to assess mitochondria-ER contact sites (Csordás *et al.*, 2010). Unfortunately, the occurrence of photobleaching and intrinsic autofluorescence of the cells examined can limit the usefulness of FRET. In addition, excitation of the acceptor fluorophore directly has been known to occur in some cases, leading to false-positive results (Xu *et al.*, 1999).

Despite the advances in the creation and optimisation of all of the above methods, they all still have their own respective limitations. A criticism of fluorescence-based studies and imaging in general for the investigation of contact sites is that any observed co-localisation or proximity between organelles is not necessarily indicative of a functional contact site (Cohen *et al.*, 2018). Therefore, these techniques should be combined with additional techniques, such as biochemical methods, to confirm the organelle interaction. Biochemical methods are often employed as a preliminary step to identify interacting proteins implicated in organelle contact sites. Common techniques of this type include the yeast two hybrid system, tandem affinity purification (TAP) and co-immunoprecipitation (coIP) (Rao *et al.*, 2014). Co-IP is most commonly used and requires a whole cell extract where proteins are present in their native form (Rao *et al.*, 2014). A drawback of biochemical methods in general, however, is that creating a cell lysate, as is required in most methods, destroys the environment of the protein. As organelle contact sites are highly organised structures, the creation of a cell lysate could compromise their integrity, making the identification of genuine interactions difficult (Eisenberg-Bord *et al.*, 2016).

1.6 Thesis aims and objectives:

It is clear that the current toolbox for the investigation of organelle contact sites is expanding, however, with our growing knowledge of contact sites, there is a requirement to optimise these methods to allow for the study of more inter-organelle contact sites. As peroxisome-organelle contact sites have only recently been identified, methods to study these sites are lacking.

Despite our advances in the understanding of peroxisome-ER contact sites, many questions are still unanswered. We understand the relevance of this organelle contact in both health and disease, however, the mechanisms underlying its formation and how this is regulated has yet to be uncovered.

Moreover, its physiological function has not been elucidated. In order for us to fully understand this organelle contact we require appropriate tools which are simple, robust and modifiable to enable their application to a range of biological questions. To this end, the main aim of this thesis is to create methods to visualise and quantify the extent of peroxisome-ER contacts using two approaches: a split fluorescent protein reporter system and the proximity ligation assay, Duolink®.

- In the split fluorescent protein reporter system, one half of a split fluorescent protein is targeted to the peroxisome membrane and the other half to the ER membrane. When the two organelles are in close apposition, the fluorescent halves should recombine, indicating contact between the organelles. To achieve this, two BiFC technologies will be used: dimerisation-dependent GFP and split superfolder GFP.
- The second approach is to optimise the proximity ligation assay, Duolink®. This will be achieved by using peroxisome-ER contact site proteins as target proteins for the assay. Additionally, the assay will be conducted using an abundant peroxisomal membrane protein not known to be implicated in contact sites as a target.
- Finally, both of these systems will be used to assess changes in the number of peroxisome-ER contacts following changes in physiological cellular conditions.

It is hoped that the findings presented in this thesis will provide two novel methods to assess this newly discovered contact site and provide indication of the stimuli altering the extent of contact site formation. Ultimately, the systems presented here could be amended for the investigation of other peroxisome-organelle contact sites to further our understanding of the important interplay between organelles.

Chapter 2:

General materials and methods

2.1 Cell culture:

Table 2.1. Cell lines used in this study

Cell line	Description	Origin
COS-7	African green monkey kidney cells	ATCC: CRL-1651
COS-7-GFP-SKL	African green monkey kidney cells stably transfected with a construct encoding for a fusion protein of green fluorescent protein (GFP) carrying a consensus peroxisomal targeting signal 1 (PTS1) of three amino acids (SKL; serine, lysine, leucine). This is sufficient to target GFP to peroxisomes in mammalian cells.	Created from ATCC: CRL-1651 G. Lüers, Univ. of Marburg, Germany (Koch *et al.*, 2004)
HeLa	Human cervical adenocarcinoma epithelial cells.	ATCC: CCL-2

Cell culture maintenance:

COS-7, COS-7-GFP-SKL and HeLa cells were cultured in DMEM (Dulbecco's Modified Eagle Medium) medium, high glucose (4.5 g/l) supplemented with 10% Fetal Bovine Serum (FBS), 100 U/ml penicillin, and 100 µg/ml streptomycin at 37°C with 5% CO_2 and 95% humidity.

All cell lines were routinely cultured in supplemented DMEM medium. The medium was replaced as needed until cells reached confluency. Confluent cells were washed with 1x sterile phosphate-buffered saline (PBS) (pH 7.4) and detached from cell culture dishes using TrypLE Express Enzyme (1x), phenol-

red free (Gibco, Thermo Fisher Scientific). The cells were harvested with supplemented DMEM medium and centrifuged at 1000rpm for 3 minutes at room temperature. The cell pellet was then resuspended in supplemented DMEM medium and plated onto cell culture dishes at the appropriate density.

2.2 DEAE-dextran transfection:

COS-7 and COS-7-GFP-SKL cells were grown on 19 mm glass coverslips in 6-cm-diameter cell culture dishes and incubated overnight at 37°C with 5% CO_2 and 95% humidity. Cells were transfected using diethylaminoethyl (DEAE)-dextran (Sigma-Aldrich). For transfections in a 6-cm-diameter cell culture dish, cells were transfected with 4 µg of DNA when using a single plasmid and 3.3 µg of DNA with transfected with two plasmids simultaneously. Cells were washed once with 1x sterile PBS (pH 7.4) and DEAE-dextran, DMEM with no supplements and DNA were added to cells. Cells were incubated at 37°C with 5% CO_2 and 95% humidity with shaking for 1.5 hours. Supplemented DMEM media containing 0.1% chloroquine was then added to cells for 3 hours to prevent lysosomal degradation of plasmids. Cells were then washed twice with 1x sterile PBS and supplemented DMEM media was added to cells. Cells were incubated overnight at 37°C with 5% CO_2 and 95% humidity.

2.3 TurboFect transfection:

HeLa cells were grown on 19 mm glass coverslips in 6-cm-diameter cell culture dishes and incubated overnight at 37°C with 5% CO_2 and 95% humidity. Cells were transfected with TurboFect (Thermo Fisher Scientific) reagent. For transfections in a 6-cm-diameter cell culture dish, cells were transfected with 4 µg of DNA when using a single plasmid and 3.3 µg of DNA with transfected with two plasmids simultaneously. Cells were washed once with 1x sterile PBS (pH 7.4) and TurboFect, DMEM with no supplements and DNA were added to cells. Cells were incubated at 37°C with 5% CO_2 and 95% humidity for 3 hours. Cells were then washed three times with 1x sterile PBS and supplemented DMEM media was added to cells. Cells were incubated overnight at 37°C with 5% CO_2 and 95% humidity.

2.4 Immunofluorescence:

Cells grown on 19 mm glass coverslips washed with 1x PBS and fixed in 4% paraformaldehyde in PBS (pH 7.4) for 20 minutes at room temperature. Cells were then washed three times for 5 minutes with PBS. Cellular membranes were then permeabilised using 0.2% Triton X-100 for 10 minutes at room temperature. Cells were washed in PBS three times for 5 minutes and then blocked with 1% bovine serum albumin (BSA) for 10 minutes. Samples were then incubated with primary antibodies diluted to the appropriate dilutions in 1x PBS for 1 hour at room temperature. After washing three times for 5 minutes in PBS, samples were incubated with fluorescently labelled secondary antibodies for 1 hour at room temperature. To prepare the slides, coverslips were washed once in Milli-Q water and mounted in Mowiol 4-88 containing n-propyl gallate as an anti-fading reagent (3:1 mowiol with n-propyl gallate).

2.5 Microscopy and image processing:

Cell imaging was performed using an IX81 microscope (Olympus) equipped with an UPlanSApo 100×/1.40 oil objective (Olympus) and a CoolSNAP HQ2 CCD camera. Digital images were taken and processed using VisiView software (Visitron Systems). Images were adjusted for contrast and brightness using MetaMorph 7 (Molecular Devices).

2.6 Quantification of fluorescent signals:

Quantification of fluorescent signals was performed using ImageJ software. Fluorescent signals from a minimum of 30 cells were quantified from each experimental repeat. In all cases, the cellular membrane was not defined, therefore, the number of fluorescent signals in close range to each visible nucleus was quantified. A custom macro was created for this purpose:

- Outline the cell of interest using the freeform selection tool.
- Edit -> Options -> Colors - Foreground white, background black.
- Edit -> Clear Outside.
- Image -> Type -> 8-bit.
- Process -> Filters -> Gaussian Blur – Sigma 1.
- Process -> Subtract Background – Rolling ball radius 20 pixels.

- Image -> Adjust -> Threshold – Manually threshold the image.
- Process -> Binary -> Convert to Mask.
- Process -> Binary -> Erode.
- Process -> Binary -> Watershed.
- Analyze -> Analyze Particles – Size 10-200, Circularity 0.10-1.00, Show Nothing.

2.7 Statistical analysis:

All statistical analysis was performed using GraphPad Prism Version 5 for Windows (GraphPad Software, La Jolla California USA). A two-tailed, unpaired *t* test was used to determine statistical differences against the indicated group (*, $P < 0.05$; **, $P < 0.01$; ***, $P < 0.001$).

Table 2.2. Plasmids used in this study

Plasmid	Source
Myc-VAPB	C. Miller, King's College London, London, UK
FLAG-ACBD5	J. Costello, Univ. of Exeter, UK
GFP-SKL	S. Grille, Univ. of Exeter, UK
Untargeted GFP1-10	Gift from T. Cali, Universita degli studi Di Padova, Italy
Kate-β11	Gift from T. Cali, Universita degli studi Di Padova, Italy

Table 2.3. Plasmids generated in this study

Plasmid	Enzymes	Vector
spGFP1-10-Pex26-ALDP	HindIII/XhoI	pcDNA3.1 (+)
spGFP1-10	HindIII/XhoI	pcDNA3.1 (+)
spGFP11x7	HindIII/XhoI	pcDNA3.1 (+)

Table 2.4. Primary and secondary antibodies used in this study

Antibodies	Type	Dilution	Source
ACBD5	pcRb	1:100	Sigma-Aldrich
VAPB	mcMs	1:200	Proteintech
PEX14	Rb	1:1400	D. Crane, Griffith University, Brisbane, Australia
Myc	pcRb	1:200	Abcam
FLAG	mcMs	1:500	Sigma-Aldrich
Alexa Fluor 488 IgG	dk anti-rb	1:500	Molecular Probes
Alexa Fluor 488 IgG	dk anti-ms	1:400	Molecular Probes
Alexa Fluor 594 IgG	dk anti-rb	1:1000	Molecular Probes
Alexa Fluor 594 IgG	dk anti-ms	1:1000	Molecular Probes

Chapter 3:

Visualising peroxisome-endoplasmic reticulum contacts using the proximity ligation assay Duolink®.

3.1 Introduction:

Cellular processes are governed by the dynamic interplay between proteins (Söderberg *et al.*, 2006). The activity of such proteins is determined by their secondary modifications and their interacting partners (Söderberg *et al.*, 2008). It is of growing importance to develop sensitive and specific techniques to visualise these endogenous proteins interactions to uncover their localisation and function. To this end, progress has been made in the development of biochemical methods such as co-immunoprecipitation (coIP) or fluorescence-based methods such as bimolecular fluorescence complementation (BiFC) or fluorescence resonance energy transfer (FRET) (Bellucci *et al.*, 2014). Though well-established, biochemical methods often fail to provide understanding of the cellular context of proteins (Bellucci *et al.*, 2014) and many fluorescence-based methods are often associated with low sensitivity and brightness (Kerppola, 2006).

To overcome these limitations, the proximity ligation assay (PLA) was developed in 2002 by Fredriksson and colleagues (Fredriksson *et al.*, 2002). This assay was first developed to allow *in vitro* detection of proteins. The first generation of PLA consisted of DNA aptamers, which are oligonucleotides specific to a target protein. When a pair of these aptamers binds the target protein, their free ends are brought in close proximity. This allows them to hybridise to a subsequently added connector oligonucleotide which allows ligation of the ends to take place. The ligation products are then replicated by nucleic acid amplification through polymerase chain reaction (PCR). The PCR products can then be detected and quantified which is indicative of the number of target protein molecules present in a sample (Fredriksson *et al.*, 2002). This assay formed the basis of the *in situ* PLA which was developed by the same group in 2006 (Söderberg *et al.*, 2006). This adaptation allows individual pairs of interacting proteins to be visualised and quantified in cell lines and fixed clinical samples using an antibody-based approach. This assay was commercialised in 2007 under the name of “Duolink®” by Olink Bioscience, a biotechnology company founded by members of the group who pioneered PLA technology (*Olink bioscience* | *AntibodyChain*, 2009). Since 2015, Duolink® is now commercially available through Sigma-Aldrich.

Duolink® relies on the targeting of specific primary antibodies raised in two different species, such as mouse or rabbit, to two proteins of interest (Gullberg and Andersson, 2010). This is followed by the addition of proximity probes, which are oligonucleotides attached to secondary antibodies which are complementary to the primary antibodies. When the proteins of interest are in close proximity (<40 nm), this brings the oligonucleotides on the proximity probes close together so they can ligate with added “connector oligonucleotides” to form a circular DNA strand. This acts as a template for rolling circle amplification (RCA). Following RCA, the resulting DNA product, still covalently attached to the proximity probes, is detected through the addition of fluorescently-labelled probes. This allows single-molecule protein interaction events to be represented by discrete fluorescent signals which can be visualised and quantified with standard fluorescent microscopy methods (Söderberg *et al.*, 2006).

The use of this assay for the detection of protein-protein interactions has increased in recent years. This is, in part, due to the sensitivity and specificity of the method, allowing it to be used to detect single-molecule, and even transient, protein interactions (Söderberg *et al.*, 2006). In addition, the ability to apply this assay to fixed cells and tissue samples offers significant advantage over other standardised methods for protein interaction studies, allowing endogenous interactions to be detected *in situ* (Bellucci *et al.*, 2014). It is known that most organelles interact through inter-organellar tethering mediated by interacting proteins in sites called membrane contact sites (MCS) (Eisenberg-Bord *et al.*, 2016). Although these interactions are vital for normal cellular function, the mechanisms underlying the formation and function of MCSs remain to be fully elucidated. The lack of knowledge in this field is, perhaps, caused by a lack of appropriate tools (Eisenberg-Bord *et al.*, 2016). Most assays to study these organelle interactions rely on over-expression of proteins to study contact sites *in situ,* which may alter the size or nature of MCSs or biochemical techniques which require denaturation of proteins, disrupting their native environment (Eisenberg-Bord *et al.*, 2016). For these reasons, assays such as Duolink® have superseded previous techniques for further characterising the nature and role of MCSs. Perhaps the best studied MCSs are those between the mitochondria and the ER. These MCSs, known as mitochondria-associated ER

membranes (MAM), are essential for lipid and calcium homeostasis (Paillusson *et al.*, 2016). The Duolink® assay has recently been optimised to study these interactions.

As Duolink® is suitable for assessing protein interactions of less than 40 nm (Gullberg and Andersson, 2010), it was thought that this assay would be ideal for the study of MCSs as interacting proteins at MCSs are usually 10-40 nm apart (Eisenberg-Bord *et al.*, 2016). Therefore, it was hypothesised that labelling a single membrane protein on each interacting organelle with a complementary primary antibody and followed by the Duolink® reagents, would allow events where the respective organelles were in close proximity to be visualised with a fluorescent readout (Tubbs *et al.*, 2014). The first use of Duolink® in this way utilised putative interaction partners ER-resident protein VAPB and outer mitochondrial membrane protein, protein tyrosine phosphatase-interacting protein 51 (PTPIP51) as target proteins (De Vos *et al.*, 2012). This study used Duolink® as one of a few techniques to demonstrate that these two proteins interact to tether the respective organelles to regulate calcium homeostasis. This was shown by the formation of fluorescent signals after labelling both VAPB and PTPIP51 with complementary primary antibodies in fixed mammalian cells and performing the Duolink® assay (De Vos *et al.*, 2012). Duolink® has subsequently been used in many studies assessing mitochondria-ER associations, some of which used the outer mitochondrial membrane protein voltage-dependent anion channel (VDAC) and ER protein inositol 1,4,5-triphosphate receptor (IP3R) as target proteins (Hedskog *et al.*, 2013; Tubbs *et al.*, 2014). These proteins are enriched at MAMs and are known to physically interact to facilitate Ca^{2+} transfer from the ER to mitochondria (Szabadkai *et al.*, 2006). The use of Duolink® in these studies has enabled the identification of many roles in which this organelle association is involved. For example, in the pathogenesis of Alzheimer's disease (Hedskog *et al.*, 2013), amyotrophic lateral sclerosis and frontotemporal dementia (ALS/FTD) (Stoica *et al.*, 2016), and also in hepatic insulin action and resistance (Tubbs *et al.*, 2014).

Following from the success of the use of Duolink® in investigating proximity between mitochondria and the ER, it was thought that this assay could also be applicable to the study of peroxisome-ER interactions (Fig 3.1). Little is known about the peroxisome-ER contact site size, however, electron microscopy data

suggests the size of these contact sites to be within the range that can be detected using the Duolink® assay (Costello *et al.*, 2017a). In the case of peroxisome-ER contact sites, the only known tethering proteins are peroxisomal membrane proteins ACBD4 and ACBD5 and ER proteins VAPA and VAPB (Costello *et al.*, 2017a; Costello *et al.*, 2017b; Hua *et al.*, 2017). It was, therefore, hypothesised that in events where peroxisomes and the ER were in close proximity, labelling ACBD4/5 and VAPA/B with complementary primary antibodies, followed by the Duolink® reagents, would allow ligation of the oligonucleotides on the proximity probes and RCA to take place. This would ultimately result in the formation of a fluorescent signal, indicating proximity between the two organelles (Fig 3.1). This assay would, again, offer the advantage of enabling visualisation of endogenous interactions within their cellular context. In addition, this assay could also be used to assess the effect of altering physiological cellular conditions on the integrity and number of peroxisome-ER contacts, shedding light on processes which are currently not well-understood.

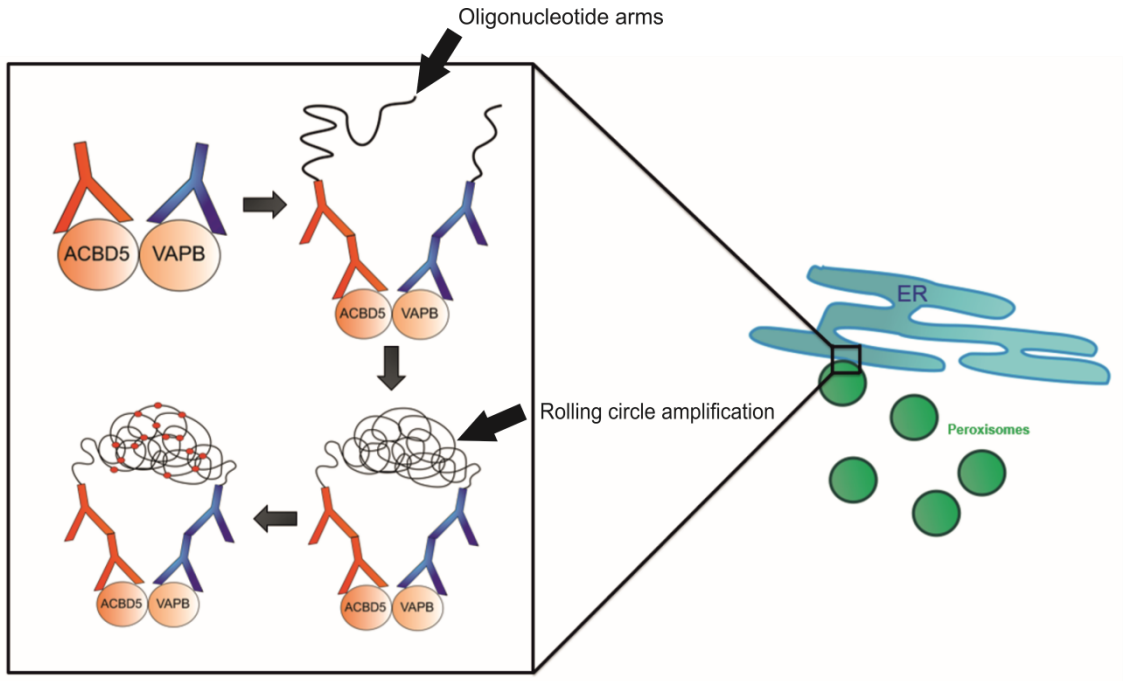

Fig. 3.1. Schematic illustration of Duolink® technology used to visualise proximity between peroxisomes and the ER using ACBD5 and VAPB as target proteins.

3.2 Materials and methods:

3.2.1. Duolink® assay:

COS-7 or COS-7-GFP-SKL cells were seeded onto 3.5-cm-diameter glass bottom dishes (Cellview; Greiner BioOne) and incubated overnight at 37°C with 5% CO_2 and 95% humidity. In some assays, cells were transfected after 24 hours incubation using DEAE-dextran, following the same protocol as described in Section 2.2. In all assays, 48 hours after seeding, cells were fixed in 4% paraformaldehyde in PBS (pH 7.4) for 20 minutes at room temperature. Cellular membranes were permeabilised with 0.2% Triton X-100 for 10 minutes at room temperature and washed three times for 5 minutes in 1x PBS. The proximity ligation assay (PLA), Duolink® (Sigma-Aldrich), was then performed.

Samples were blocked by adding Duolink® blocking solution and incubating for 30 minutes at 37°C in a humidity chamber. The blocking solution was then removed and samples were incubated with primary antibodies diluted to the appropriate dilutions in antibody diluent supplied with the kit for 1 hour in a humidity chamber. Primary antibodies used are listed in Table 2.4. Samples were then washed twice for 5 minutes in 1x wash buffer A at room temperature. Samples were incubated with PLA probes (proximity probes) supplied in the kit, diluted 1:5 in antibody diluent, for 1 hour at 37°C in a humidity chamber. Samples were washed twice for 5 minutes in 1x wash buffer A at room temperature. PLA probes were ligated by incubating with ligase enzyme diluted 1:40 in ligation buffer supplied with the kit for 30 minutes at 37°C in a humidity chamber. Samples were again washed in 1x wash buffer A at room temperature before incubation with polymerase enzyme diluted 1:80 in amplification buffer supplied with the kit for 100 minutes at 37°C in a humidity chamber. Following incubation, samples were washed twice for 10 minutes in 1x wash buffer B at room temperature and then washed once in 0.01x wash buffer B for 1 minute. 19 mm coverslips were then mounted onto culture dishes using Mowiol 4-88 (3:1 mowiol with n-propyl gallate) prior to imaging. Slides were then analysed with fluorescence microscopy as described in Section 2.5. Quantification of the fluorescent signals produced was performed as described in Section 2.6.

3.3 Results:

3.3.1. ACBD5/VAPB-mediated peroxisome-ER proximity can be visualised using the proximity ligation assay, Duolink®:

To optimise the Duolink® assay to visualise endogenous proximity between peroxisomes and the ER, the peroxisomal tethering protein ACBD5 and the ER tethering protein VAPB were used as target proteins for the assay. The primary antibody used against ACBD5 has been validated in COS-7 cells in a previous study by our group (Costello *et al.*, 2017a) and the primary antibody against VAPB was validated by others in COS-7 cells to show specific binding to VAPB at the ER (Zhao *et al.*, 2018).

COS-7 cells stably expressing peroxisome-targeted GFP (GFP-SKL) (referred to as COS-7-GFP-SKL cells) were grown on glass-bottom dishes and fixed. This cell line was chosen to enable consistent labelling of peroxisomes to allow for assessment of whether the fluorescent signals produced from the Duolink® assay would co-localise with peroxisomes, confirming specificity of the assay. ACBD5 and VAPB were labelled with rabbit anti-ACBD5 and mouse anti-VAPB primary antibodies respectively. The Duolink® assay was then performed using mouse and rabbit secondary antibodies (proximity probes) complementary to the primary antibodies used. This resulted in the formation of red fluorescent signals, some of which are found in close proximity to peroxisomes. Controls were also performed to confirm specificity of the assay where the Duolink® assay was performed on fixed COS-7 cells but only one of each primary antibody or no primary antibody was used (Fig. 3.2).

After performing the Duolink® assay, the slides were analysed with fluorescence microscopy and the number of fluorescent signals per cell (nucleus) were quantified in 30 cells. An average of 7.28 ± 1.20 fluorescent signals were formed per cell (nucleus). In the cases of the controls, cells had none or very few fluorescent signals. The average number of fluorescent signals for the anti-ACBD5 antibody alone was 0.4 ± 0.11. The average number of fluorescent signals produced when the anti-VAPB antibody was used alone was 0.37 ± 0.11 and when no primary antibody was used 0.57 ± 0.16 fluorescent signals were produced (Fig. 3.5).

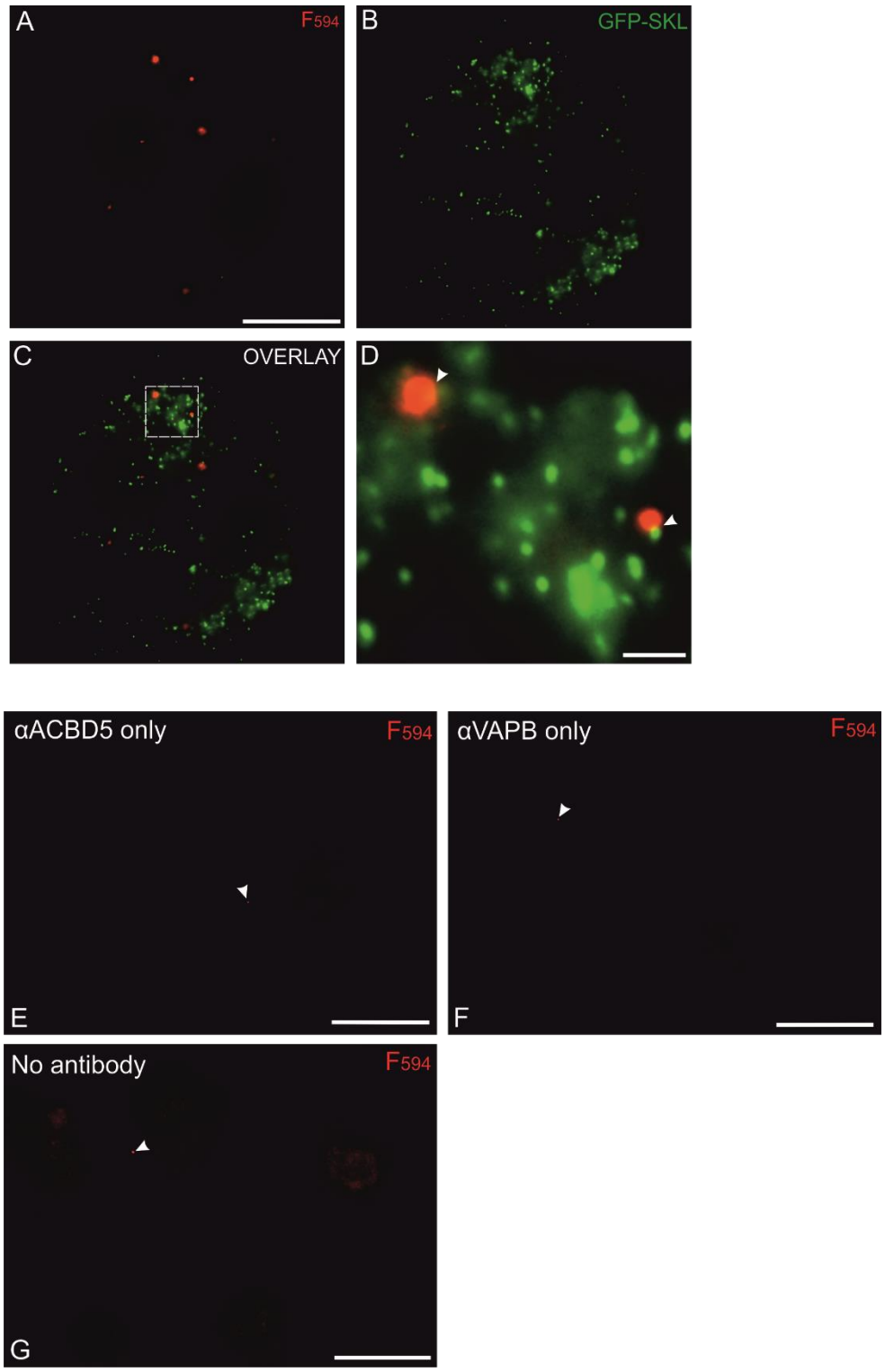

Fig. 3.2. **Duolink® allows proximity between peroxisomes and the ER to be visualised by the formation of fluorescent signals.** (A) Proximity between peroxisomes and the ER depicted as red fluorescent signals. (B) Peroxisomes labelled with GFP. (C) Overlay of red fluorescent signals from the Duolink® assay with labelled peroxisomes. (D) Zoom of (C), arrows indicate close

proximity of fluorescent signals with peroxisomes. (E-G) Negative controls using the Duolink® assay with anti-ACBD5 or anti-VAPB primary antibodies alone or no antibody. Arrows indicate a single fluorescent signal formed. Scale bars (main): 20µm (zoom): 2µm.

3.3.2. An increase in peroxisome-ER association can be visualised using Duolink®:

As indicated by previously published work from our group, overexpression of ACBD5 and VAPB increases contact between peroxisomes and the ER (Costello *et al.*, 2017a). Therefore, it was hypothesised that the increase in association between the two organelles following overexpression of ACBD5 and VAPB would be visible by an increase in the number of fluorescent signals produced from the Duolink® assay. COS-7 cells were first transfected with a GFP-SKL plasmid to label peroxisomes. The cells were also transfected with Myc-tagged VAPB and FLAG-tagged ACBD5. Following fixation of the transfected cells the Duolink® assay was performed. First, the Myc and FLAG epitope tags were probed with rabbit anti-Myc and mouse anti-FLAG primary antibodies and the Duolink® assay was performed (Fig. 3.3). The Duolink® assay was then performed in the same way following overexpression of the tagged proteins but using primary antibodies against the ACBD5 and VAPB proteins (Fig. 3.4).

Following analysis of the resulting slides it was found that overexpression of the tethering proteins dramatically increased the number of fluorescent signals produced using the Duolink® assay. When antibodies against the Myc and FLAG epitope tags were used, an average of 72.01 ± 5.52 fluorescent signals were formed per cell (nucleus) and when antibodies against the tethering proteins were used the number of fluorescent signals produced was 60.05 ± 9.12 per cell (nucleus). Controls were also performed using the anti-Myc or anti-FLAG primary antibodies individually on transfected cells to confirm specificity of the use of these antibodies with the Duolink® assay. In both cases, again, most cells had none or very few fluorescent signals. When the anti-Myc primary antibody was used alone an average of 0.1 ± 0.07 fluorescent signals were produced per cell (nucleus) and 0.37 ± 0.11 fluorescent signals were produced per cell (nucleus) when the anti-FLAG primary antibody was used alone. (Fig. 3.5).

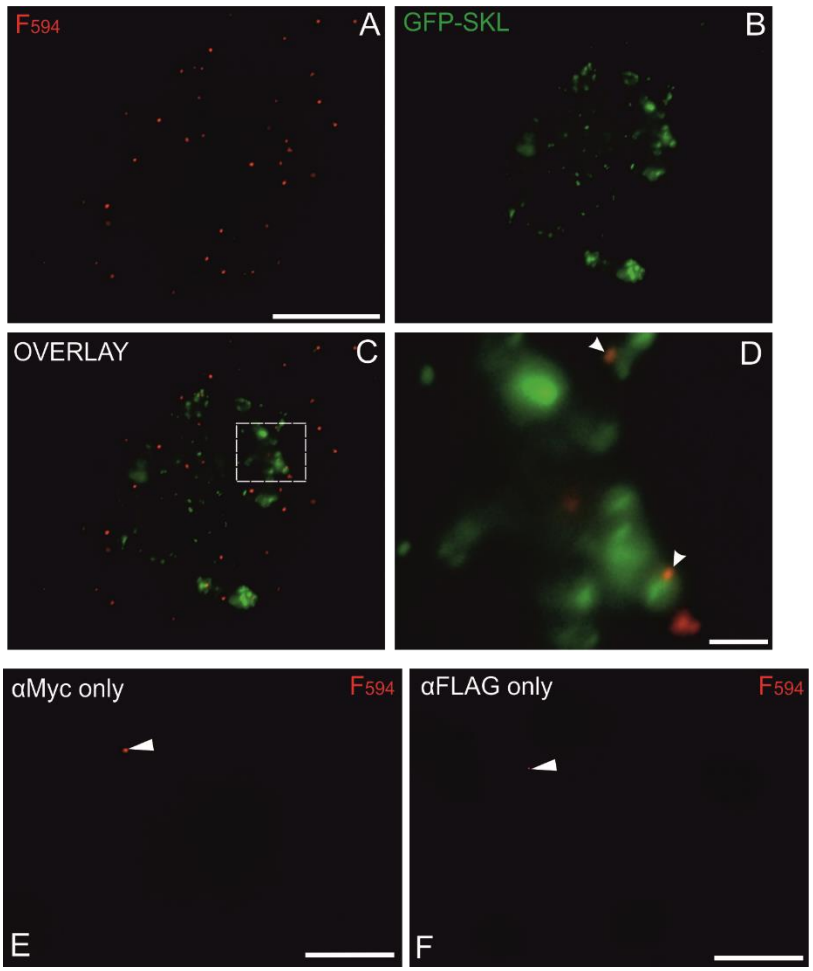

Fig. 3.3. **An increase in peroxisome-ER associations can be visualised by an increase in fluorescent signals formed from the Duolink® assay using antibodies against epitope tags.** (A) COS-7 cells transfected with GFP-SKL, Myc-VAPB and FLAG-ACBD5. The Duolink® assay was performed using the Myc and FLAG epitope tags as target proteins. Proximity between peroxisomes and the ER is depicted as red fluorescent signals. (B) Peroxisomes labelled with GFP-SKL. (C) Overlay of red fluorescent signals from the Duolink® assay with labelled peroxisomes. (D) Zoom of (C), arrows indicate close proximity of fluorescent signals with peroxisomes. (E-F) Negative controls using the Duolink® assay with anti-Myc or anti-FLAG primary antibodies alone. Arrows indicate a single fluorescent signal formed. Scale bars (main): 20µm (zoom): 2µm.

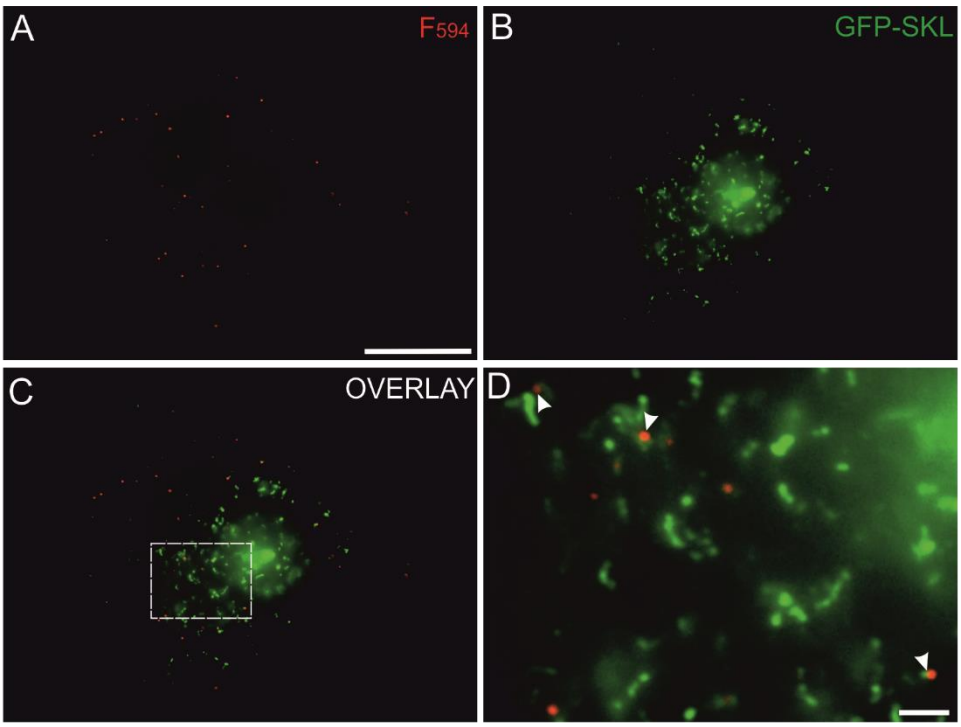

Fig. 3.4. **An increase in peroxisome-ER associations can be visualised by an increase in fluorescent signals formed from the Duolink® assay using antibodies against the tethering proteins.** (A) COS-7 cells transfected with GFP-SKL, Myc-VAPB and FLAG-ACBD5. The Duolink® assay was performed using ACBD5 and VAPB as target proteins. Proximity between peroxisomes and the ER is depicted as red fluorescent signals. (B) Peroxisomes labelled with GFP-SKL. (C) Overlay of red fluorescent signals from the Duolink® assay with labelled peroxisomes. (D) Zoom of (C), arrows indicate close proximity of fluorescent signals with peroxisomes. Scale bars (main): 20µm (zoom): 2µm.

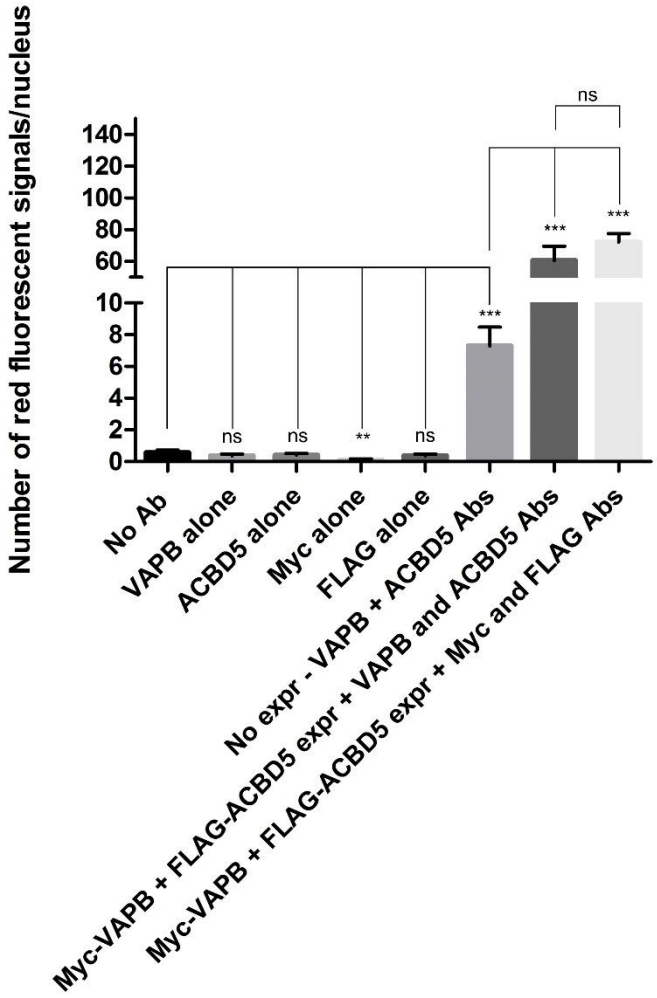

Fig. 3.5. Quantitative analysis of the number of red fluorescent signals produced per cell (nucleus) following the use of the Duolink® assay to measure endogenous proximity between peroxisomes and the ER and proximity following overexpression of ACBD5 and VAPB. The number of red fluorescent signals produced per cell (nucleus) following the use of each primary antibody alone is shown. Data are presented as mean ± standard error of the mean (SEM). Data were analysed with a two-tailed, unpaired *t* test (ns, not significant, **, P < 0.01; ***, P < 0.001). n = 30 cells. Data shown are the result of three independent experiments.

3.3.3. Duolink® can be used to visualise proximity between peroxisomes and the ER using target proteins not known to be involved in inter-organelle tethering:

Following the success of using ACBD5 and VAPB as target proteins for the Duolink® assay, it was decided to assess whether other ubiquitous peroxisomal membrane proteins can be used as target proteins for the assay. VAPB was still

used as a target for the ER membrane, however, in this case, the peroxisomal membrane protein PEX14 was used as the peroxisomal target. PEX14 is a key component of the peroxisomal import machinery, acting as a docking factor for the PTS1 receptor, PEX5 (Fransen *et al.,* 1998). The PEX14 antibody used was made and validated in a previous study (Nguyen *et al.*, 2006).

COS-7-GFP-SKL cells were grown and fixed and the Duolink® assay was performed as described in Section 3.2.1 but the peroxisomal membrane was targeted with rabbit anti-PEX14 primary antibody and the ER membrane with mouse anti-VAPB primary antibody as previously. Controls were also performed using the anti-PEX14 or anti-VAPB antibody individually (Fig. 3.6). Analysis of the resulting slides showed that an average of 14.18 ± 1.81 fluorescent signals were formed per cell (nucleus) when the anti-PEX14 and anti-VAPB antibodies were used together. This is significantly higher than the number of fluorescent signals produced when ACBD5 and VAPB were used as target proteins ($P \leq 0.001$). When the anti-VAPB primary antibody was used alone, an average of 0.37 ± 0.11 fluorescent signals were formed per cell (nucleus) and when the anti-PEX14 primary antibody was used alone, an average of 0.57 ± 0.12 fluorescent signals were formed per cell (nucleus) (Fig. 3.6).

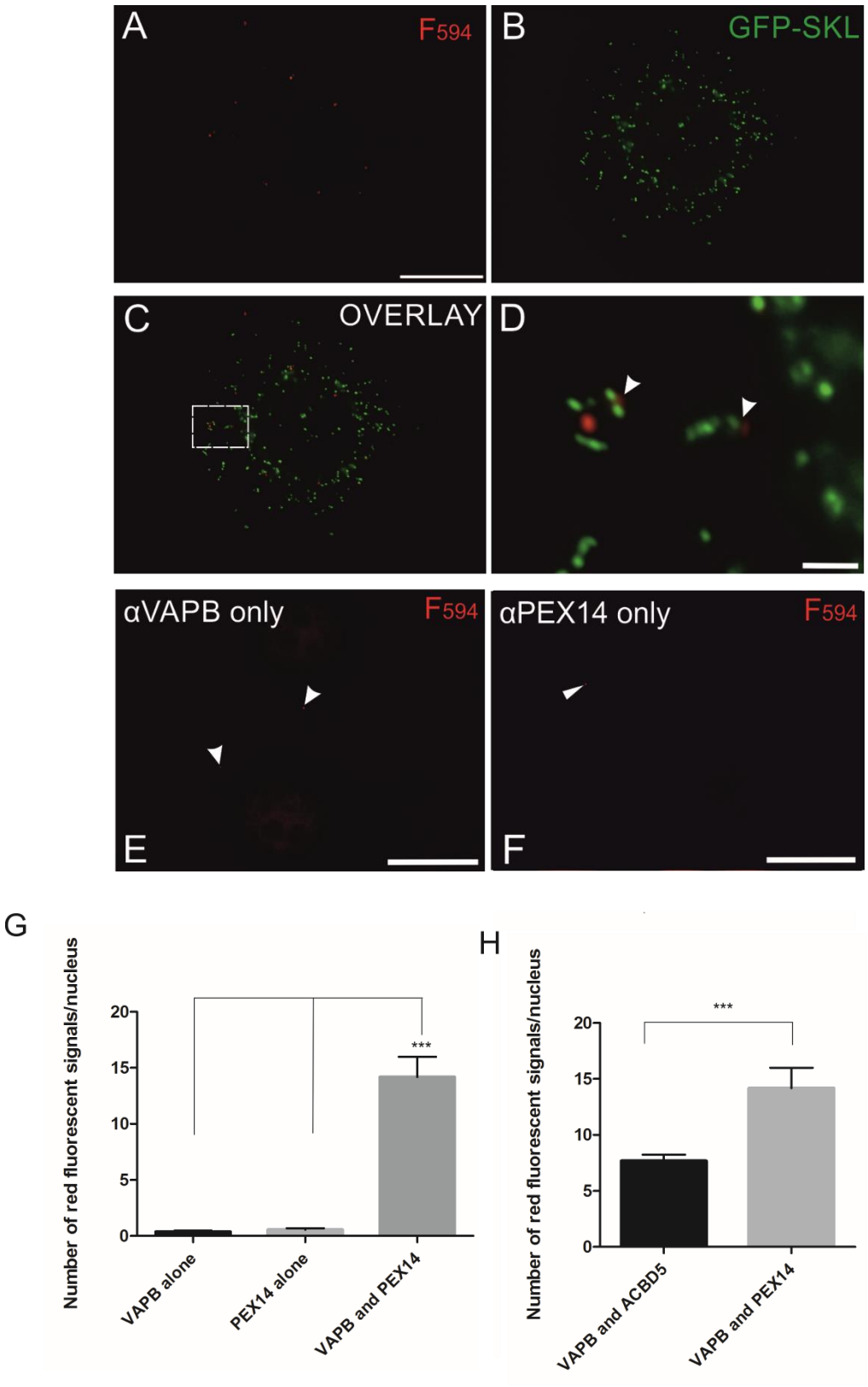

Fig. 3.6. – **Proximity between peroxisomes and the ER can be visualised by Duolink® using PEX14 and VAPB as targets.** (A) Proximity between peroxisomes and the ER depicted as red fluorescent signals. (B) Peroxisomes labelled with GFP-SKL. (C) Overlay of red fluorescent signals from the Duolink® assay with labelled peroxisomes. (D) Zoom of (C), arrows indicate close

proximity of fluorescent signals with peroxisomes. (E-F) Negative control using the Duolink® assay with anti-VAPB or anti-PEX14 primary antibody alone. Arrows indicate fluorescent signals formed. Scale bars (main): 20µm (zoom): 2µm. (G) Quantitative analysis of the number of red fluorescent signals produced following use of anti-VAPB and anti-PEX14 antibodies as targets. The number of red fluorescent signals produced following the use of each primary antibody alone is also shown (H) A quantitative comparison of the number of fluorescent signals produced using the Duolink® assay to assess peroxisome-ER interactions using either VAPB and ACBD5 or VAPB and PEX14 as targets. Data are presented as mean ± SEM. Data were analysed with a two-tailed, unpaired *t* test (***, $P < 0.001$). n = 30 cells. Data shown are the result of three independent experiments.

3.4 Discussion:

It is now recognised that cellular organelles cooperate extensively in order to carry out their essential functions. However, our understanding of these sites, thus far, has been hampered by a lack of effective tools. The growing understanding of peroxisome-organelle contact sites and the relevance of these sites in health and disease, has led to a further push to develop robust and reliable methods to enable their study. The results presented here show that the *in situ* PLA, Duolink®, is an effective method to visualise and quantify proximity between these organelles. This study is, to date, the first to utilise this method to visualise peroxisome-ER contact sites in mammalian cells.

Employing Duolink® for the study of inter-organelle contact sites raises several significant advantages. Primarily, Duolink® is an incredibly simple tool which does not require any specialist expertise, unlike other techniques such as EM. Any laboratory group which frequently performs immunofluorescence experiments will be capable to carry out the Duolink® assay with their existing knowledge and equipment. The only specialised equipment required for the assay is a heat transfer block or incubator which can be heated to 37°C to enable a few of the steps in the assay to be carried out efficiently. However, both of these are standard equipment in most laboratories, particularly if Duolink® is performed on fixed cell samples as maintenance of the cell lines used will require an incubator. Additionally, unlike many other commonly used techniques to study protein interactions, Duolink® (when used to monitor endogenous protein interactions) does not require any molecular cloning, which can be complicated and time-consuming.

One of the greatest strengths of the Duolink® assay is its unparalleled sensitivity and brightness. Weak, or even transient, single molecule interaction events are labelled by one RCA product which is visible as a robust and bright signal due to the exponential nature of DNA amplification. This allows high visibility of the signals over any background fluorescence in a fluorescence microscope. Additionally, the sensitivity can be increased by altering the amplification conditions, for example, by increasing incubation time for amplification (Weibrecht *et al.*, 2010). Moreover, since the binding of two different primary antibodies is required for a signal to be produced, the risk of unspecific binding events is significantly minimised (Leuchowius *et al.*, 2009).

As Duolink® is an *in situ* assay, it also hosts the advantage of allowing protein interaction events to be monitored within their native cellular environment, avoiding the need for cell lysis, as is required for many biochemical assays and also avoids the occurrence of artifacts caused by protein overexpression or ectopic expression (Söderberg *et al.*, 2006). As protein expression is not required, this also means that the assay can be carried out in fixed clinical samples, raising a significant advantage over many other methods used to study protein interactions such as FRET and BiFC (Leuchowius *et al.*, 2009).

The results presented in this study show that Duolink® is an effective method to study peroxisome-ER associations. The use of Duolink® in this context led to the formation of discrete fluorescent signals in areas where the target proteins, ACBD5 and VAPB were in close proximity (Fig. 3.2). These could be easily visualised and quantified using fluorescence microscopy providing an indication of the frequency of contacts between peroxisomes and the ER. In addition, the fluorescent signals produced were found in close proximity to peroxisomes, suggesting that these signals indicate peroxisomal interactions (Fig. 3.2). An increase in the number of sites of contact between peroxisomes and the ER, following overexpression of ACBD5 and VAPB was shown by an increase in the number of fluorescent signals produced (Fig. 3.3, Fig. 3.4). When using antibodies against the epitope tags on the expressed proteins, the number of fluorescent signals increased 10-fold compared to no protein expression ($P \leq 0.001$) (Fig. 3.5). Using antibodies against ACBD5 and VAPB following overexpression showed about an 8.5-fold increase compared to no protein expression ($P \leq 0.001$) (Fig. 3.5). This result is consistent with previously reported EM data showing that the number of peroxisome-ER contacts increases when the tethering proteins are overexpressed (Costello *et al.*, 2017a). This result is also comparable to data obtained in a similar study investigating mitochondria-ER associations when a protein known to increase these associations was overexpressed (Tubbs *et al.*, 2014). Slightly less fluorescent signals (~10 per nucleus) were produced on average when using antibodies against the tethering proteins compared to using antibodies against the epitope tags following overexpression (Fig. 3.5). Although non-significant, the discrepancy between these results is interesting. It can be assumed that this difference is because the antibodies against the epitope tags are more specific,

especially considering that these antibodies are more widely used and are better established than those against the tethering proteins, therefore, they may label their target proteins more efficiently. It is also possible that the epitope tags may be more accessible than the tethering proteins in the contact site.

When each of the antibodies was used individually with the Duolink® system, or no antibody was used at all, none or very few signals were present in cells (Fig 3.5). This has also been observed through using this system to investigate mitochondria-ER interactions (Gomez-Suaga *et al.*, 2017). It is not specifically known why this occurs, however, it is possible that this could be caused by non-specific association of the added proximity probes resulting in RCA and a fluorescent product.

It was also shown in this study that proximity between peroxisomes and the ER can also be assessed by using proteins which are not known to be involved in contact sites as target proteins. In this case, the abundant peroxisomal membrane protein PEX14 was used. The number of fluorescent signals produced using PEX14 as a target protein was approximately double the number using ACBD5 as a target protein with VAPB ($P \leq 0.001$) (Fig. 3.6). PEX14 has never been reported to physically interact with VAPB, which suggests that Duolink® is capable of reporting physical proximity of proteins, as well as protein interactions. So as long as the target proteins are within a distance of ≤40 nm, a fluorescent signal should be produced using the Duolink® system. This finding can be used to our advantage as this means that we are now capable of using a variety of abundant organelle membrane proteins to study organelle interactions, provided that 1) the chosen membrane proteins are localised at the interface at which the two organelles interact; 2) they reside within a distance of ≤40 nm when the two organelles interact; and 3) specific antibodies against the proteins are available. Using these proteins as target proteins is advantageous as will enable future studies to be conducted in which the known tethering proteins are silenced or knocked out using genome editing strategies. This will aid in uncovering the physiological roles of tethering proteins through observing the effect of their absence. Moreover, this will also enable patient cell conditions to be emulated, for example, the effect of the lack of function of ACBD5 could be observed. This would obviously not be possible if the assay relied on targeting the tethering proteins of interest. In addition, this

also means that previous knowledge of the tethering proteins is not necessary in order to study organelle interactions with this system.

Despite the clear advantages of this finding, it also means that results using this assay should be analysed cautiously. The formation of fluorescent signals using the Duolink® assay may solely indicate proximity between the two target proteins, not a genuine interaction. Therefore, this system should not be used exclusively to test for an interaction between two putative interacting partners, instead, it should be combined with other methods to confirm a genuine interaction.

Although Duolink® is a simple and effective system to study organelle interactions, it does harbour some limitations. The main drawback of Duolink® is the cost. The cost of the entire Duolink® starter kit from Sigma-Aldrich is over £600 for 30 reactions (as of September 2018) (*Duolink® PLA Technology - Protein Interaction | Sigma-Aldrich*, 2017). This, combined with the high cost of primary antibodies also required for the assay, renders Duolink® a very expensive method which may not be feasible for all laboratory groups. Despite this, it is possible to make some of the reagents required for the assay in-house, such as the wash buffers and the recipes for these have been published (Mendez and Banerjee, 2017). Sigma-Aldrich also sell a PLA “Probemaker” kit which allows the user to create their own PLA probes using antibodies of their choice (*Duolink® PLA Technology - Protein Interaction | Sigma-Aldrich*, 2017). Employing both of these alternatives could help to significantly reduce the cost of the assay long-term. Another limitation of Duolink® is that the samples need to be fixed, similarly to other immunofluorescence methods. This means that the dynamic nature of contact site formation cannot be assessed.

Despite the ease of use of the Duolink® system, it should be noted that there are many steps required for the assay. If these are all carried out correctly, at the recommended temperatures and times, the assay should produce reliable results. However, if this is not the case, it will affect the results obtained. The number of incubation steps and wash steps required for this assay also increases the risk of losing cells at each step, however, the assay can also be performed in a 96-well plate format allowing several reactions to be performed simultaneously to maintain a high throughput (Leuchowius *et al.*, 2009). The efficacy of the Duolink® assay is also dependent on the availability of

appropriate antibodies, in many cases, well-established antibodies against the target proteins may not be available. Moreover, Duolink® requires antibodies from two different species to be used, in the case of this study, mouse and rabbit antibodies were required, but other species combinations are offered with the Duolink® starter kits. In some cases, it may not be possible to obtain the required antibodies from the two different species specified in the starter kits, however, this could be rectified by customising complementary PLA probes. As demonstrated in this study, it may also be possible to use other abundant organelle membrane proteins as target proteins if the desired antibodies are not available.

An interesting observation in this study was that the number of fluorescent signals produced when using the Duolink® assay to study endogenous peroxisome-ER interactions (with no protein expression and ACBD5 and VAPB primary antibodies) was much lower than the number of contact sites observed between the organelles using EM. In EM, it has been observed that approximately 65-70% of peroxisomes in COS-7 cells are in contact with the ER at a given time (Costello *et al.*, 2017a), however, using the Duolink® assay, an average of just 7 fluorescent signals are formed under the same conditions. It can be seen in Figure 3.2 that the average number of fluorescent signals is not close to this percentage considering the number of peroxisomes in the cell. This result was obtained in every cell and every repeat of the experiment. It has been assumed in the past, that the number of fluorescent signals produced in this assay should be proportional to the number of protein associations in the cell (Mocanu *et al.*, 2011), however, this result suggests that this is not the case. Moreover, similar discrepancies have also been reported in another study (Leuchowius *et al.*, 2009). This prompted a full comparative analysis of the Duolink® system with FRET (Mocanu *et al.*, 2011). Through this, it was suggested that the number of fluorescent signals formed using this system can become “saturated” at medium to high expression levels of the proteins of interest. At this point, no more signals are formed despite subsequent protein interactions that are shown to occur through the use of FRET. It was hypothesised in this study that the saturation phenomenon is due to steric hindrance between densely packed proximity probes which might prevent enzymes from taking part in the amplification process. Therefore, the Duolink®

assay only detects a fraction of the interacting molecules as it depends on both molecular proximities and also the equilibrium of association/dissociation reactions and enzymatic processes. It should be noted, however, that in this investigation it was suggested that saturation occurs when the proteins reach an expression level of about 1–2 million molecules/cell (Mocanu *et al.*, 2011). This is likely much higher than the expression level of the proteins investigated in the present study. Therefore, the reason for the comparatively low number of fluorescent signals is not fully understood, however, it is clear that the Duolink® reaction is incredibly complex and will require full molecular analysis in order to completely understand this phenomenon. For this reason, it can be suggested that Duolink® should be considered a semi-quantitative tool for measuring protein associations.

Chapter 4:

Visualising peroxisome-endoplasmic reticulum contact sites using fluorescent reporter systems.

4.1 Introduction:

The prevailing question we face in the postgenomic era is how to characterise the roles of ~20,000 proteins encoded in the human genome. To this end, progress has been made in devising methods to tag proteins to uncover their function. This includes the use of peptides such as epitope tags, which have no function individually, but can be recognised by other expressed proteins (Kamiyama *et al.*, 2016), or fluorescent proteins, such as green fluorescent protein (GFP). GFP was first discovered in 1962 by Shimomura and colleagues as a companion protein to aequorin, the chemiluminescent protein from *Aequorea* jellyfish (Shimomura *et al.*, 1962). Since the discovery of these proteins, they have been used extensively in proteomic studies to track the localisation of putative proteins (through fluorescence-based methods) and gain insight into their interacting partners (using epitope tags and immunoprecipitation) (Leonetti *et al.*, 2016). Following the success of the use of GFP, it was hypothesised that the use of this protein could be extended to *in vivo* protein-protein interaction studies. The first advancement in this direction was the advent of bimolecular fluorescence complementation (BiFC) assays. This began with the creation of a split GFP molecule whose reassembly could be directed by antiparallel leucine zippers (Ghosh *et al.,* 2000). When dissected between amino acids 157 and 158, both halves of GFP are non-fluorescent and it is only when they recombine, following heterodimerisation of the leucine zippers attached to each half, that fluorescence can be restored. Unfortunately, this system harboured the disadvantage of expressing very large halves of GFP, which may interfere with the biological system of interest and resulted in poor re-folding of GFP (Ghosh *et al.*, 2000).

In order to expand the range of split fluorescent protein technologies and overcome some of the issues associated with previous attempts, several new systems have been created. This includes split Venus BiFC assays which are the most widely used for testing protein interactions under physiological conditions (Miller *et al.*, 2015). Venus is a yellow fluorescent protein (YFP) variant carrying a F46L mutation which allows for faster chromophore maturation (Nagai *et al.*, 2002). Several split Venus variants have been made and successfully used for the *in vivo* study of protein-protein interactions (Shyu *et al.*, 2006; Ohashi and Mizuno, 2014). Furthermore, a dimerisation-dependent

fluorescent protein (ddFP) variant was created in 2012 by Alford and colleagues (Alford *et al.*, 2012b). This technology involves the reversible binding of two "dark" fluorescent protein monomers which can recombine to form a fluorescent heterodimeric complex (Alford *et al.*, 2012a) (Fig. 4.1). The first generation construct was a dimerisation-dependent red fluorescent protein (RFP), which proved to be effective in many biosensing applications, but had limited brightness and contrast (Alford *et al.*, 2012b). To improve this system, efforts were made to expand the colour palette of ddFPs and improve their brightness and contrast. Through a process of site-directed mutagenesis of the original ddRFP construct followed by rounds of directed evolution and gene shuffling, dimerisation-dependent GFP (ddGFP) was created (Alford *et al.*, 2012a). This variant was greatly improved in terms of brightness and contrast and also displayed a much lower dissociation constant, making it ideal for use as a reversible reporter of protein-protein interactions. In the same way as ddRFP, ddGFP can be split into two monomers, designated "ddGFP-A" and "ddGFP-B". The ddGFP-A half contains the preformed, but quenched, chromophore, whereas the ddGFP-B half lacks a chromophore. It is only when these two halves recombine that fluorescence is restored (Alford *et al.*, 2012a). This feature suggested that ddFPs could be useful for visualising organelle contact sites. It was thought that if one half of the ddFP was targeted to the surface of one organelle, and the other half to the surface of an interacting organelle, then fluorescence would only be restored when the respective organelles were in close proximity, allowing the two halves of the ddFP to recombine.

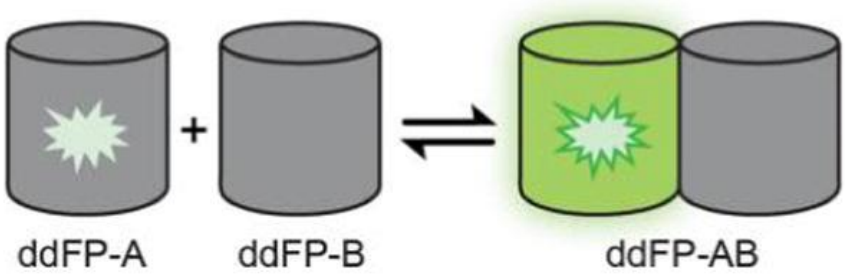

Fig. 4.1. Schematic illustration of the ddFP technology. (From: Alford *et al.*, 2012a)

In this way, the ddGFP system was first used to assess mitochondria-ER contact sites. The ddGFP-A half was targeted to the ER via fusion to the C-terminus of the ER protein calnexin and the ddGFP-B half was targeted to

mitochondria via fusion to the C-terminus of mitochondrial protein translocase of outer membrane-20 (Tom20) (Alford *et al.*, 2012a). When co-expressed in HeLa cells, bright green fluorescence was observed in the perinuclear region of the cells, indicating that the mitochondria and ER were in close proximity. No fluorescence was observed when the constructs were expressed individually. It was thought that this system could also be applied to investigating peroxisome-ER contact sites. To achieve this, we created a peroxisome-targeted ddGFP-B construct (Fig. 4.2). This construct was targeted to peroxisomes via the transmembrane domain and tail (TMD-T) region of the peroxisomal contact site protein ACBD5 (amino acids 503-534) (Fig. 4.2.). This was previously found to target specifically to peroxisomes through binding to the peroxisomal import receptor PEX19 (Costello *et al.*, 2017c). This sequence was connected to a 10 amino acid linker and fused to the C-terminus of ddGFP-B. A FLAG epitope tag was also fused to the N-terminus of ddGFP-B to allow for tracking of the subcellular localisation of the construct following transfection into mammalian cells using immuno-staining methods (Fig. 4.2). As the ER has been shown to 'wrap around' peroxisomes (Novikoff and Novikoff, 1972; Zaar *et al.,* 1987; Grabenbauer *et al.*, 2000) it was thought that the calnexin-targeted ddGFP-A half, localised to the cytosolic face of the ER, should be in an appropriate location to contact the peroxisome-targeted ddGFP-B half and heterodimerise when the organelles are in close proximity, thereafter producing a fluorescent signal (Fig. 4.2).

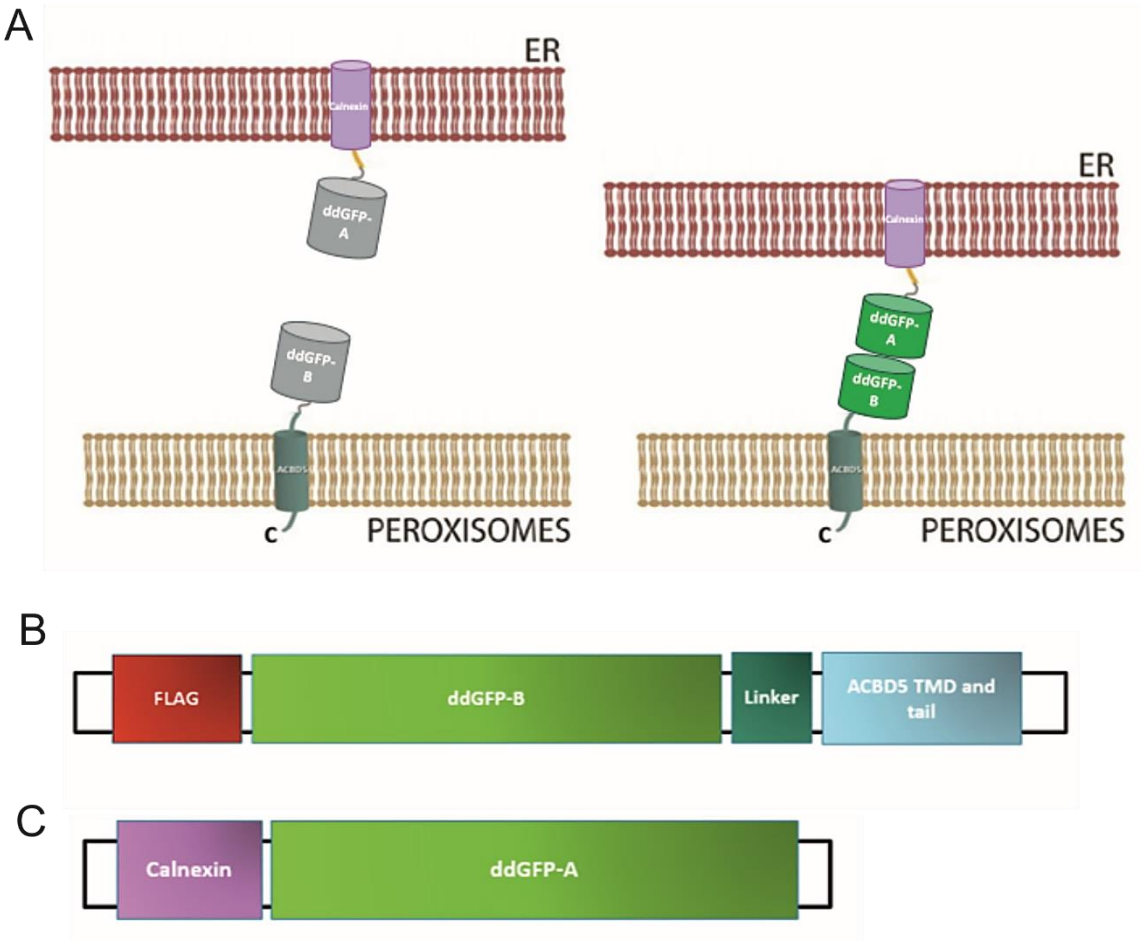

Fig. 4.2. (A) Schematic illustration of the targeting of the ddGFP fragments to the peroxisomal and ER membranes to visualise peroxisome-ER contact sites. The fragments recombine when the organelles are in close proximity, producing a fluorescent signal. (B) Schematic illustration of the peroxisome-targeted ddGFP-B half. (C) Schematic illustration of the ER-targeted ddGFP-A half.

For the analysis of peroxisome-ER contact sites, both the peroxisome and ER-targeted ddGFP constructs were first transfected into COS-7 cells and the cells were subsequently fixed prior to analysis with fluorescence microscopy. Following analysis, it was found that no fluorescent signal could be observed, only natural autofluorescence of the cells was visible (Fig. 4.3). In order to ascertain that the peroxisome-targeted construct was correctly localised following transfection, transfected cells were immuno-stained in order to detect the localisation of the FLAG epitope tag. This showed that the construct targeted correctly to peroxisomes (Fig. 4.3). The same could not be confirmed for the ER-targeted construct due to the absence of an epitope tag. HeLa cells were subsequently transfected with both constructs, consistent with the previous literature, and cells were either fixed or analysed via live cell imaging.

In both cases, no fluorescent signal was observed above the autofluorescence of the cells (Fig. 4.3). It is possible that the lack of fluorescent signal observed was due to the recombined fluorescent signal displaying low brightness (Alford *et al.*, 2012a). This system consequently has not been used extensively in the field.

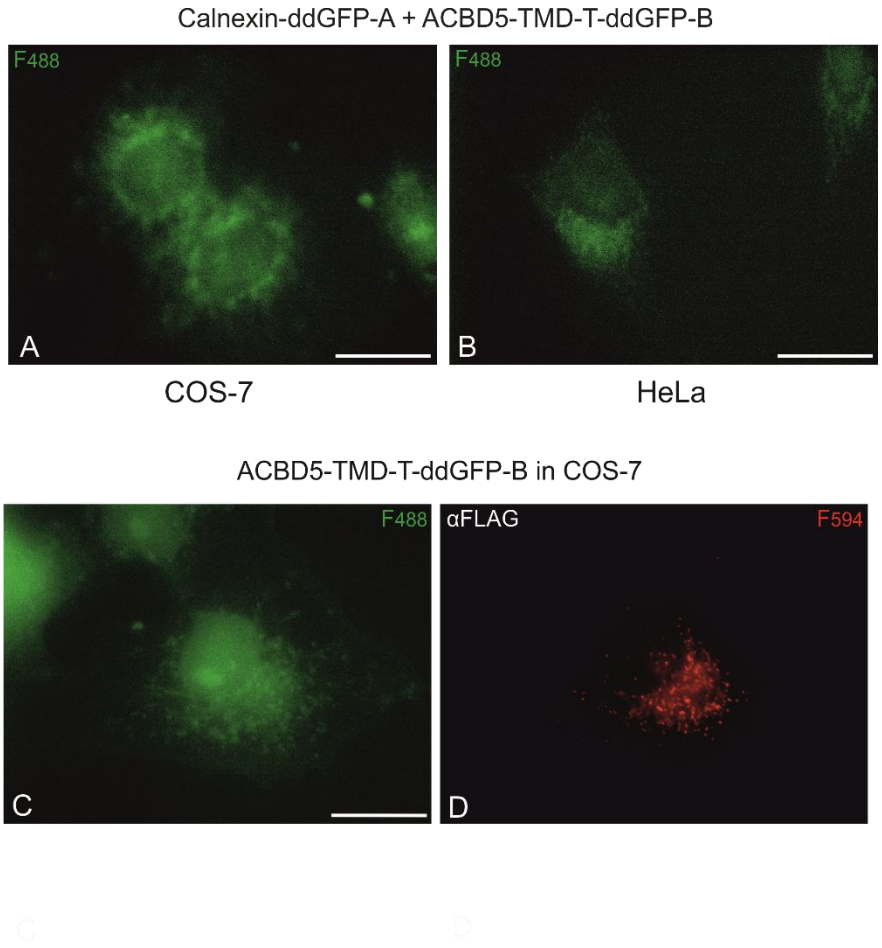

Fig. 4.3. **The ddGFP signal is not bright enough to be seen over autofluorescence.** (A) ER-targeted ddGFP-A and peroxisome-targeted ddGFP-B expressed in COS-7 cells. Only autofluorescence of the cells can be seen. (B) ER-targeted ddGFP-A and peroxisome-targeted ddGFP-B expressed in HeLa cells. Only autofluorescence of the cells can be seen. (C-D) Peroxisome-targeted ddGFP-B expressed in COS-7 cells and immuno-stained with anti-FLAG antibody. No fluorescence seen at 488 nm (C). Punctate red fluorescent structures can be seen at 594 nm, indicating correct targeting of ddGFP-B to peroxisomes. Scale bars: 20µm.

To overcome the issues observed with the use of ddFP systems, a new split GFP system was used. This system was created by Cabantous and colleagues

(Cabantous *et al.,* 2005) and consists of soluble fragments of 'superfolder' GFP which can self-associated without the assistance of other protein-protein interactions. Superfolder GFP is a variant of GFP which was created following the observation that GFP is prone to misfolding when expressed as fusions with other proteins (Tsien, 1998). This robustly folded version of GFP was created from a previous variant of GFP which was optimised for folding called 'folding reporter GFP'. Folding reporter GFP contains the 'cycle-3' mutations (F99S, M153T, V163A (Crameri *et al.*, 1996), F64L and S65T (Patterson *et al.*, 1997)). Superfolder GFP contains the folding reporter GFP mutations and six new mutations (S30R, Y39N, N105T, Y145F, I171V and A206V), creating a variant of GFP which displays enhanced folding and higher fluorescence when expressed as a protein fusion (Pédelacq *et al.*, 2006).

In order to create a split version of this protein to assess protein-protein interactions, the superfolder GFP molecule is split between the tenth and eleventh β-strand, creating two fragments; GFP1-10 (amino acids 1-214) and GFP11 (amino acids 214-230) (Fig. 4.4). GFP1-10 is non-fluorescent individually but contains the three residues that constitute the GFP chromophore (Kamiyama *et al.*, 2016). Fluorescence can only be produced following maturation of the chromophore which requires the conserved E222 residue on GFP11 (Barondeau *et al.*, 2003) (Fig. 4.4). This split system has been successfully used for many different applications, such as protein quantification (Cabantous *et al.,* 2005), protein localisation studies (Kaddoum *et al.*, 2010; Van Engelenburg and Palmer, 2010; Hyun *et al.,* 2015) and cell-cell contact detection (Feinberg *et al.*, 2008). More recently, this split superfolder GFP (spGFP) system has been used to study contact sites between mitochondria and the ER in mammalian cells (Cieri *et al.*, 2018; Kakimoto *et al.*, 2018; Yang *et al.*, 2018). All of these studies capitalised on the idea that if one fragment of split GFP was targeted to one organelle membrane and the other fragment targeted to the opposing membrane, then the two fragments would only recombine and produce fluorescence if the organelles were in close proximity, thereby providing an indication of contact site formation.

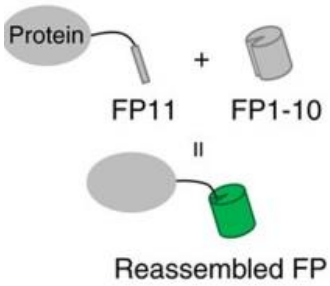

Fig. 4.4. Schematic illustration of spGFP technology. (From: Kamiyama *et al.*, 2016)

Following the success of the use of spGFP technology in assessing mitochondria-ER contact sites, it was hypothesised that this system could also be used to assess similar peroxisome-ER contact sites. In this case, it was reasoned that if the GFP1-10 portion of spGFP was targeted to the peroxisomal membrane and the GFP β-strand 11 to the ER membrane, then fluorescence would only be restored if the two organelles were in close proximity (Fig. 4.5).

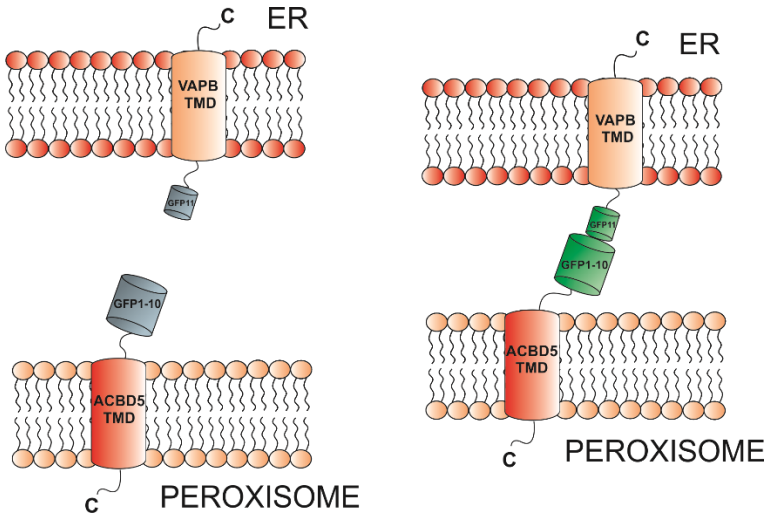

Fig. 4.5. Schematic illustration of the targeting of the spGFP fragments to the peroxisomal and ER membranes to visualise peroxisome-ER contact sites. The fragments recombine when the organelles are in close proximity, producing a fluorescent signal.

To target the GFP1-10 and 11 fragments to the peroxisome and ER membrane, the targeting sequences used in both cases were small in size. This ensured that only the closest associations of the membranes would be detected. In addition, a restriction enzyme site was place before the targeting sequence in all cases to allow the targeting sequence to be modified for future studies. The GFP1-10 fragment was targeted to peroxisomes using a PEX26-ALDP chimera

protein (Fig. 4.6). PEX26 is a tail anchored protein of the peroxisomal membrane which is targeted to peroxisomes via PEX19, an import receptor for most peroxisomal membrane proteins (Halbach *et al.*, 2006). The C-terminal targeting signal of PEX26 contains two binding sites for PEX19, one in the transmembrane domain (TMD) of the protein and the other in the luminal domain, the latter being more important for correct targeting of the protein to peroxisomes with no mitochondrial mistargeting (Halbach *et al.*, 2006). The adrenoleukodystrophy protein, ALDP, is another peroxisomal membrane protein that is a member of the ATP-binding cassette transporter protein family (Gärtner *et al.*, 2002). Previous literature showed that expression of a fusion of the luminal PEX19-binding site of PEX26 (amino acids 2-274) with a fragment of the membrane protein-targeting signal of ALDP (amino acids 87-164) led to complete peroxisomal localisation (Halbach *et al.*, 2006; Castro *et al.*, 2018a). Therefore, it was hypothesised that this would provide robust peroxisomal targeting of the GFP1-10 fragment. This sequence was fused to the C-terminus of the GFP1-10 sequence to create a targeted spGFP construct. This construct will henceforth be referred to as spGFP1-10-Pex26-ALDP (Fig. 4.6).

A second peroxisome-targeted GFP1-10 construct was also created. This construct was targeted to peroxisomes via the TMD and tail (TMD-T) region of the peroxisomal contact site protein ACBD5 (amino acids 503-534) (Fig. 4.6). This was previously found to target specifically to peroxisomes through binding to the peroxisomal import receptor PEX19 (Costello *et al.*, 2017c). This was fused to the C-terminus of the GFP1-10 sequence. This construct will be referred to as spGFP1-10 (Fig. 4.6).

The GFP11 fragment was targeted to the ER via the TMD-T region of ER membrane protein VAPB (amino acids 223-243) (Fig. 4.6). This targeting sequence was chosen as recent work using a split-Venus fluorescent reporter system to study interactions between mitochondria and the ER showed that this sequence is sufficient to target proteins to the cytoplasmic face of the ER membrane (Harmon *et al.*, 2017). Due to the small size of the GFP11 fragment, it can be arranged into tandem arrays in order to amplify the fluorescent signal (Kamiyama *et al.*, 2016); this helps in reducing issues such as low fluorescence intensity or photobleaching that can often occur with fluorescence imaging. According to previously published literature, seven copies of the GFP11

fragment with a 15 amino acid linker length between the repeats produced the highest fluorescent signal (Kamiyama *et al.*, 2016). Synonymous codons were used in the tandem arrays in order to avoid deleterious recombination during cloning which can be caused by repetitive nucleic acid sequences (Kamiyama *et al.*, 2016). This construct will be referred to as spGFP11x7 (Fig. 4.6).

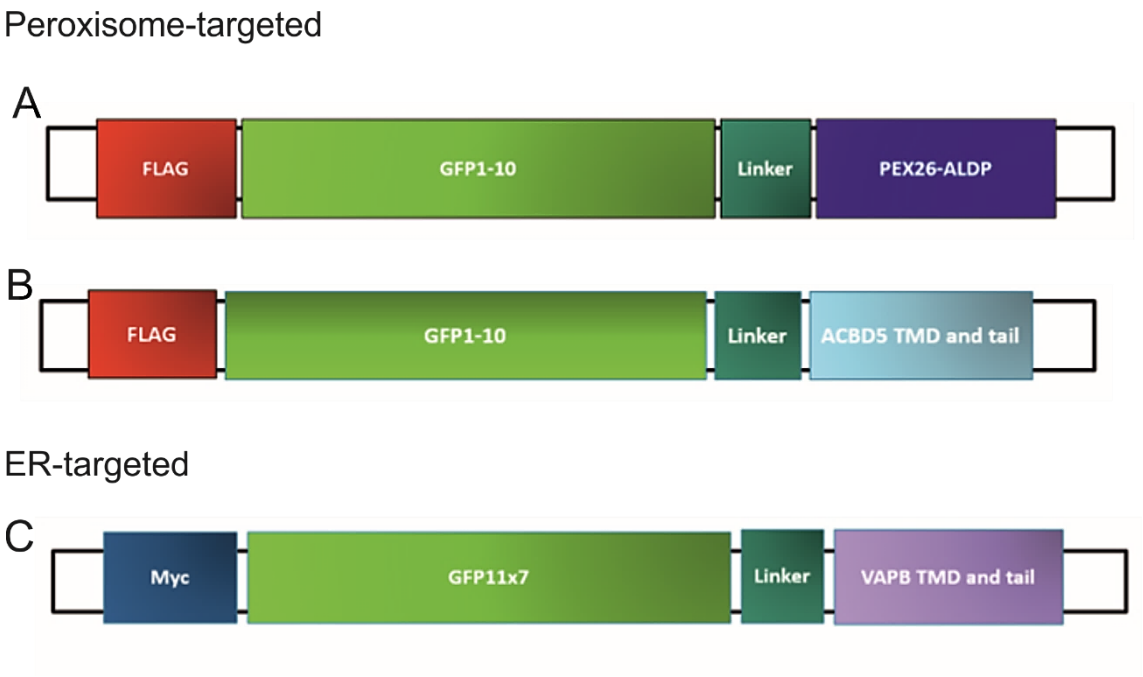

Fig. 4.6. Schematic illustration of the spGFP constructs created in this study. (A) Pex26-ALDP-targeted GFP1-10. (B) ACBD5 TMD-T-targeted GFP1-10. (C) VAPB-TMD-T-targeted GFP11.

The GFP1-10 and 11 sequences were obtained from previously published literature (Kamiyama *et al.*, 2016). A 17 amino acid linker (GTGGGGSGTGGGGSGGG) was inserted between GFP1-10/11 fragment and the targeting sequence in all cases. A FLAG epitope tag was fused to the N-terminus of the GFP1-10 constructs and a Myc epitope tag was fused to the N-terminus of the GFP11 construct to allow for tracking of the subcellular localisation of the construct following transfection into mammalian cells.

The overall size of the recombined targeted spGFP constructs was also considered. As the average distance between organelle membranes at contact sites is between 10-40 nm (Eisenberg-Bord *et al.*, 2016), the overall size of the recombined constructs would need to be ~100 amino acids. This is because unstructured peptide chains can extend up to 0.38nm per residue (Pillardy *et al.*, 2001). The linker length of each of the constructs created, combined with

the size of the spGFP fragments should be sufficient to span this contact site without disrupting endogenous organelle associations.

This system should allow peroxisome-ER contact sites to be easily visualised and quantified. This will allow further understanding and characterisation of contacts between these organelles, and ultimately contacts between peroxisomes and other organelles.

4.2 Materials and methods:

4.2.1. Molecular cloning:

Specific details of the design of the spGFP constructs can be found in Section 4.1. The sequences used are listed in Table 4.1. Gene synthesis was performed by Eurofins (Eurofins Genomics, Ebersberg, Germany). The resulting construct was transformed into the transient host DH5α competent *Escherichia coli* cells (Thermo Fisher Scientific). DNA was extracted through minipreparation using the NucleoSpin plasmid kit (Macherey-Nagel). The resulting DNA was ligated into a pcDNA3.1 (+) vector using restriction enzymes HindIII and XhoI. Correctly ligated DNA was obtained through agarose gel electrophoresis and gel extraction. Ligated plasmids were transformed into XL-10 Gold ultracompetent *E. coli* cells (Agilent Technologies) and DNA was extracted through midipreparation using the NucleoSpin plasmid kit (Macherey-Nagel).

Table 4.1. Sequences used to design spGFP constructs

Name	Sequence
GFP1-10 (From: Kamiyama *et al.*, 2016)	ATGTCCAAAGGAGAAGAACTGTTTACCGGTGTTGTGCCAA TTTTGGTTGAACTCGATGGTGATGTCAACGGACATAAGTT CTCAGTGAGAGGCGAAGGAGAAGGTGACGCCACCATTGG AAAATTGACTCTTAAATTCATCTGTACTACTGGTAAACTTC CTGTACCATGGCCGACTCTCGTAACAACGCTTACGTACGG AGTTCAGTGCTTTTCGAGATACCCAGACCATATGAAAAGA CATGACTTTTTTAAGTCGGCTATGCCTGAAGGTTACGTGC AAGAAAGAACAATTTCGTTCAAAGATGATGGAAAATATAAA ACTAGAGCAGTTGTTAAATTTGAAGGAGATACTTTGGTTAA CCGCATTGAACTGAAAGGAACAGATTTTAAAGAAGATGGT AATATTCTTGGACACAAACTCGAATACAATTTTAATAGTCAT AACGTATACATCACTGCTGAAAGCAAAAGAACGGAATTAA AGCGAATTTCACAGTACGCCATAATGTAGAAGATGGCAGT GTTCAACTTGCCGACCATTACCAACAAAACACCCCTATTG GAGACGGTCCGGTACTTCTTCCTGATAATCACTACCTCTC AACACAAACAGTCCTGAGCAAAGATCCAAATGAAAAA

GFP11x7 (From: Kamiyama *et al.*, 2016)	ATGCGTGACCACATGGTCCTTCATGAGTATGTAAATGCTG CTGGGATTACAGGTGGCTCTGGAAGTTCAGGTGGAGGCT CGGGTGGCGGCAGTTCGAGAGATCATATGGTTCTCCACG AATACGTTAACGCCGCAGGCATCACTGGCAGTGGTGGAT CTGGCAGCGGGAGCGGCTCTGGAGGTAGCAGTCGCGAC CATATGGTACTACATGAATATGTCAATGCAGCCGGAATAA CCGGATCCGGAAGTGGCTCAAGCGGAGGAGGAAGTAGTG GAAGTTCTCGGGATCACATGGTGCTGCATGAGTATGTGAA CGCGGCGGGTATAACTGGTTCGGGAGGCTCAGGTAGCGG CAGTTCAGGAGGAAGCGGGTCCCGAGACCATATGGTGCT TCACGAATACGTAAACGCAGCTGGCATTACTGGGTCAGGA GGTTCAGGAGGGTCTGGTTCTGGATCAGGAGGTAGCAGG GATCACATGGTACTCCATGAGTACGTGAACGCTGCTGGAA TCACAGGCGGTAGCAGTGGTGGAAGTAGCGGCAGCGGC GGCAGTAGCTCACGGGACCATATGGTCCTGCACGAATAT GTCAATGCTGCCGGTATCACCGGGAGTGGTGGGTCCGGC GGGAAATTCATG
Pex26-ALDP	TCCTCCCTGCACTTCCTCTACAAGCTGGCCCAGCTCTTCC GCTGGATCCGGAAGGCTGCATTTTCTCGCCTCTACCAGCT CCGCATCCGTGACGGATTCCTGTGCCGGGAGACGGGGCT GCTGGCCCTGCACTCGGCCGCCTTGGTGAGCCGCACCTT CCTGTCGGTGTATGTGGCCCGCCTGGACGGAAGGCTGGC CCGCTGCATCGTCCGCAAGGACCCGCGGGCTTTTGGCTG GCAGCTGCTGCAGTGGCTCCTCATCGCCCTCCCTGCTAC CTTCGTCAACAGTGCCATCCGTTACCTGGAGGGCCAACTG GCCCTGTCGTTCCGCAGCTGA
ACBD5 TMD-T	TCTCCTGGTGTGCTAACGTTTGCCATCATATGGCCTTTTAT TGCACAGTGGTTGGTGTATTTATACTATCAAAGAAGGAGA AGAAAAAGAAACTGA
VAPB TMD-T	CTTAGCACCCGGCTCTTGGCTCTGGTGGTTTTGTTCTTTAT CGTTGGTGTAATTATTGGGAAGATTGCC

4.3 Results:

4.3.1. Split superfolder green fluorescent protein (spGFP) technology can be used to assess contacts between peroxisomes and the ER:

In order to create a fluorescence-based sensor of organelle proximity, the split superfolder variant of GFP (spGFP) was used. The GFP1-10 fragment (spGFP1-10-Pex26-ALDP) was targeted to the peroxisomal membrane and the GFP11 fragment (spGFP11x7) was targeted to the ER membrane. The specific details on the design and cloning of these constructs are outlined in Sections 4.1 and 4.2.

The constructs were first tested for their correct localisation. For this, two untargeted fragments of spGFP were used; Untargeted GFP1-10 and Kate-β11. Individually both fragments produce no green fluorescent signal, however, Kate-β11 is fused to RFP so is visible at 594 nm. Both fragments also have a cytosolic localisation individually, however, when bound to a targeted complementary spGFP fragment, they should localise at the targeted organelle (Cieri *et al.*, 2018).

In order to confirm that these constructs were completely untargeted and only localised to the cytosol, both untargeted-GFP1-10 and Kate-β11 were co-transfected in COS-7 cells. This produced a green fluorescent signal that could be observed in the cytosol (Fig. 4.7).

To confirm that the spGFP1-10-Pex26-ALDP construct localised to peroxisomes, the construct was co-transfected in COS-7 cells with Kate-β11. This produced small, evenly distributed punctate structures identical to those seen with traditional peroxisomal staining, suggesting that this construct successfully targets to peroxisomes. The spGFP11x7 construct was co-transfected in COS-7 cells with the untargeted GFP1-10 construct. This showed a clear staining of the ER network surrounding the nucleus of the cell (Fig. 4.7).

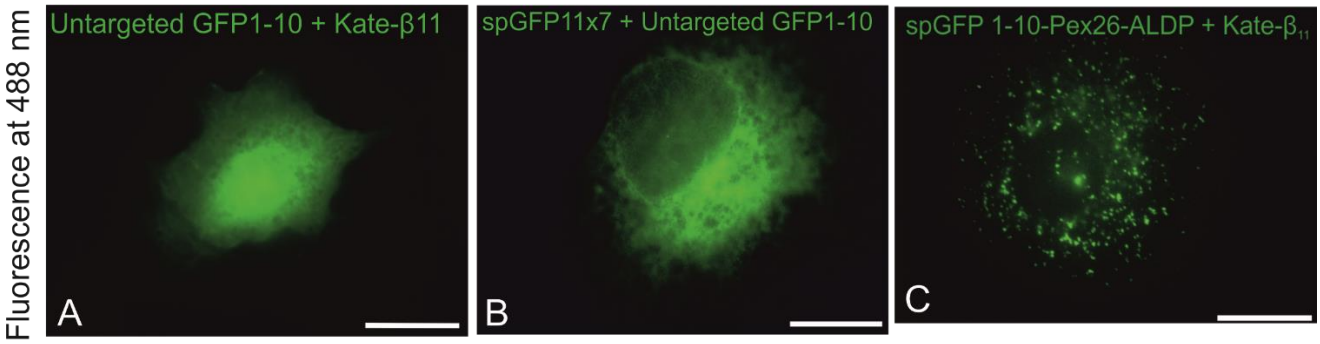

Fig. 4.7. **Untargeted spGFP constructs show correct targeting of spGFP1-10-Pex26-ALDP and spGFP11x7.** COS-7 cells were transfected with (A) untargeted GFP1-10 and Kate-β11 showing clear cytosolic localisation of the recombined spGFP fragments; (B) spGFP11x7 and untargeted GFP1-10 showing clear staining of the ER network, and (C) spGFP1-10-Pex26-ALDP and Kate-β11 showing clear peroxisomal staining. Scale bars: 20μm.

To confirm whether the recombined spGFP1-10-Pex26-ALDP and spGFP11x7 constructs would label peroxisome-ER contact sites, both constructs were transfected into COS-7 cells. In most cells, this resulted in the formation of many green fluorescent signals. The transfected cells were also immuno-stained with the peroxisomal membrane maker PEX14 to label peroxisomes. This was to provide an indication of whether the fluorescent signals observed recognised areas of peroxisome-ER juxtaposition. The green fluorescent signals appeared to colocalise with peroxisomes. COS-7 cells were also transfected with each spGFP construct individually to confirm that, when expressed alone, the constructs did not produce any fluorescence. In both cases, no fluorescence was seen, only autofluorescence of the cells could be observed (data not shown).

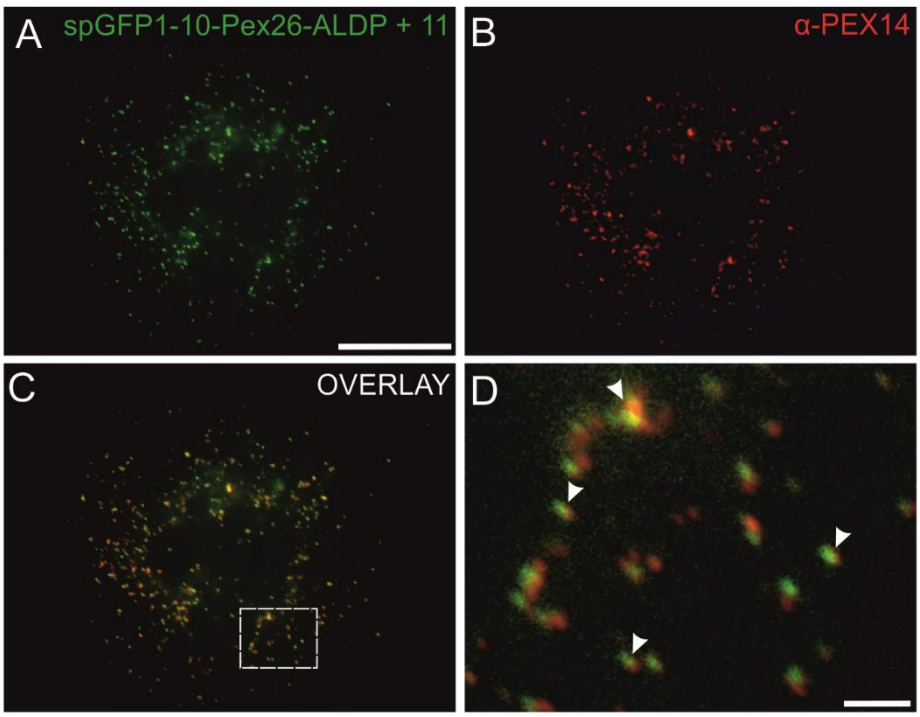

Fig. 4.8. **spGFP1-10-Pex26-ALDP and spGFP11x7 can label peroxisome-ER contact sites.** (A) COS-7 cells expressing both spGFP1-10-Pex26-ALDP and spGFP11x7. Clear green fluorescent punctate structures can be seen, indicating contacts between peroxisomes and the ER (B) Peroxisomes labelled with PEX14. (C) Overlay of green fluorescent signals from the recombined spGFP fragments with labelled peroxisomes. (D) Zoom of (C), arrows indicate co-localisation of fluorescent signals with peroxisomes. Scale bars (main): 20µm (zoom): 2µm.

In some cells, however, a different phenotype was observed. In these cells, there appeared to be a reduction in the number of peroxisomes and the recombined spGFP constructs appeared to localise to other cellular structures (Fig. 4.9). This change in phenotype was also observed in control cells where the spGFP1-10-Pex26-ALDP construct was expressed alone but this was not observed when the spGFP11x7 construct was expressed alone (data not shown), suggesting that the change in phenotype was caused by expression of the spGFP1-10-Pex26-ALDP construct and not caused by recombination of the spGFP constructs. In addition, the same phenotype was also observed when the spGFP1-10-Pex26-ALDP construct was expressed with untargeted Kate-β11 (Fig. 4.9).

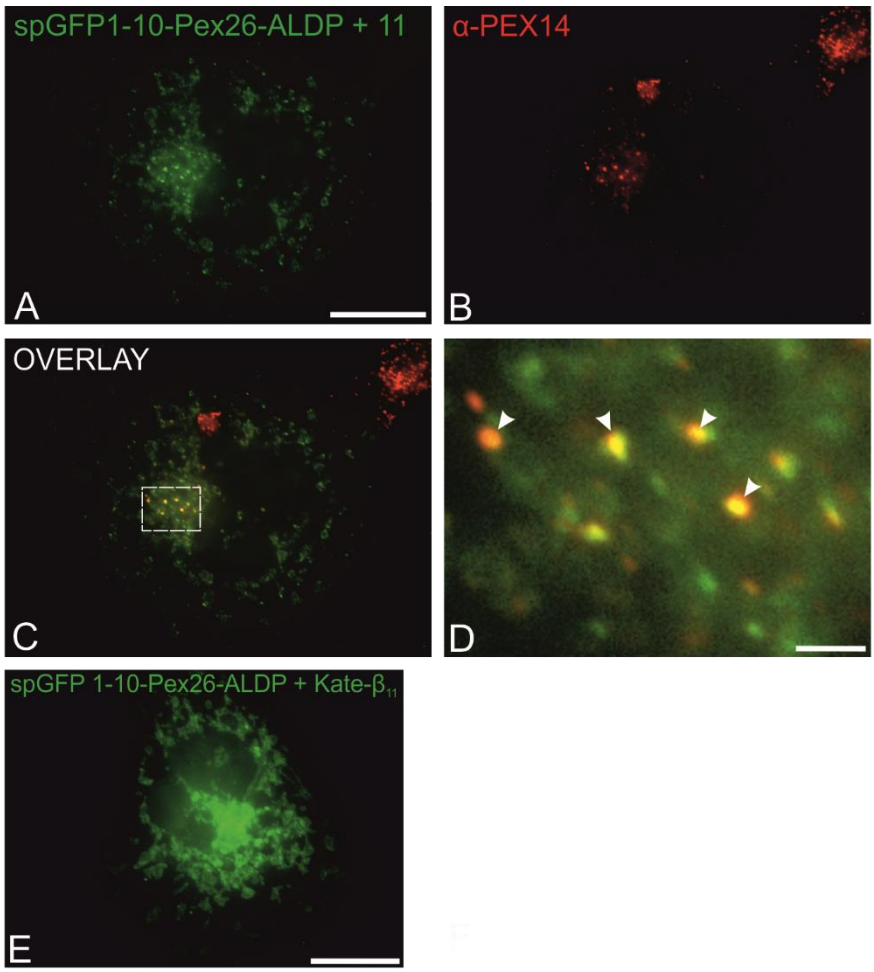

Fig. 4.9. **Expression of spGFP1-10-Pex26-ALDP leads to mistargeting and a reduction in peroxisome number in some cells.** (A) COS-7 cells expressing both spGFP1-10-Pex26-ALDP and spGFP11x7. Some green fluorescent punctate structures can be seen, as well as other structures (B) Peroxisomes labelled with PEX14. Peroxisomes appear clustered and their number is reduced (C) Overlay of green fluorescent signals from the recombined spGFP fragments with labelled peroxisomes. (D) Zoom of (C), arrows indicate co-localisation of fluorescent signals with peroxisomes. (E) spGFP1-10-Pex26-ALDP expressed with Kate-β11 showing mistargeting of green fluorescent signals to other cellular structures. Scale bars (main): 20µm (zoom): 2µm.

The structures to which the spGFP1-10-Pex26-ALDP construct and the recombined spGFP constructs colocalised appeared to be mitochondria. To confirm this, COS-7 cells expressing both spGFP constructs were immuno-stained with the mitochondrial marker ATPB. In some cells, the recombined

spGFP constructs co-localised with the labelled mitochondria, however, in most cells, this co-localisation was not seen (Fig. 4.10).

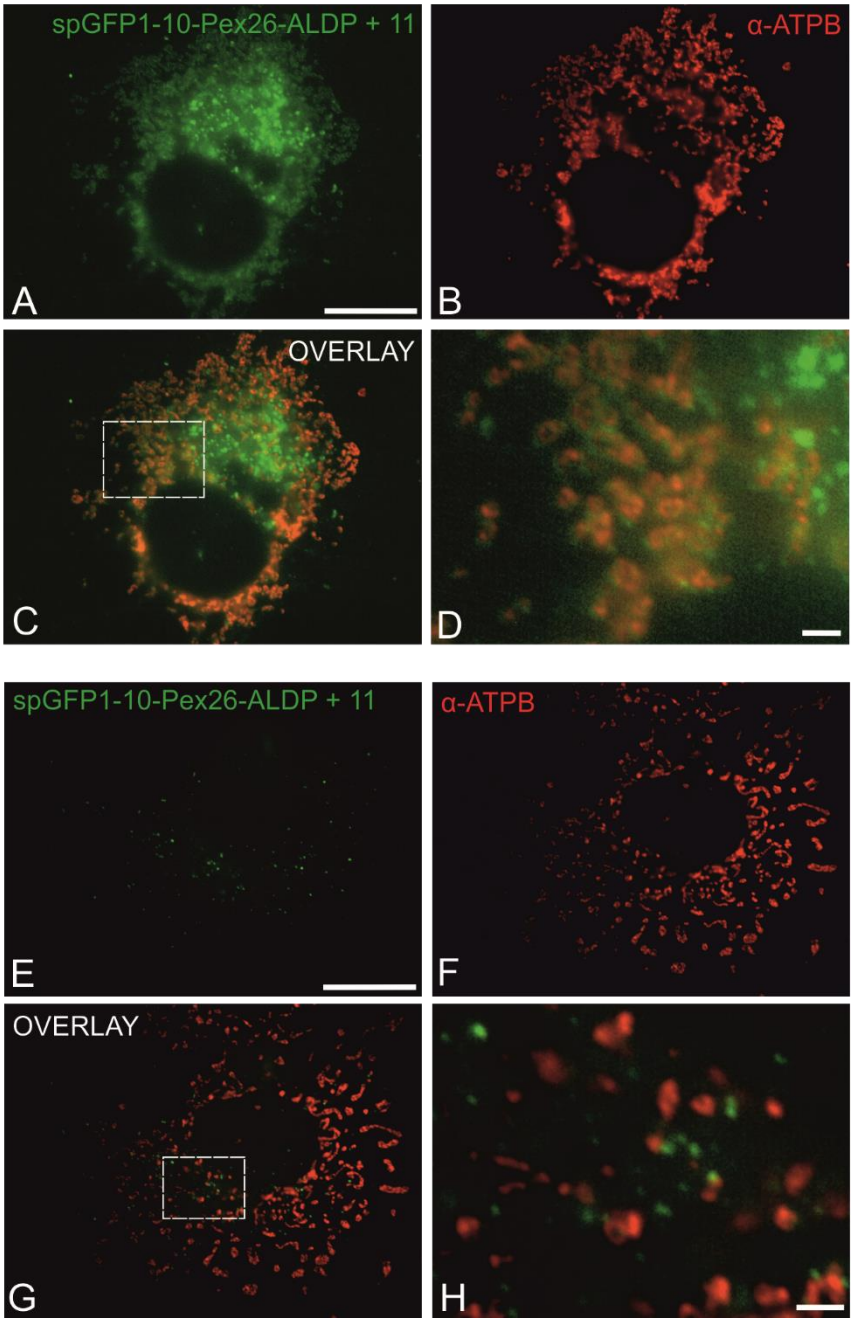

Fig. 4.10. **Staining with mitochondrial marker ATPB reveals that spGFP1-10-Pex26-ALDP can mistarget to mitochondria.** (A) COS-7 cells expressing both spGFP1-10-Pex26-ALDP and spGFP11x7 where mistargeting is apparent. (B) Mitochondria are labelled with ATPB (C) Overlay of green fluorescent signals from the recombined spGFP fragments with labelled mitochondria. Co-localisation with mitochondria can be seen (D) Zoom of (C), to show co-localisation of green fluorescent staining with mitochondria. (E) COS-7 cells expressing both spGFP1-10-Pex26-ALDP and spGFP11x7 where no

mistargeting appears. (F) Mitochondria are labelled with ATPB (G) Overlay of green fluorescent signals from the recombined spGFP fragments with labelled mitochondria. No co-localisation with mitochondria can be seen (H) Zoom of (G), to show a lack of co-localisation of the green fluorescent signals with mitochondria. Scale bars (main): 20µm (zoom): 2µm.

The number of green fluorescent signals and the number of peroxisomes per cell (nucleus) were also quantified. For this, a total of 30 cells were chosen from each of 3 experimental repeats. In this case, only cells with a normal phenotype and no mistargeting of the constructs were chosen for quantification. An average of 96.87 ± 13.19 fluorescent signals were produced per cell (nucleus) and there was an average of 204.7 ± 39.24 peroxisomes per cell (nucleus). The average percentage of peroxisomes in contact with the ER is therefore 58.46 ± 4.21% (Fig. 4.11).

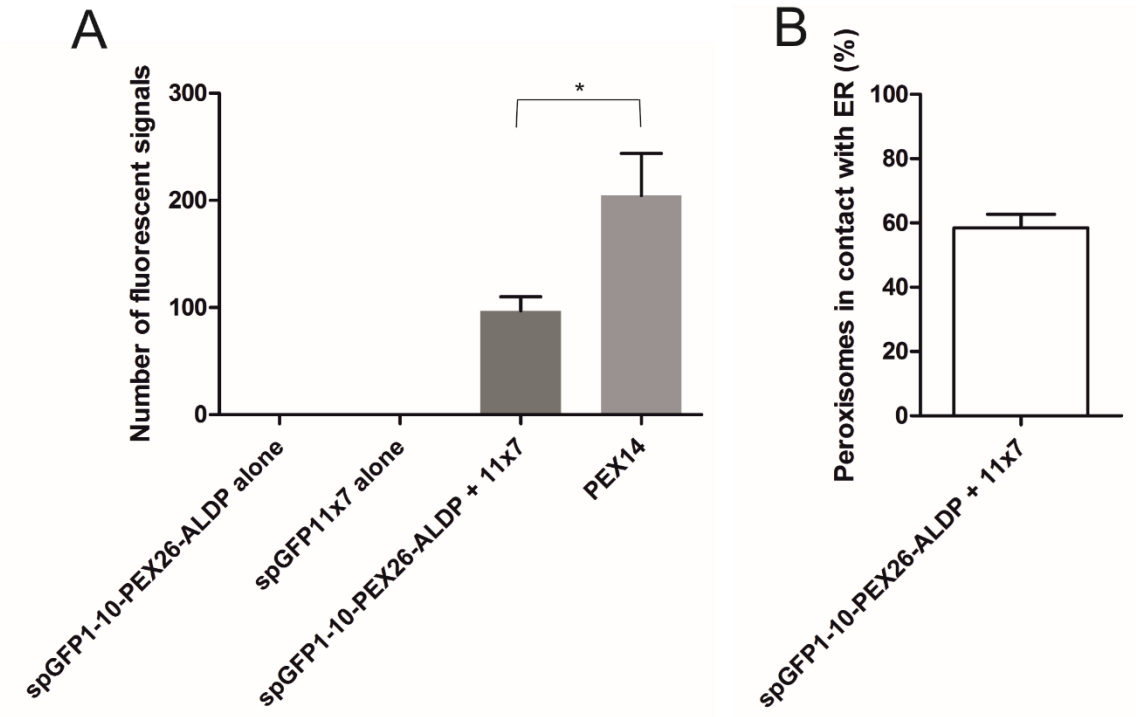

Fig. 4.11. (A) Quantitative analysis of the number of fluorescent signals per cell (nucleus) formed when spGFP1-10-Pex26-ALDP and spGFP11x7 are expressed individually and together in COS-7 cells and the mean number of peroxisomes labelled with PEX14. (B) The representative percentage of peroxisomes in contact with the ER as shown by the co-expression of spGFP1-10-Pex26-ALDP and spGFP11x7. Data are presented as mean ± SEM. Data

were analysed with a two-tailed, unpaired *t* test (*, P < 0.05). n = 30 cells. Data shown are the result of three independent experiments.

4.3.2. A spGFP1-10 construct targeted to peroxisomes via the ACBD5 TMD-T region shows improved targeting:

Although the spGFP1-10-Pex26-ALDP construct produced desirable results in most cells, obvious mistargeting to mitochondria occurred in other cells. Therefore, it was decided to try a new peroxisome-targeted GFP1-10 construct with a different targeting sequence to allow for more uniform results following transfection into cells. This construct was targeted to peroxisomes via the transmembrane domain and tail (TMD-T) region of peroxisome contact site protein ACBD5.

This construct was first tested for its correct localisation in cells. COS-7 cells were transfected with the spGFP1-10 construct and the untargeted Kate-β11 construct. The resulting recombined spGFP targeted to structures resembling peroxisomes, confirming that the construct is correctly targeted (Fig. 4.12).

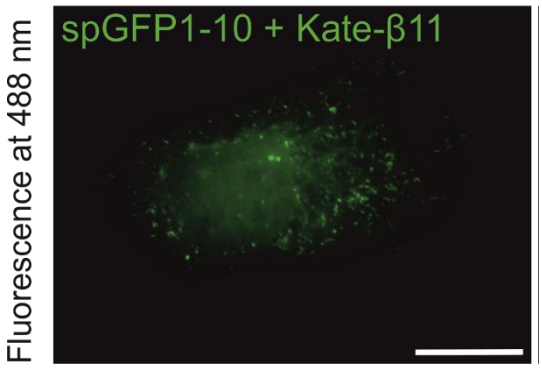

Fig. 4.12. **spGFP1-10 correctly targets to peroxisomes.** COS-7 cells were transfected with spGFP1-10 and Kate-β11. The resulting green fluorescent punctate structures resemble peroxisomes. Scale bar: 20µm

COS-7 cells were then transfected with spGFP1-10 and spGFP11x7. This resulted in the formation of many green fluorescent signals (Fig. 4.13). Cells were again immuno-stained with peroxisome membrane marker PEX14 which showed clear co-localisation of the green fluorescent signals with peroxisomes (Fig. 4.13). This indicates that the recombined constructs also recognise peroxisome-ER juxtapositions. The problem of overexpression leading to mistargeting of the constructs was not observed with this version of the spGFP1-10 construct, suggesting that this is a more robust peroxisome-

targeted construct. As a control, the spGFP1-10 construct was also transfected into COS-7 cells alone to confirm that the construct does not produce fluorescence individually. No fluorescence was observed, only natural autofluorescence of the cells was seen (data not shown).

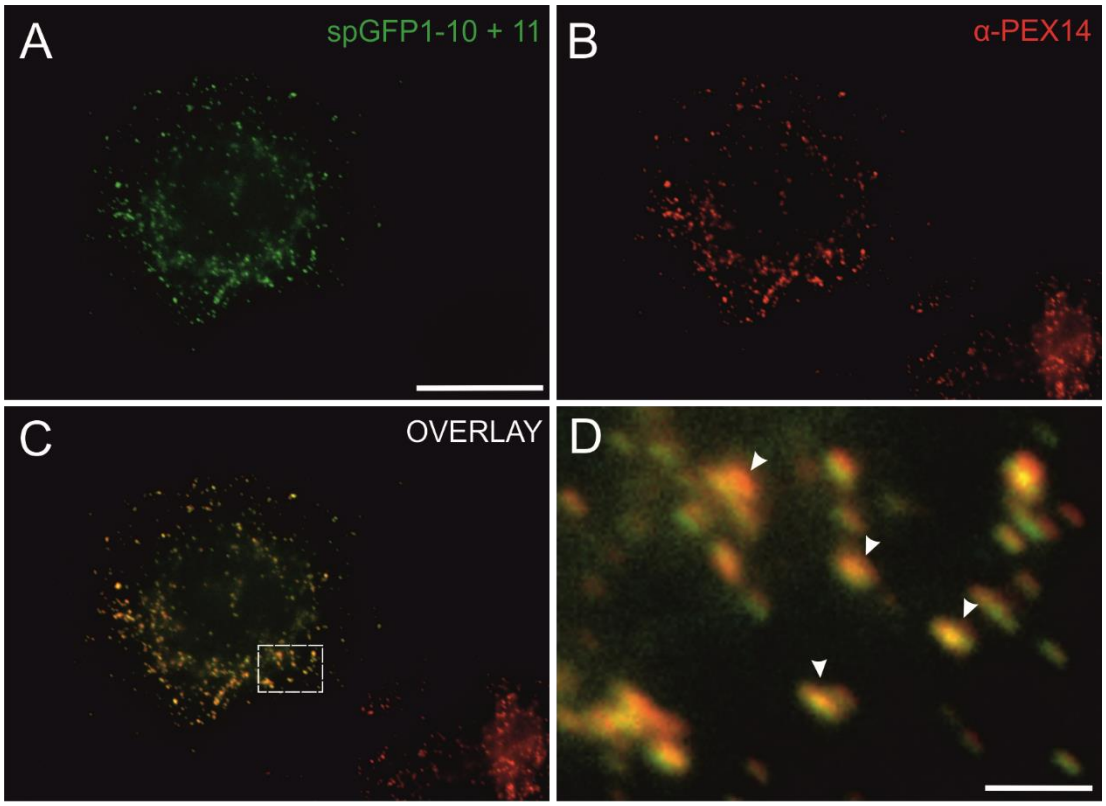

Fig. 4.13. **spGFP1-10 and spGFP11x7 can label peroxisome-ER contact sites.** (A) COS-7 cells expressing both spGFP1-10 and spGFP11x7. Clear green fluorescent punctate structures can be seen, indicating contacts between peroxisomes and the ER (B) Peroxisomes labelled with PEX14. (C) Overlay of green fluorescent signals from the recombined spGFP fragments with labelled peroxisomes. (D) Zoom of (C), arrows indicate co-localisation of fluorescent signals with peroxisomes. Scale bars (main): 20µm (zoom): 2µm.

The number of green fluorescent dots and the number of peroxisomes was also quantified in 30 cells from each of 3 experimental repeats. In this case, an average of 64.98 ± 4.45 green fluorescent signals were formed per cell (nucleus) and there was an average of 94.12 ± 6.79 peroxisomes per cell (nucleus). This shows that an average of 78.83 ± 3.67% of peroxisomes are in contact with the ER (Fig. 4.14).

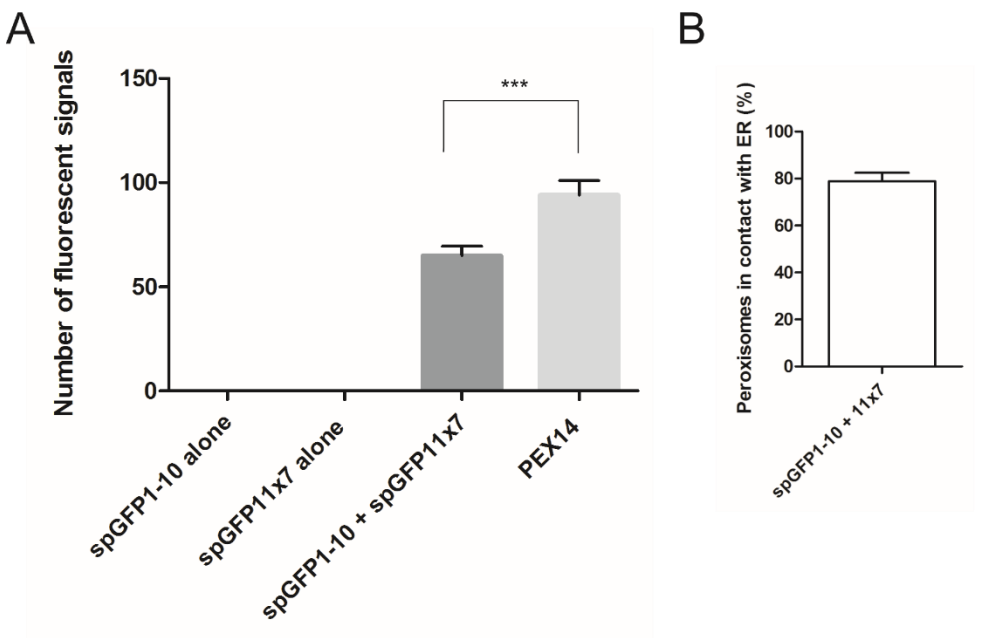

Fig. 4.14. (A) Quantitative analysis of the number of fluorescent signals per cell (nucleus) formed when spGFP1-10 and spGFP11x7 are expressed individually and together in COS-7 cells and the mean number of peroxisomes labelled with PEX14 (B) The representative percentage of peroxisomes in contact with the ER as shown by the co-expression of spGFP1-10 and spGFP11x7. Data are presented as mean ± SEM. Data were analysed with a two-tailed, unpaired *t* test (***, $P < 0.001$). n = 30 cells. Data shown are the result of three independent experiments.

4.3.3. Expression of split superfolder GFP appears to increase contacts between peroxisomes and the ER:

Since the introduction of split superfolder GFP technology and its use in analysing contacts between organelles, literature in the field has been conflicted regarding whether the binding of the GFP1-10 and 11 fragments is reversible. The concern lies within the idea that if the binding between the two fragments is irreversible, this would lead to artificial tethering between the two organelles to which the fragments are targeted, subsequently altering the results observed.

It was considered that artificial tethering of organelles could be a possibility in this peroxisome-ER-targeted spGFP system. In order to assess whether this was taking place when co-expressing the peroxisome and ER-targeted spGFP1-10 and 11 fragments, the Duolink® assay was performed on cells expressing targeted spGFP constructs. It was established from previous

experiments in this study that overexpressing proteins which are known to increase peroxisome-ER contact sites leads to a significant increase in the number of fluorescent dots produced from the Duolink® assay. Therefore, the hypothesis was made that if the expression of targeted spGFP constructs increased peroxisome-ER contact sites, then a significant increase in the number of fluorescent dots produced from the Duolink® assay would be observed.

COS-7 cells were grown on glass-bottom dishes prior to transfection with both spGFP1-10 and spGFP11x7 as in previous experiments. As a control, cells were only transfected with GFP-SKL to label peroxisomes. 24 hours post-transfection, the Duolink® assay was performed. Peroxisomal protein ACBD5 and ER protein VAPB were labelled with rabbit anti-ACBD5 and mouse anti-VAPB primary antibodies respectively, and the Duolink® assay was performed (Fig. 4.15). Before carrying out this experiment, it was confirmed that these antibodies will not bind to the ACBD5 or VAPB targeting sequences on the spGFP fragments through comparing the immunogen sequence of these antibodies to the targeting sequences used. This ensures that the Duolink® assay will only label endogenous ACBD5 and VAPB proteins. The resulting slides were analysed and the number of red fluorescent dots produced from 30 cells transfected with spGFP1-10 and spGFP11x7 constructs was quantified. An average of 15.12 ± 1.23 red fluorescent signals were formed per cell (nucleus). In control cells, an average of 7.68 ± 0.57 red fluorescent signals were formed per cell (nucleus). The number of red fluorescent signals produced from cells expressing spGFP constructs was significantly higher than the control cells ($P \leq 0.001$). This suggests that expression of peroxisome/ER-targeted spGFP constructs may increase contact between the organelles (Fig 4.15).

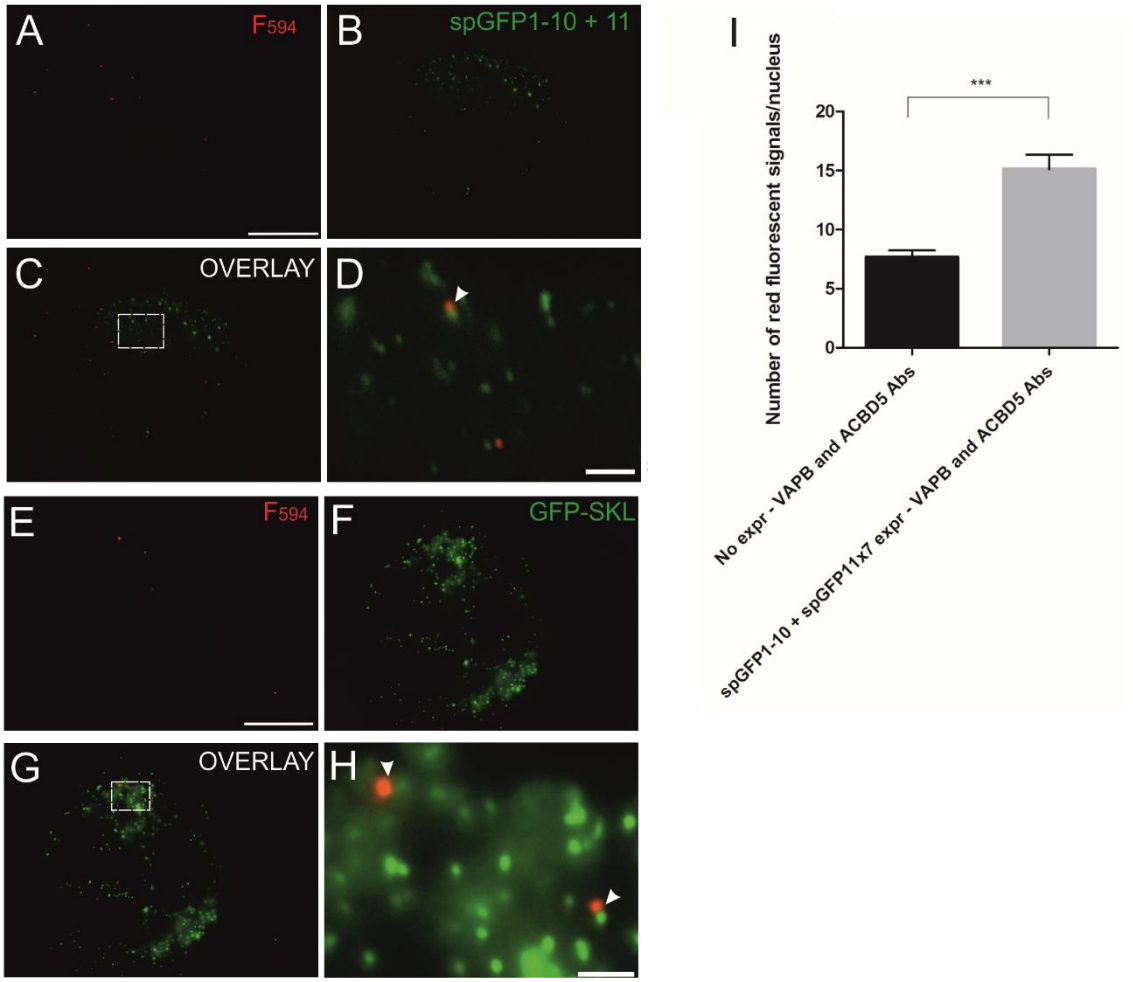

Fig. 4.15. **Expression of spGFP1-10 and spGFP11x7 increases the number of fluorescent signals formed by the Duolink® assay.** (A) COS-7 cells transfected with spGFP1-10 and spGFP11x7. The Duolink® assay was performed using ACBD5 and VAPB as target proteins. Proximity between peroxisomes and the ER is depicted as red fluorescent signals. (B) Green fluorescent signals produced from recombination of the spGFP fragments (C) Overlay of red fluorescent signals from the Duolink® assay with recombined spGFP signals (D) Zoom of (C), arrow indicates close proximity of red fluorescent Duolink® signals with recombined spGFP signals. (E) COS-7 cells transfected with GFP-SKL. The Duolink® assay was performed using ACBD5 and VAPB as target proteins. Proximity between peroxisomes and the ER is depicted as red fluorescent signals. (F) Peroxisomes labelled with GFP-SKL. (G) Overlay of red fluorescent signals from the Duolink® assay with labelled peroxisomes. (H) Zoom of (G), arrows indicate close proximity of fluorescent signals with peroxisomes. Scale bars (main): 20µm (zoom): 2µm. (I) Quantitative analysis of the number of red fluorescent signals produced per cell

(nucleus) following the use of the Duolink® assay to assess the change in the number of peroxisome-ER contact sites following expression of spGFP1-10 and spGFP11x7. Data are presented as mean ± SEM. Data were analysed with a two-tailed, unpaired *t* test (***, $P < 0.001$). n = 30 cells. Data shown are the result of three independent experiments.

4.4 Discussion:

Another tool optimised in this study was the split superfolder (spGFP) system. This represents an additional robust method to investigate intracellular protein and organelle interactions. In this study, the spGFP system has been shown to be a powerful tool to study peroxisome-ER contact sites, allowing them to be effectively visualised and quantified. To date, the present study is the first application of a split GFP system to study peroxisome-ER interactions in mammalian cells.

The spGFP system has many advantages as a tool to monitor protein and organelle interactions. Most importantly, the spGFP system is conceptually simple and due to its high modularity and flexibility it can be used to visualise complexes formed between virtually any combination of proteins in a wide variety of cell types and organisms (Kerppola, 2006). For this reason, it has been successfully employed in a recent study to investigate contact sites between multiple organelle pairs in both yeast and mammalian cells (Kakimoto *et al.*, 2018). It has also been shown to be capable of monitoring organelle interactions over a range of distances through varying the length of the spacer between the GFP11 fragment and its targeting sequence (Cieri *et al.*, 2018), permitting its application in a range of biological systems. Moreover, this system is praised for its intrinsic brightness and stability (Cieri *et al.*, 2018), traits that are not often seen with the use of other split fluorescent proteins, such as ddGFP (Alford *et al.*, 2012a).

Another advantage of this system, and other BiFC methods, over standard biochemical methods to study protein interactions, such as coIP, is that the interactions can be visualised within their native cellular environment, reducing the potential for disruption of endogenous interactions (Kerppola, 2006). Although in this study, the spGFP system was only employed in fixed cells, the system can also easily be used in live cells and visualised with live cell imaging. This not only allows for dynamic, or even transient, interactions to be visualised, but it also eliminates potential artifacts that can be caused by fixation of cells (Kerppola, 2006). Furthermore, the spGFP system is a relatively inexpensive method for the study of organelle contact sites, particularly when compared to other methods commonly used for this purpose, such as EM. It also does not require any specialist equipment. Moreover, this system is technically

straightforward in its application. The design of the spGFP fragments is the most challenging step as this requires knowledge of the sequence of an abundant organelle membrane protein or contact site protein that will be sufficient to target the fragments to the correct location in the cell.

The results shown in this study demonstrate that spGFP is an effective system to visualise peroxisome-ER contact sites. The peroxisome-targeted spGFP1-10 construct and the ER-targeted spGFP11x7 construct were shown to target specifically to peroxisomes and the ER, respectively (Fig. 4.7, Fig. 4.12). When co-transfected, the resulting fluorescence was also shown to co-localise with peroxisomes, indicating that this system specifically labels peroxisome-ER contact sites (Fig. 4.13). The punctate fluorescent structures produced from the recombination of these spGFP fragments are consistent with those seen using this system to assess mitochondria-ER contact sites in mammalian cells (Cieri *et al.*, 2018; Kakimoto *et al.*, 2018; Yang *et al.*, 2018). Using the spGFP1-10 construct, the percentage of peroxisomes in contact with the ER was 80% (Fig. 4.14). This is only slightly higher than published EM data which shows that at a given moment around 65-70% of peroxisomes are in contact with the ER in COS-7 cells (Costello *et al.*, 2017a), suggesting that this system is a reliable method to study peroxisome-ER interactions. Moreover, when each construct was tested individually in cells, no fluorescent signal could be observed whatsoever (data not shown), indicating that the signals produced from co-expressing the constructs is indicative of genuine recombination of the fluorescent fragments.

In contrast, the first construct created for this study, spGFP1-10-Pex26-ALDP, was not as effective. It appeared to localise incorrectly in some cells when expressed both with the untargeted Kate-β11 construct and with the ER-targeted spGFP11x7 (Fig. 4.9). Immunostaining with the mitochondrial marker ATPB confirmed that the construct mistargeted to mitochondria (Fig. 4.10). This mistargeting was not expected as the PEX26-ALDP sequence has previously been reported to target specifically to peroxisomes (Halbach *et al.*, 2006; Castro *et al.*, 2018a).

Despite the many benefits of using the spGFP system to study organelle contact sites, it does harbour some limitations to its applicability which should be taken into consideration when interpreting results. The main question

surrounding the use of all BiFC methods, including spGFP is whether the formation of the reconstituted fluorescent complex is reversible. Ideally, this system should be reversible in order to minimise disruption of the biological system, especially as we now understand that interactions between organelles can often be dynamic and transient (Eisenberg-Bord *et al.*, 2016). Therefore, an irreversible reaction between the spGFP fragments could have the potential to artificially tether the organelles, creating new contacts and altering interpretation of the results. *In vitro* studies utilising split GFP systems have shown that this reaction is often irreversible (Cabantous *et al.,* 2005; Magliery *et al.*, 2005; Pédelacq *et al.*, 2006), however, it had never been tested whether this reaction would be reversible if there were forces to pull the two fragments apart, which may occur if they were tethered to opposing organelle membranes *in vivo.* Several studies that have recently employed spGFP to study mitochondria-ER interactions have investigated this possibility. One such study took the approach of comparing the number of mitochondria-ER interactions using EM in a cell line where the spGFP fragments were not expressed and in a cell line stably transfected with mitochondria and ER-targeted spGFP fragments. In this case, it was found that expression of the spGFP fragments did not change the number or size of mitochondria-ER contacts, suggesting that the association of the spGFP fragments is reversible in these settings (Yang *et al.*, 2018). In contrast, another publication assessing mitochondria-ER contact sites using the spGFP system had conflicting results regarding the reversibility of the system. In this study, expression of the spGFP probes on the mitochondria and the ER was shown to rescue the growth defects of cells which are unable to form mitochondria-ER contacts, analogous to the effect of expressing a genuine artificial tethering protein (Kakimoto *et al.*, 2018). This suggests that expression of the spGFP fragments can form new, irreversible contacts between organelles. The primary difference between these two studies is that the first used a cell line which stably expresses the spGFP fragments, whereas the second did not. It could be possible that stable expression of the constructs enables an optimal expression level at which irreversible binding of the fragments does not occur.

It was not known whether complementation of the spGFP fragments was reversible in the present study. In order to test this, the Duolink® assay was

performed on cells expressing spGFP fragments targeted to peroxisomes and the ER. Cells expressing the spGFP fragments produced a significantly higher number of fluorescent signals in the Duolink® assay than cells not expressing the system (Fig. 4.15). As Duolink® shows an increase in proximity between organelles, this suggests that expression of the spGFP fragments increases the frequency of contacts between peroxisomes and the ER. The ideal control for this experiment would have been to express a genuine peroxisome-ER artificial tethering protein and compare these results to cells expressing the spGFP fragments, however, due to time constraints, this was not possible in this study. It would also be interesting to express the spGFP fragments in a cell line where the ACBD5 protein is either silenced or knocked-out as it is known that silencing ACBD5 significantly reduces peroxisome-ER contacts (Costello *et al.*, 2017a). Thus, if expressing the spGFP fragments significantly increases the number of peroxisome-ER contacts in this context to the wild-type level, it could be concluded that the reconstitution of these fragments is irreversible and leads to artificial tethering of the organelles.

Another issue with the use of spGFP which has been noted in several studies is that high expression levels of both fragments can lead to alteration of the morphology of one of the targeted organelles. Both of the aforementioned studies reported changes in mitochondrial morphology when the spGFP fragments were expressed at high levels in both yeast and mammalian cells (Kakimoto *et al.*, 2018; Yang *et al.*, 2018). In the present study, it was noted that in cells with high expression levels of the spGFP constructs, that “clustering” of peroxisomes seemed to occur. This was the case with both the spGFP1-10-Pex26-ALDP and spGFP1-10 constructs (Fig. 4.16). It is not known specifically why this phenotype occurs, however, as the ER is known to wrap around peroxisomes (Novikoff and Novikoff, 1972; Zaar *et al.*, 1987; Grabenbauer *et al.*, 2000), it is possible that artificial tethering of the two organelles, potentially caused by expression of the spGFP fragments could lead to peroxisomes clustering in areas where they are bound by the ER. Moreover, peroxisomal clustering is also known to occur prior to pexophagy (Yamashita *et al.*, 2014), suggesting that high expression levels of the spGFP fragments may be toxic to the peroxisomes, leading to the onset of pexophagy. This phenotype could be avoided with the creation of a cell line which stably expresses the spGFP

fragments to ensure that the expression level of the fragments is at an optimal level.

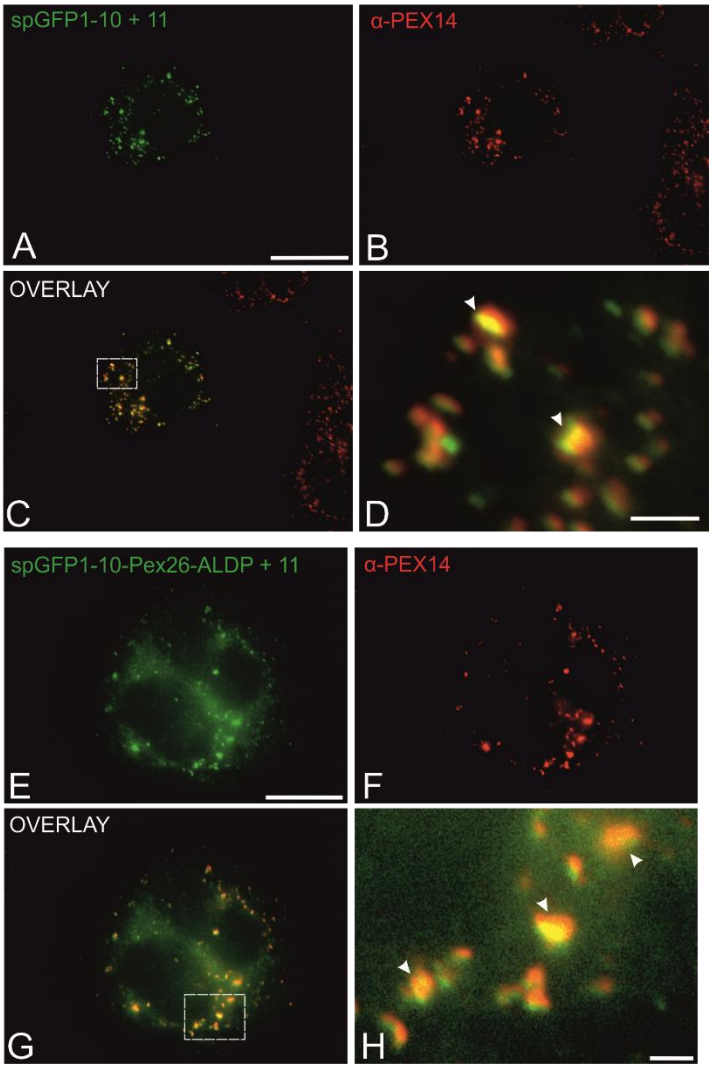

Fig. 4.16. **Clustering of peroxisomes seems to occur with high expression levels of the spGFP constructs.** (A) spGFP1-10 or (E) spGFP1-10-Pex26-ALDP and spGFP11x7 expressed in COS-7 cells. Clustering of the green fluorescent signal can be observed. (B, F) Peroxisomes labelled with PEX14. Peroxisome number appears reduced and clustering is visible. (C, G) Overlay of green fluorescent signals with labelled peroxisomes. (D, H) Zoom of (C, G). Clusters of the recombined spGFP fragments co-localise with clustered peroxisomes. Arrows indicate co-localisation. Scale bars (main): 20µm (zoom): 2µm.

Considering both the advantages and the disadvantages of the spGFP system, it can be concluded that it is an effective system to study peroxisome-ER interactions, however, the results should be analysed with caution. The potential

of spGFP to perturb the natural biological system, by inducing organelle interactions or by altering organelle morphology, cannot completely be ruled out by this study or by others. The creation of a stably expressing cell line in the future could help to minimise these effects by ensuring an optimal expression level. Until then, this system can be used to detect and analyse peroxisome-ER contact sites and help to uncover the physiological roles of these sites.

Chapter 5:

Using Duolink® and split superfolder GFP systems to assess changes in peroxisome-endoplasmic reticulum contact sites following changes in physiological cellular conditions.

5.1. Introduction:

Following optimisation of both Duolink® and the spGFP fluorescent reporter system to visualise and quantify peroxisome-ER interactions, these systems were used to assess the effect of altering the physiological cellular conditions on the integrity and number of peroxisome-ER contact sites formed.

It is known that peroxisome-ER associations are required for several essential peroxisomal metabolic processes including the production of polyunsaturated fatty acids (Sprecher and Chen, 1999), bile acid synthesis (Mihalik *et al.*, 2002) and the biosynthesis of plasmalogens (Braverman and Moser, 2012), which has been shown to be impacted when peroxisome-ER associations are disrupted (Hua *et al.*, 2017; Herzog *et al.*, 2018). Additionally, cooperation between these organelles has been implicated in *de novo* peroxisome biogenesis and also peroxisomal growth and division (Raychaudhuri and Prinz, 2008; Hettema *et al.*, 2014) likely through the transfer of membrane lipids. This is corroborated by the finding that an absence of contact between peroxisomes and the ER leads to a reduction in peroxisomal membrane expansion (Costello *et al.*, 2017a). Specific details of these processes and interplay between peroxisomes and the ER can be found in Section 1.4.6.

Despite our growing understanding of the importance of cooperation between these organelles, the specific role of peroxisome-ER contact sites in these processes is still not fully understood. At present, it cannot be ascertained whether contact sites play a direct role in these processes, for example, through enabling transfer of the substrates or end products of peroxisome metabolism between the organelles (Wanders *et al.*, 2016), or an indirect role through simply providing proximity between the organelles to enable vesicular transfer of products. Currently, the only evidence for the involvement of peroxisome-ER tethering in a physiological role is the finding that plasmalogen production is reduced when contact site formation is disrupted (Hua *et al.*, 2017; Herzog *et al.*, 2018). However, some hypotheses have been made for the cooperation of these organelles. One such hypothesis is that contact between these organelles may play a direct or indirect role in peroxisomal β-oxidation (Castro *et al.*, 2018b). Interestingly, all patients with defects in the peroxisomal contact site protein, ACBD5, have elevated levels of VLCFAs, which are exclusive substrates of peroxisomal β-oxidation (Ferdinandusse *et al.*, 2017; Yagita *et al.*,

2017a). It is possible that this functional defect could be caused as ACBD5 has been hypothesised to bind directly to ER-derived and cytosolic VLCFAs and recruit them to peroxisomes where β-oxidation can take place (Ferdinandusse *et al.*, 2017).

Previous studies have successfully used both Duolink® and split fluorescent reporter systems to detect changes in the number of mitochondria-ER contact sites formed following induction of stress conditions, changes in organelle morphology and the addition of stimuli (Stoica *et al.*, 2016; Cieri *et al.*, 2018; Yang *et al.*, 2018). Therefore, it was hypothesised that these systems could be used to assess changes in the number of peroxisome-ER contacts sites in response to altered physiological conditions. Following initial observations, it was decided that the Duolink® system may be better suited to assess an increase in the number of contact sites formed, rather than showing a decrease. This is because it was found that the number of fluorescent signals formed using this system is much lower than the estimated number of endogenous contact sites which has been calculated through the use of EM (Costello, *et al.*, 2017a). However, the number of fluorescent signals formed seems to increase significantly following an induction in contact site formation, for example through the overexpression of contact site proteins.

Following from the hypothesis that peroxisome-ER contact may be implicated in peroxisomal fatty acid β-oxidation, it was decided to test whether the addition of excess oleic acid would increase contacts between peroxisomes and the ER in response to increased β-oxidation. Oleic acid (18:1) is a long chain monounsaturated fatty acid and is known to be broken down by fatty acid β-oxidation (Ren and Schulz, 2003). It was hypothesised that an excess of this fatty acid would induce fatty acid β-oxidation in the cell, thereby increasing the number of peroxisome-ER contacts if, indeed, these play a role in the process. Moreover, addition of excess oleic acid has been shown to affect the number of contacts between peroxisomes and other organelles in a previous study (Valm *et al.*, 2017).

In addition, it was decided to test the effect of adding excess arachidonic acid, a polyunsaturated fatty acid, on the number of peroxisome-ER contact sites formed. Arachidonic acid is a very long chain polyunsaturated fatty acid (C20:4) which can be broken down by β-oxidation (Gordon *et al.*, 1994). It is known to

induce the formation of tubular peroxisomes (Schrader *et al.*, 1998) as well as stimulating peroxisome proliferation (Reddy and Mannaerts, 1994). It has been reported that the ER transfers membrane lipids to peroxisomes, mainly for peroxisome biogenesis (Raychaudhuri and Prinz, 2008) and that organelle tethering can facilitate this transfer (Prinz, 2010). Therefore, it was thought that a stimulation of peroxisome proliferation through the addition of excess arachidonic acid may increase contacts between peroxisomes and the ER to facilitate lipid transfer for peroxisome biogenesis. For the addition of both oleic and arachidonic acid, cells were treated with an appropriate concentration of the respective fatty acid and the Duolink® assay was carried out in order to assess whether a change in peroxisome-ER contact sites could be reflected by a change in the number of fluorescent signals produced.

The effect of cellular stresses on the formation of peroxisome-ER contact sites is also not well understood. It is known that conditions, such as nutrient-starvation, lead to autophagic degradation of peroxisomes (Hara-Kuge and Fujiki, 2008), which could potentially reduce the number of peroxisome-ER contact sites present in a cell. However, it has also been identified, using a split fluorescent reporter system, that the number of mitochondria-ER contact sites increases following nutrient-starvation (Yang *et al.*, 2018). Due to the similarity and frequent cross-over between peroxisomal and mitochondrial phenotypes (Schrader and Yoon, 2007), it was thought that this effect may also be present in peroxisome-ER contacts following the same conditions. In order to investigate this, the spGFP system was used and the number of fluorescent signals were quantified in both starved and un-starved cells to reflect changes in the number of peroxisome-ER contact sites formed.

5.2. Materials and methods:

5.2.1. Oleic acid and arachidonic acid treatment:

COS-7-GFP-SKL cells were grown on 19 mm glass coverslips at 37°C with 5% CO_2 and 95% humidity for 8 hours. After this time, oleic acid was added to cells at three different concentrations: 25, 50 and 100 µM or arachidonic acid was added to cells at two different concentrations: 25 and 50 µM. Ethanol was added as a control. In the case of oleic acid treatment, BODIPY 558/568 C_{12} was added to cells to stain lipid droplets. Cells were then incubated at 37°C with 5% CO_2 and 95% humidity overnight. After this time, the cells were washed with 1x PBS and fixed in 4% paraformaldehyde in PBS (pH 7.4) for 20 minutes at room temperature. Cells were then washed three times for 5 minutes with PBS. To prepare the slides, coverslips were washed once in Milli-Q water and mounted in Mowiol 4-88 containing n-propyl gallate as an anti-fading reagent (3:1 mowiol with n-propyl gallate). The cells were then imaged using fluorescence microscopy as described in Section 2.5.

5.2.2. Duolink® assay with fatty acid treatment:

COS-7-GFP-SKL cells were grown 3.5-cm-diameter glass bottom dishes (Cellview; Greiner BioOne) and incubated for 8 hours at 37°C with 5% CO_2 and 95% humidity. After this time, cells were treated with 25 µM oleic acid or arachidonic acid or the same quantity of ethanol as a control. Following overnight incubation, the Duolink® assay was performed as described in Section 3.2.1. Slides were then analysed with fluorescence microscopy as described in Section 2.5. Quantification of the fluorescent signals produced was performed as described in Section 2.6.

5.2.3. spGFP assay following nutrient starvation:

COS-7 cells were transfected using DEAE-dextran transfection with peroxisome-targeted spGFP1-10 and ER-targeted spGFP11x7 as described in Section 2.2. Following overnight incubation at 37°C with 5% CO_2 and 95% humidity, media was changed to Hank's Balanced Salt Solution (HBSS), a medium which lacks amino acids but contains sufficient glucose to ensure cell survival over a 24-hour period (Sargent *et al.*, 2016). Cells were nutrient starved for 24 hours. As a control, media was replaced with complete media (DMEM

+/+) at this time point. Following this 24-hour incubation, cells were fixed and immuno-stained with anti-PEX14 antibody to label peroxisomes as described in Section 2.4. Slides were then analysed with fluorescence microscopy as described in Section 2.5. Quantification of the fluorescent signals produced was performed as described in Section 2.6.

5.3. Results:

5.3.1. Addition of excess oleic acid increases the size of lipid droplets:

In order to first determine the appropriate concentration of oleic acid to use in this experiment, increasing concentrations of oleic acid were individually added to COS-7-GFP-SKL cells. The concentrations used were 0, 25, 50 and 100 µM. The cells were also stained with BODIPY 558/568 C_{12} to label lipid droplets. Cells were fixed and analysed by fluorescence microscopy to assess the overall appearance of the cells, including the number and distribution of peroxisomes and the formation of lipid droplets. The size of lipid droplets increased as the concentration of oleic acid increased. With all concentrations, peroxisome number and distribution were uniform (Fig. 5.1). It was decided to use a concentration of 25 µM oleic acid for subsequent experiments as this appeared to be sufficient to induce an effect within the cells, as seen by a clear increase in the size of lipid droplets but was still a low concentration to reduce the potential of causing toxicity within the cell.

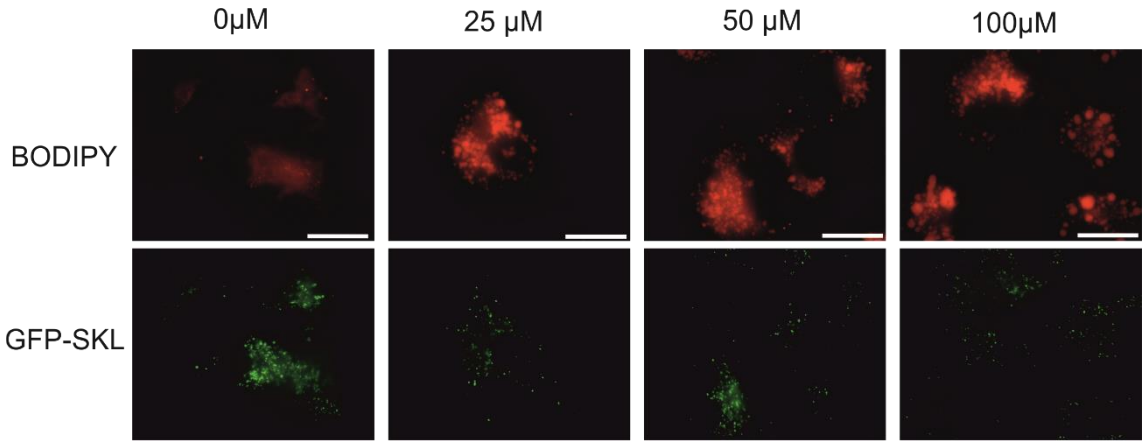

Fig. 5.1. **COS-7-GFP-SKL cells were treated with increasing concentrations of oleic acid.** Lipid droplets were stained with BODIPY and appear to increase in size following increasing concentrations of oleic acid. The number and distribution of peroxisomes remains consistent. Scale bars: 20µm.

5.3.2. Addition of excess arachidonic acid induces peroxisome tubulation:

A similar approach was taken for determining the appropriate concentration of arachidonic acid. COS-7-GFP-SKL cells were treated with increasing concentrations of arachidonic acid (0, 25 and 50 µM). Cells were fixed and observed using fluorescence microscopy. In this case, it was necessary to

identify the minimum concentration of fatty acid that would induce peroxisomal tubulation without producing any toxic effects in the cell. It was decided that 25 µM arachidonic acid was the optimum concentration to use as some tubulation could be observed, however, the number and distribution of peroxisomes was normal (Fig. 5.2). At concentrations of 50 µM, peroxisomal tubulation occurred, however, the number of peroxisomes appeared to be reduced and peroxisomes seemed to cluster around the nucleus of the cell, indicating potential toxicity to the cells (Fig. 5.2).

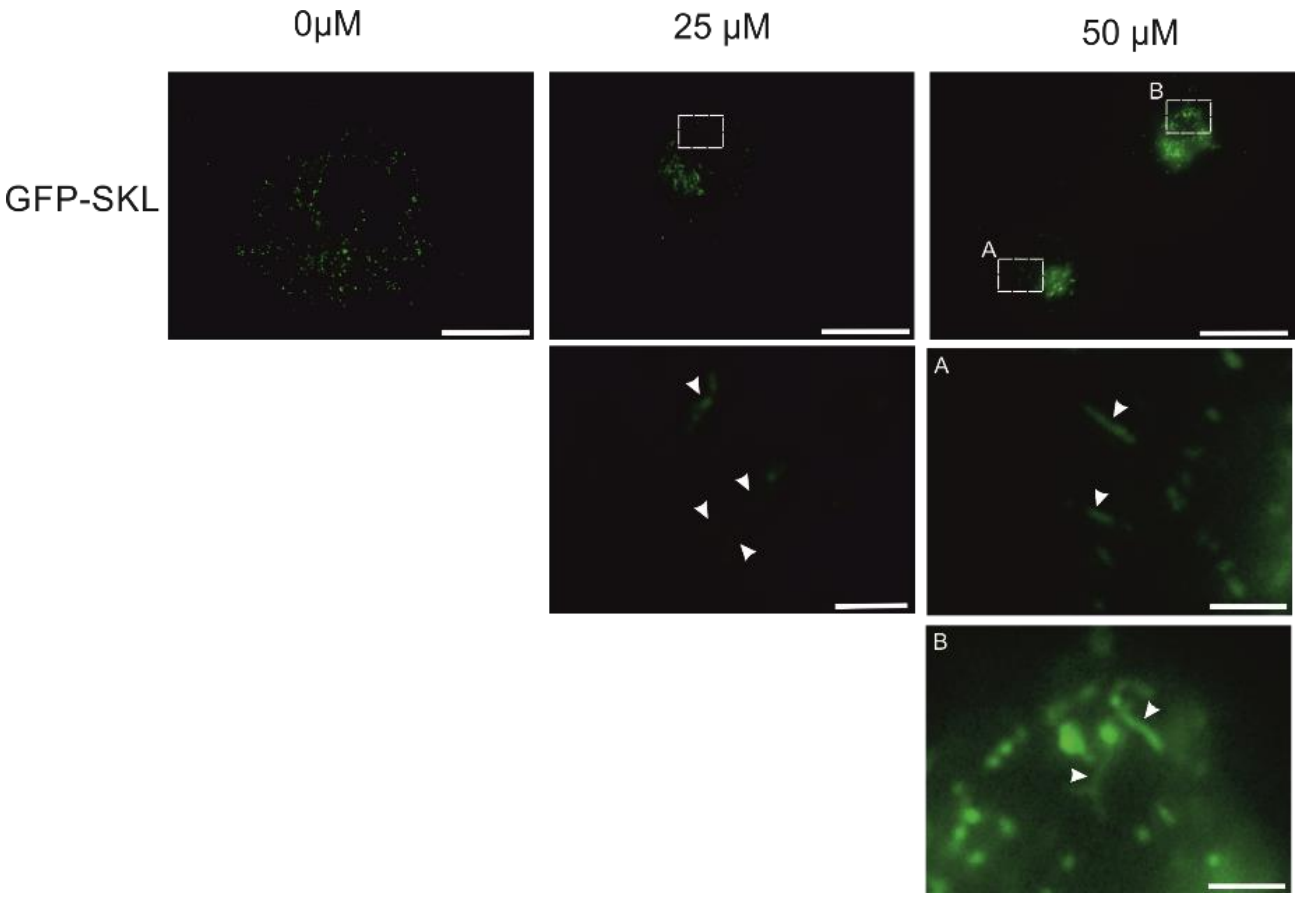

Fig. 5.2. **COS-7-GFP-SKL cells were treated with increasing concentrations of arachidonic acid.** Peroxisomal tubulation is indicated by arrows at 25 and 50 µM arachidonic acid. Scale bars: 20µm.

5.3.3. Adding excess oleic acid to cells has no effect on the number of peroxisome-ER contact sites as visualised by the Duolink® system:

After determining the optimal concentration of oleic acid to use for experimentation, the effect of adding an excess of this fatty acid to cells on the formation of peroxisome-ER contact sites was investigated. For this, the Duolink® system was used. COS-7-GFP-SKL cells were treated with 25 µM

oleic acid. The oleic acid used for this study was dissolved in ethanol, therefore, as a control, cells were treated with the same amount of solvent. The Duolink® assay was performed as described; peroxisomal protein ACBD5 and ER protein VAPB were labelled with rabbit anti-ACBD5 and mouse anti-VAPB primary antibodies, respectively. Following analysis of the slides, it was found that an average of 8.26 ± 0.79 fluorescent signals were formed per cell (nucleus) in cells treated with oleic acid compared to an average of 7.97 ± 0.66 fluorescent signals in control cells. The difference in the number of fluorescent signals was not significant, suggesting that the addition of excess oleic acid has no effect on the number of peroxisome-ER contact sites that can be visualised using the Duolink® system (Fig. 5.3).

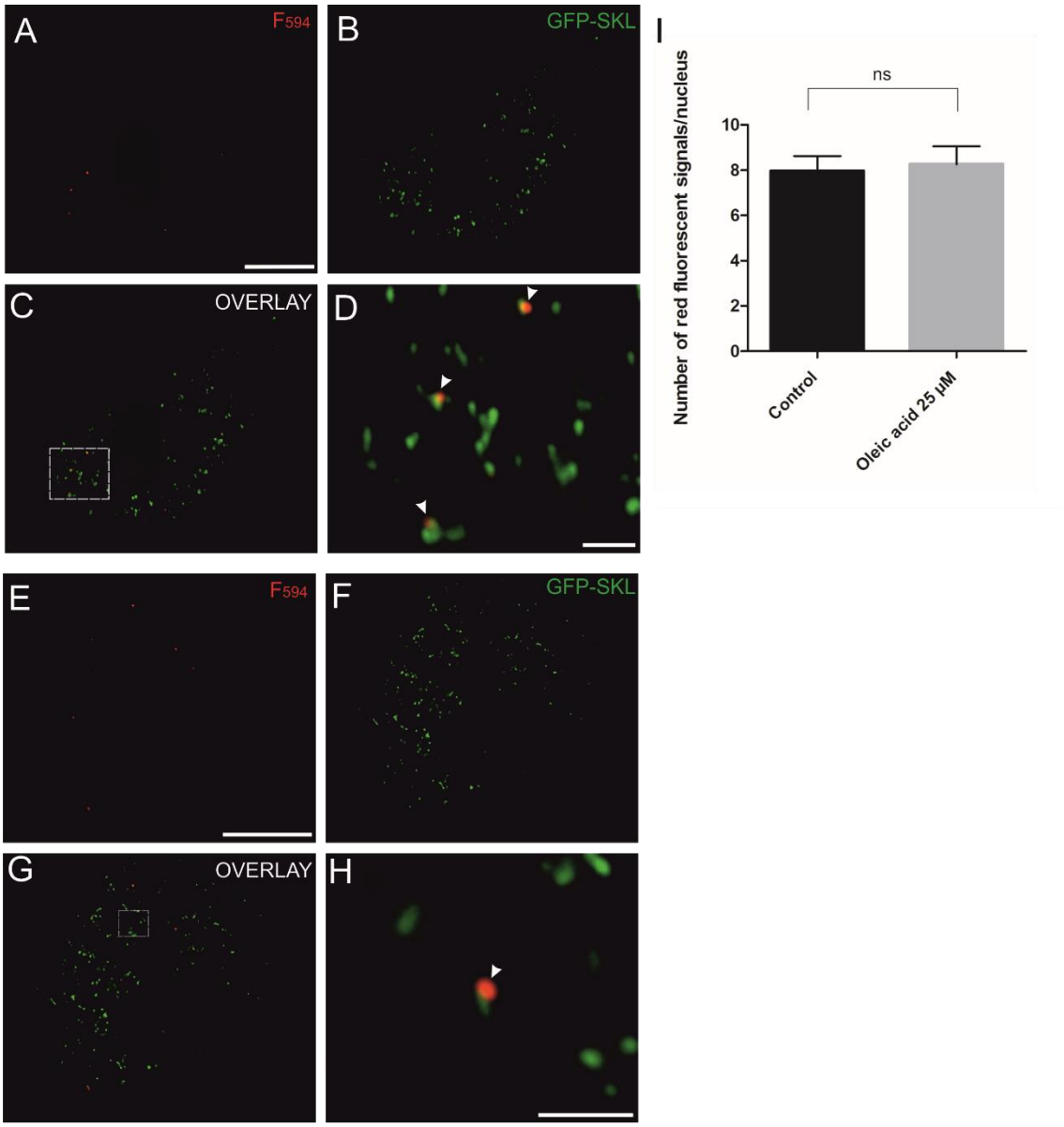

Fig. 5.3. **Addition of excess oleic acid does not change the number of fluorescent signals formed by the Duolink® assay.** (A) Control COS-7-GFP-SKL cells were treated with ethanol. The Duolink® assay was performed using ACBD5 and VAPB as target proteins. Proximity between peroxisomes and the ER is depicted as red fluorescent signals. (B) Peroxisomes labelled with GFP-SKL. (C) Overlay of red fluorescent signals from the Duolink® assay with labelled peroxisomes (D) Zoom of (C), arrows indicate close proximity of red fluorescent Duolink® signals with peroxisomes (E) COS-7-GFP-SKL cells treated with 25 µM oleic acid. The Duolink® assay was performed using ACBD5 and VAPB as target proteins. Proximity between peroxisomes and the ER is depicted as red fluorescent signals. (F) Peroxisomes labelled with GFP-SKL. (G) Overlay of red fluorescent signals from the Duolink® assay with labelled peroxisomes. (H) Zoom of (G), arrow indicates close proximity of fluorescent signals with peroxisomes. Scale bars (main): 20µm (zoom): 2µm. (I) Quantitative analysis of the number of red fluorescent signals produced per cell (nucleus) following the use of the Duolink® assay to assess the change in the number of peroxisome-ER contact sites following treatment with excess oleic acid. Data are presented as mean ± SEM. Data were analysed with a two-tailed, unpaired *t* test (ns, not significant). n = 30 cells. Data shown are the result of three independent experiments.

5.3.4. Adding excess arachidonic acid to cells has no effect on the number of peroxisome-ER contact sites as visualised by the Duolink® system:

COS-7-GFP-SKL cells were treated with 25 µM arachidonic acid to assess the effect of the presence of an excess of this fatty acid on the formation of peroxisome-ER contact sites. As a control, COS-7-GFP-SKL cells were also treated with the same amount of ethanol, which was the diluent of the arachidonic acid used. The Duolink® assay was performed as described; peroxisomal protein ACBD5 and ER protein VAPB were labelled with rabbit anti-ACBD5 and mouse anti-VAPB primary antibodies, respectively. Analysis of the slides showed that an average of 10.23 ± 1.35 fluorescent signals were formed per cell (nucleus) in cells treated with arachidonic acid compared to an average of 12.11 ± 0.77 fluorescent signals formed in control cells. The difference in the number of fluorescent signals formed was not significant, suggesting that the addition of excess arachidonic acid has no effect on the

number of peroxisome-ER contact sites that can be visualised using the Duolink® system (Fig. 5.4).

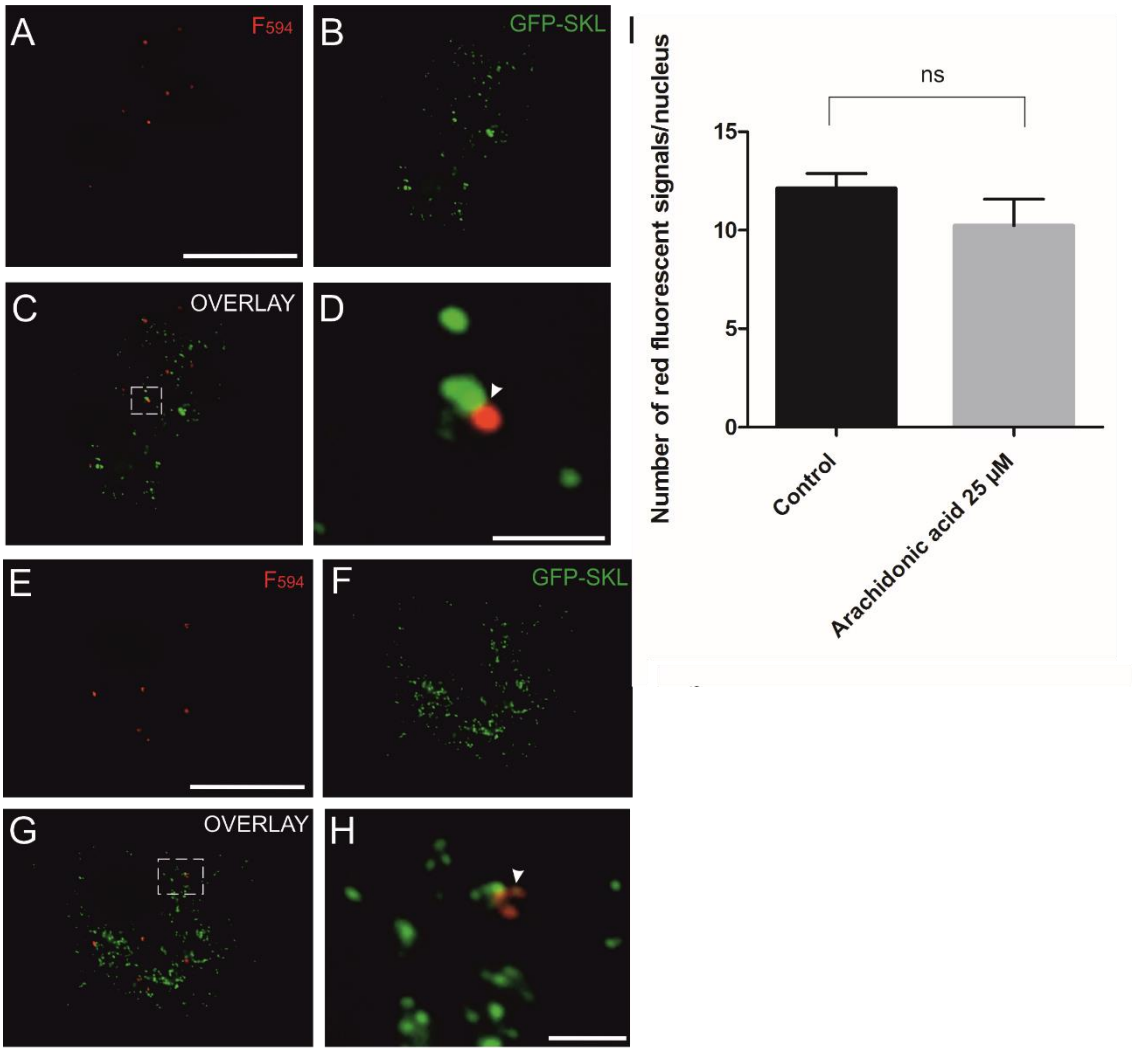

Fig. 5.4. **Addition of excess arachidonic acid does not change the number of fluorescent signals formed by the Duolink® assay.** (A) Control COS-7-GFP-SKL cells were treated with ethanol. The Duolink® assay was performed using ACBD5 and VAPB as target proteins. Proximity between peroxisomes and the ER is depicted as red fluorescent signals. (B) Peroxisomes labelled with GFP-SKL. (C) Overlay of red fluorescent signals from the Duolink® assay with labelled peroxisomes (D) Zoom of (C), arrow indicates close proximity of red fluorescent Duolink® signals with peroxisomes (E) COS-7-GFP-SKL cells treated with 25 µM arachidonic acid. The Duolink® assay was performed using ACBD5 and VAPB as target proteins. Proximity between peroxisomes and the ER is depicted as red fluorescent signals. (F) Peroxisomes labelled with GFP-SKL. (G) Overlay of red fluorescent signals from the Duolink® assay with labelled peroxisomes. (H) Zoom of (G), arrow indicates close proximity of

fluorescent signals with peroxisomes. Scale bars (main): 20µm (zoom): 2µm. (I) Quantitative analysis of the number of red fluorescent signals produced per cell (nucleus) following the use of the Duolink® assay to assess the change in the number of peroxisome-ER contact sites following treatment with excess arachidonic acid. Data are presented as mean ± SEM. Data were analysed with a two-tailed, unpaired *t* test (ns, not significant). n = 30 cells. Data shown are the result of three independent experiments.

5.3.5. Nutrient starvation has no effect on the number of peroxisome-ER contact sites formed that can be visualised by split fluorescent protein technology:

Following transfection with the spGFP fragments and nutrient starvation, 30 cells were analysed from both control and starved culture conditions. The number of peroxisomes and the number of fluorescent signals produced from the recombined spGFP fragments (representing peroxisome-ER contact sites) were quantified. The number of peroxisomes appeared to decrease following starvation compared to control cells (99.56 ± 19.64 control, 65.5 ± 15.5 starved), however, this reduction in number was not significant. The number of fluorescent signals per cell (nucleus) also decreased following starvation (69.69 ± 16.83 control, 40.67 ± 6.9 starved) however, this reduction was also not significant. The percentage of peroxisomes in contact with the ER remained relatively constant (73.25 ± 8.59% control, 81.04 ± 12.08% starvation - ns) (Fig. 5.5).

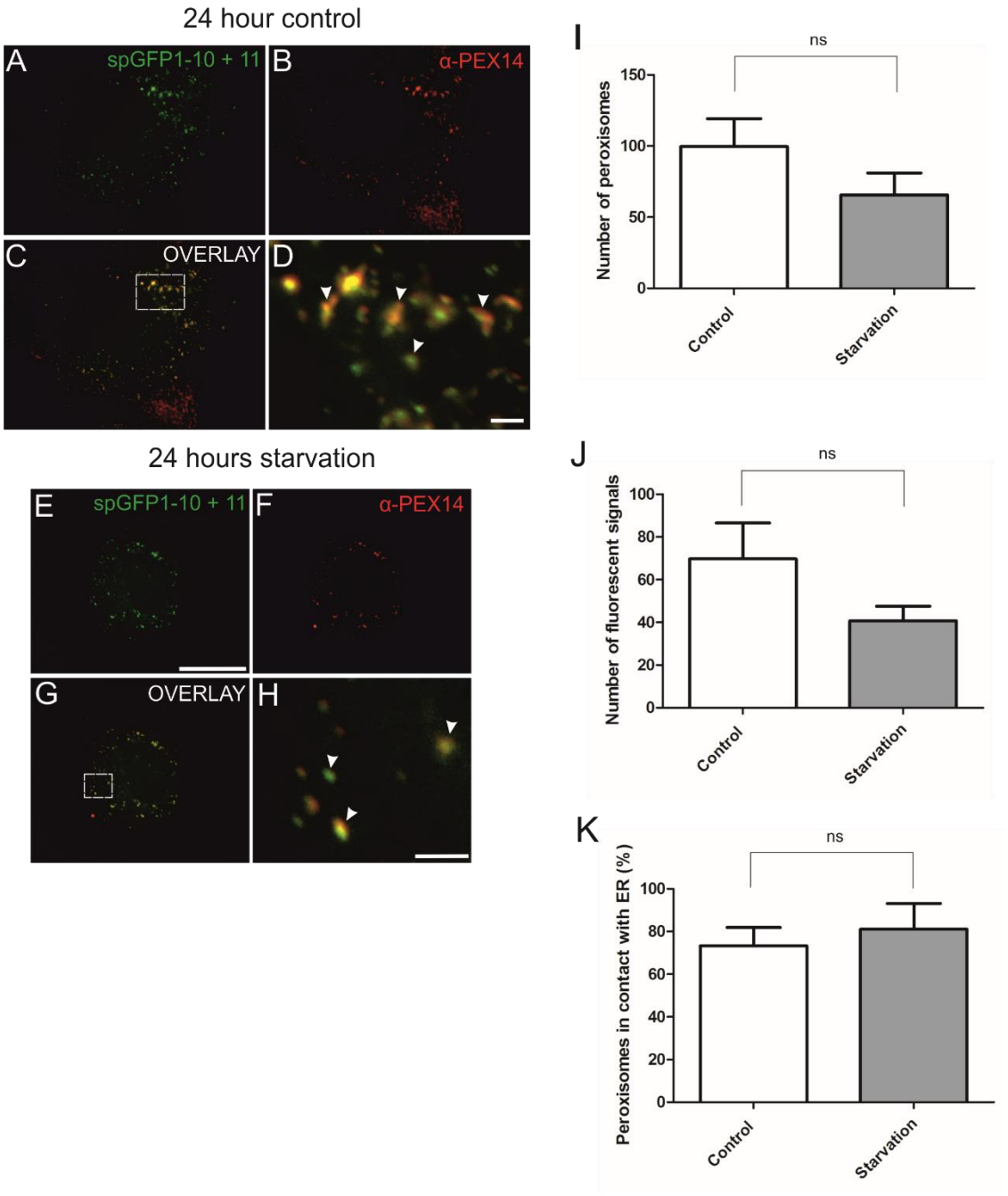

Fig. 5.5. **Nutrient starvation does not affect the number of peroxisome-ER contacts reported by the spGFP system.** (A) Control COS-7 cells transfected with spGFP1-10 and spGFP11x7. (B) Peroxisomes labelled with PEX14. (C) Overlay of green fluorescent signals from the recombined spGFP fragments with labelled peroxisomes. (D) Zoom of (C), arrows indicate co-localisation of fluorescent signals with peroxisomes. (E) COS-7 cells starved for 24 hours transfected with spGFP1-10 and spGFP11x7. (F) Peroxisomes labelled with PEX14. (G) Overlay of green fluorescent signals from the recombined spGFP fragments with labelled peroxisomes. (H) Zoom of (G), arrows indicate co-

localisation of fluorescent signals with peroxisomes. Scale bars (main): 20µm (zoom): 2µm. (I) Quantification of the number of peroxisomes between control and starved cells. (J) Quantification of the number of fluorescent signals formed per cell (nucleus) following recombination of the spGFP fragments between control and starved cells. (K) Comparison of the percentage of peroxisomes in contact with the ER as reported by the spGFP system between control and starved cells. Data are presented as mean ± SEM. Data were analysed with a two-tailed, unpaired *t* test (ns, not significant). n = 30 cells. Data shown are the result of one experiment.

5.4 Discussion:

Although much progress has been made in understanding the structure of peroxisome-ER contact sites, the physiological roles of these sites have yet to be uncovered. Following from the success of using both the Duolink® and spGFP systems to study peroxisome-ER interactions, it was hypothesised that these systems could be used to help uncover the physiological roles of this inter-organelle contact.

It was evident from results obtained earlier in this study that the Duolink® system is capable of reporting a significant increase in the number of peroxisome-ER contacts formed in a cell following protein overexpression (Fig. 3.3, Fig.3.4). For this reason, the Duolink® system was employed to assess the effect of adding an excess of oleic acid to the cells on the number of peroxisome-ER contacts formed. It was hypothesised that this would increase the number of peroxisome-ER contacts due to the suggestion that cooperation between these organelles may be implicated in fatty acid β-oxidation. However, following the addition of oleic acid to cells, no significant change was observed in the number of fluorescent signals produced in control cells and treated cells, suggesting no change in the number of peroxisome-ER contact sites formed (Fig. 5.3). The concentration of fatty acid used was shown to have an effect on the cell by inducing an increase in the size of cellular lipid droplets (Fig. 5.1), therefore, it can be ruled out that the lack of change observed in the results is due to insufficient concentrations of the fatty acid. It is possible that oleic acid is not of a sufficient chain length that would be metabolised in peroxisomes. It is known that peroxisomes only break down fatty acids of a chain length of ≥C22 (Wanders, 2004), however, the chain length of oleic acid is only C18. Thus, it is possible that addition of this fatty acid may impact mitochondrial fatty acid β-oxidation, which metabolises fatty acids of this chain length (Wanders *et al.*, 2001a), but not that which occurs in peroxisomes. Before ruling out the involvement of peroxisome-ER contacts in β-oxidation, it would be interesting to investigate the effect of adding an excess of a fatty acid with a longer chain length, in particular, C26 fatty acids, as such have shown elevated levels in a patient with a lack of function mutation in ACBD5 (Ferdinandusse *et al.*, 2017; Yagita *et al.*, 2017a). Moreover, it has been hypothesised that C26-CoA binds directly to ACBD5 before being shuttled into peroxisomes for β-oxidation

(Ferdinandusse *et al.*, 2017). It would also be useful to investigate the effect of adding C24:0-CoA as ACBD5 has also been shown to preferentially bind to this substrate (Yagita *et al.*, 2017).

The effect of adding excess arachidonic acid was subsequently investigated in this study. It was shown that, at concentrations of 25 µM, peroxisomal tubulation was induced (Fig. 5.2). This indicated that peroxisome proliferation may have been triggered as this morphology is induced during early stages of peroxisome biogenesis (Schrader *et al.,* 2012). Therefore, this suggested that there may be an increase in the number of contacts formed between peroxisomes and the ER as cooperation between these organelles is known to be involved in peroxisome biogenesis (Raychaudhuri and Prinz, 2008). However, when analysed with the Duolink® assay, there was no significant change in the number of fluorescent signals produced between treated and untreated cells, suggesting no change in the number of peroxisome-ER contact sites formed (Fig. 5.4). It is possible that the ACBD5/VAPB-mediated contact sites that were investigated in this case, are not involved in the transfer of membrane lipids for peroxisome biogenesis, therefore, there was no visible increase in the number of these sites. It is also possible, with both arachidonic and oleic acid treatment, that the increase in the number of peroxisome-ER contact sites formed following stimulation was not sufficient to produce a significant increase in the number of fluorescent signals formed using the Duolink® assay. This is because it was observed earlier in this study that the number of fluorescent signals produced using this system is not identical to the actual number of peroxisome-ER contact sites in a cell. Therefore, it may be possible that only a small increase in contact sites may not be represented by an increase in fluorescent signals using this system.

The effect of nutrient starvation on the number of peroxisome-ER contact sites formed was also assessed. In this case, it was decided to investigate this effect by using the spGFP system. It was not known whether nutrient starvation would have any effect on the number of peroxisome-ER contacts formed. It was found that the number of peroxisomes per cell (nucleus) and the number of fluorescent signals, indicating the number of peroxisome-ER contact sites formed, appear to reduce following starvation. Although the result appears to be approaching significance, the change was not significant (Fig. 5.5). Accordingly, the percentage of peroxisomes in contact with the ER did not change

significantly between starved and control cells (Fig. 5.5). As this experiment was only conducted once, it is possible that repeats could help to clarify this. It has been shown in previous studies that 24 hours starvation is a sufficient period of time to observe an effect on the number of peroxisomes in a cell (Sargent *et al.*, 2016), however, that study was conducted in HeLa cells, therefore, the period of starvation used in this study may not have been a suitable time frame to see an effect in COS-7 cells. Our current understanding of the function of peroxisome-ER contact sites under conditions of cellular stress is not extensive. Therefore, it was hoped that the use of this system in this way may shed light on their role in these processes. However, from this data it can be suggested that either peroxisome-ER contact sites do not play a role in the response to cellular stresses such as nutrient starvation, or expression of the spGFP system affects the intrinsic biological response, potentially due to irreversible binding of the fragments. The latter, however, should be unlikely as changes in the number of contact sites following starvation and refeeding has been shown to occur using the spGFP system to study mitochondria-ER contact sites in the past (Yang *et al.*, 2018). Nonetheless, it is still not clear from previous data in this study whether peroxisome-ER contact sites are subject to artificial tethering following expression of this system. Moreover, even if the system is reversible, the stable nature of the resulting refolded GFP might make subtle changes in contacts difficult to detect. In the future, this experiment should be repeated using the Duolink® assay to rule out the potential of disruption through spGFP expression. It would also be useful to assess the level of spGFP expression in both control and starved cells, using western blotting, to confirm that the level of expression does not change in these conditions, as this could affect the results observed.

No significant changes in the number of peroxisome-ER contact sites was observed in these data. Unlike contact sites between organelles such as mitochondria and the ER, which are very well characterised, contact sites between peroxisomes and the ER have only recently been discovered in mammalian cells and little is known about their function. Therefore, it was difficult to know which stimuli would affect these structures. For this reason, it is unclear whether the lack of change seen in these data was due to limitations of the systems used, or perhaps the stimuli tested were not those that would affect

contact site formation between the organelles. In the case of Duolink®, data in this study has shown that an increase in the number of contact sites formed can easily be reported by an increase in fluorescence signals using the assay, however, as mentioned previously, it is not known whether small changes can be detected by the assay. Moreover, as the spGFP system has been successfully used in the past to investigate changes in contact site formation following changes in physiological cellular conditions, it is unlikely that the systems used here are to blame for the apparent lack of change observed.

To clarify the discrepancies seen here, it would, perhaps, be better to first use these systems to investigate a contact site function for which we have more evidence. For example, it would be interesting to use these systems to investigate the effect of altering a biochemical pathway in which cooperation between peroxisomes and the ER is known to be required and observe the effect on the number of contact sites formed. For example, cooperation between peroxisomes and the ER is known to be involved in plasmalogen biosynthesis and disruption of ACBD5-VAPA/B mediated contacts have been shown to result in a reduction in plasmalogen production (Hua *et al.*, 2017). Therefore, it would be interesting to employ the Duolink® system to assess cells from a patient suffering from RCDP as plasmalogen synthesis is impaired in this disease (Brites *et al.*, 2004).

Chapter 6:

Final conclusions and future directions.

The field of peroxisome-organelle contact sites is still very much in its beginning stages, and it is likely that we have only just touched the surface of understanding peroxisome-ER contacts. With increasing data to suggest the existence of physical contacts with other organelles, such as mitochondria and lysosomes, it has become imperative that effective and simple tools are readily available to study these interactions and uncover their function. The systems presented in this study are not only efficient and robust in their current use but are readily modifiable in order to easily allow visualisation of other contact sites, either by employing alternate target proteins in the case of Duolink®, or by altering the targeting sequences in the case of spGFP. It would also be possible to design a screening experiment to identify new proteins involved in the formation of contact sites, for example, by fusing the GFP1-10 fragments to various candidate interactors and the GFP11 fragment to an organelle of interest, or by conducting the Duolink® assay in a 96-well plate and using a variety of target proteins. This would allow simple, high-throughput screening which would be very difficult or even impossible before the advent of these systems.

An exciting future perspective for these systems would be to employ them in imaging multiple interactions in one cell. For example, the GFP1-10 fragment of the spGFP system can easily be mutated to create either a cyan fluorescent protein or yellow fluorescent protein (Kamiyama *et al.*, 2016). This could be targeted to mitochondria with the ER-targeted spGFP11 fragment, for instance, alongside the peroxisome-ER spGFP system in this study to allow simultaneous detection of multiple contact sites. As organelles are known to cooperate extensively, this could be useful in determining how changes in one contact site could affect another. Moreover, this could help elucidate the role of multiple organelle interactions in one process. For example, β-oxidation of fatty acids is known to require cooperation between peroxisomes and mitochondria (Wanders *et al.*, 2001a) and also may require involvement from the ER (Ferdinandusse *et al.*, 2017). Using this system to detect changes in contact site formation between the respective organelles could aid in characterising the role contact sites play in this essential process. It would also be possible to employ the Duolink® system in this way as there is a variety of fluorophore colours that can be used with the system.

Moreover, with the increasing relevance of these sites in health and disease, these systems would make it possible to screen patient cells in order to assess whether the symptoms observed are, in fact, due to a defect in contact site formation between peroxisomes and the ER. For this, the Duolink® system could be used to assess ACBD5/VAPB-mediated peroxisome-ER interactions in a variety of patient cell samples in a 96-well plate to enable high-throughput, rapid screening without the need for full genomic analysis of the patients.

Of course, no single technique to study protein or organelle interactions is gold-standard, as shown in this study and many others, each has their own individual strengths and limitations, and the optimisation of these systems is still an on-going process. At this current time, it can be suggested that the strengths and limitations of these systems may render them better suited to different purposes. The key differences between the Duolink® and spGFP system are summarised in Table 6.1.

Table 6.1. A summary of the key differences between Duolink® and spGFP technologies.

	Duolink®	spGFP
Can be used in fixed cell studies	✔	✔
Can be used in live cell studies	X	✔
Can be used on clinical samples	✔	X
Requires transfection	X	✔
Requires specific antibodies	✔	X
Representative of the actual number of contact sites in a cell	X	✔

One general limitation of the present study is that the only imaging performed for the quantitative analysis of fluorescent signals in both the Duolink® and spGFP systems was fluorescence microscopy. This type of imaging only images a single plane, however, when focusing on the cells, it was evident that fluorescent signals could be observed in different focal planes. As quantification of the fluorescent signals was performed using the resulting fluorescent microscopy images, it is possible that fluorescent signals in other focal planes may not have be counted. To overcome this issue in future studies, confocal microscopy could be used as this would enable imaging of several focal planes, allowing all the fluorescent signals produced from either system to be quantified (Jonkman and Brown, 2015). Additionally, it may be possible to analyse the resulting fluorescence from the cells using flow cytometry as this would avoid any discrepancies in imaging or the quantification of fluorescent signals. Indeed, this has been carried out successfully in a study using Duolink® to study protein interactions (Mocanu *et al.*, 2011). Moreover, Sigma-Aldrich now sell a Duolink® kit optimised for analysis in this way, called flowPLA, making this process incredibly simple to carry out (*Duolink® PLA Technology - Protein Interaction | Sigma-Aldrich*, 2017). In addition, flow cytometry analysis could also be used to assess spGFP fluorescent signals.

Both Duolink® and the spGFP system presented in this study have been shown to allow effective visualisation and quantification of peroxisome-ER contact sites, enabling simple, rapid and, importantly, *in situ* visualisation of these sites which has never before been possible. Both systems used here are significantly more straightforward and affordable long-term than many other commonly used methods, like EM and are much easier to image with lower false-positive rates than systems such as FRET. Moreover, both systems are easily modifiable to enable the detection of other contact sites between these organelles, and contact sites between peroxisomes and other organelles allowing them to adapt to the needs of future research. Like all techniques to study organelle interactions, both systems also have their potential caveats and are, accordingly, better suited to different purposes. Nevertheless, these systems represent excellent additions to the toolbox for the study of peroxisome-ER contact sites.

Bibliography:

Abu-Safieh, L. *et al.* (2013) 'Autozygome-guided exome sequencing in retinal dystrophy patients reveals pathogenetic mutations and novel candidate disease genes.', *Genome research*. Cold Spring Harbor Laboratory Press, 23(2), pp. 236–47. doi: 10.1101/gr.144105.112.

Van Ael, E. and Fransen, M. (2006) 'Targeting signals in peroxisomal membrane proteins.', *Biochimica et biophysica acta*, 1763(12), pp. 1629–1638. doi: 10.1016/j.bbamcr.2006.08.020.

Alford, S. C. *et al.* (2012a) 'Dimerization-dependent green and yellow fluorescent proteins.', *ACS synthetic biology*. PMC Canada manuscript submission, 1(12), pp. 569–75. doi: 10.1021/sb300050j.

Alford, S. C. *et al.* (2012b) 'A fluorogenic red fluorescent protein heterodimer.', *Chemistry & biology*. PMC Canada manuscript submission, 19(3), pp. 353–60. doi: 10.1016/j.chembiol.2012.01.006.

Aranovich, A. *et al.* (2014) 'PEX16 contributes to peroxisome maintenance by constantly trafficking PEX3 via the ER.', *Journal of cell science*. The Company of Biologists Ltd, 127(Pt 17), pp. 3675–86. doi: 10.1242/jcs.146282.

Aubourg, P. and Wanders, R. (2013) 'Peroxisomal disorders', *Handbook of Clinical Neurology*. Elsevier, 113, pp. 1593–1609. doi: 10.1016/B978-0-444-59565-2.00028-9.

Barondeau, D. P. *et al.* (2003) 'Mechanism and energetics of green fluorescent protein chromophore synthesis revealed by trapped intermediate structures.', *Proceedings of the National Academy of Sciences of the United States of America*. National Academy of Sciences, 100(21), pp. 12111–6. doi: 10.1073/pnas.2133463100.

Beller, M. *et al.* (2010) 'Lipid droplets: A dynamic organelle moves into focus', *FEBS Letters*. Wiley-Blackwell, 584(11), pp. 2176–2182. doi: 10.1016/j.febslet.2010.03.022.

Bellucci, A. *et al.* (2014) 'The "In Situ" Proximity Ligation Assay to Probe Protein–Protein Interactions in Intact Tissues', in. Humana Press, New York, NY, pp. 397–405. doi: 10.1007/978-1-4939-0944-5_27.

Bernhard, W. and Rouiller, C. (1956) ‘Close topographical relationship between mitochondria and ergastoplasm of liver cells in a definite phase of cellular activity.’, *The Journal of biophysical and biochemical cytology*. Rockefeller University Press, 2(4 Suppl), pp. 73–8. doi: 10.1083/JCB.2.4.73.

Bolte, K. *et al.* (2015) ‘The evolution of eukaryotic cells from the perspective of peroxisomes’, *BioEssays*. Wiley-Blackwell, 37(2), pp. 195–203. doi: 10.1002/bies.201400151.

Bonekamp, N. A. *et al.* (2009) ‘Reactive oxygen species and peroxisomes: struggling for balance.’, *BioFactors*, 35(4), pp. 346–355. doi: 10.1002/biof.48.

Bonekamp, N. A. *et al.* (2012) ‘Transient complex interactions of mammalian peroxisomes without exchange of matrix or membrane marker proteins.’, *Traffic (Copenhagen, Denmark)*, 13(7), pp. 960–978. doi: 10.1111/j.1600-0854.2012.01356.x.

Bowen, P. *et al.* (1964) ‘A familial syndrome of multiple congenital defects.’, *Bulletin of the Johns Hopkins Hospital*, 114, pp. 402–14. Available at: http://www.ncbi.nlm.nih.gov/pubmed/14169466 (Accessed: 24 July 2018).

Braverman, N. E. *et al.* (2013) ‘Peroxisome biogenesis disorders: Biological, clinical and pathophysiological perspectives’, *Developmental Disabilities Research Reviews*. Wiley-Blackwell, 17(3), pp. 187–196. doi: 10.1002/ddrr.1113.

Braverman, N. E. and Moser, A. B. (2012) ‘Functions of plasmalogen lipids in health and disease.’, *Biochimica et biophysica acta*. Elsevier B.V. doi: 10.1016/j.bbadis.2012.05.008.

Brites, P. *et al.* (2004) ‘Functions and biosynthesis of plasmalogens in health and disease’, *Biochimica et Biophysica Acta (BBA) - Molecular and Cell Biology of Lipids*. Elsevier, 1636(2–3), pp. 219–231. doi: 10.1016/J.BBALIP.2003.12.010.

Brown, A. J. and Snyder, F. (1982) ‘Alkyldihydroxyacetone-P synthase. Solubilization, partial purification, new assay method, and evidence for a ping-pong mechanism.’, *The Journal of biological chemistry*, 257(15), pp. 8835–9. Available at: http://www.ncbi.nlm.nih.gov/pubmed/7096336 (Accessed: 9 August 2018).

Cabantous, S. *et al.* (2005) ‘Protein tagging and detection with engineered self-assembling fragments of green fluorescent protein’, *Nature Biotechnology*. Nature Publishing Group, 23(1), pp. 102–107. doi: 10.1038/nbt1044.

Castro, I. G. *et al.* (2018a) ‘A role for Mitochondrial Rho GTPase 1 (MIRO1) in motility and membrane dynamics of peroxisomes’, *Traffic*, 19(3), pp. 229–242. doi: 10.1111/tra.12549.

Castro, I. G. *et al.* (2018b) ‘Mind the Organelle Gap – Peroxisome Contact Sites in Disease’, *Trends in Biochemical Sciences*. Elsevier Current Trends, 43(3), pp. 199–210. doi: 10.1016/J.TIBS.2018.01.001.

Celler, K. *et al.* (2016) ‘Microtubules in Plant Cells: Strategies and Methods for Immunofluorescence, Transmission Electron Microscopy, and Live Cell Imaging.’, *Methods in molecular biology (Clifton, N.J.)*. Europe PMC Funders, 1365, pp. 155–84. doi: 10.1007/978-1-4939-3124-8_8.

Chaffey, N. (2010) ‘Plant Cuttings’, *Annals of Botany*. Oxford University Press, 106(6), pp. iv–vi. doi: 10.1093/aob/mcq231.

Cho, D.-H. *et al.* (2018) ‘Pexophagy: Molecular Mechanisms and Implications for Health and Diseases.’, *Molecules and cells*. Korean Society for Molecular and Cellular Biology, 41(1), pp. 55–64. doi: 10.14348/molcells.2018.2245.

Choudhary, O. P. and Priyanka (2017) ‘Scanning Electron Microscope: Advantages and Disadvantages in Imaging Components’, *International Journal of Current Microbiology and Applied Sciences*, 6(5), pp. 1877–1882. doi: 10.20546/ijcmas.2017.605.207.

Chu, B.-B. *et al.* (2015) ‘Cholesterol Transport through Lysosome-Peroxisome Membrane Contacts’, *Cell*. Elsevier Inc., 161(2), pp. 291–306. doi: 10.1016/j.cell.2015.02.019.

Cieri, D. *et al.* (2018) ‘SPLICS: a split green fluorescent protein-based contact site sensor for narrow and wide heterotypic organelle juxtaposition’, *Cell Death & Differentiation*. Nature Publishing Group, 25(6), pp. 1131–1145. doi: 10.1038/s41418-017-0033-z.

Cohen, S. *et al.* (2018) ‘Interacting organelles’, *Current Opinion in Cell Biology*. Elsevier Current Trends, 53, pp. 84–91. doi: 10.1016/J.CEB.2018.06.003.

Cohen, Y. *et al.* (2014) ‘Peroxisomes are juxtaposed to strategic sites on mitochondria.’, *Molecular bioSystems*, 10(7), pp. 1742–1748. doi: 10.1039/c4mb00001c.

Copeland, D. E. and Dalton, A. J. (1959) ‘An association between mitochondria and the endoplasmic reticulum in cells of the pseudobranch gland of a teleost.’, *The Journal of biophysical and biochemical cytology*. Rockefeller University Press, 5(3), pp. 393–6. doi: 10.1083/JCB.5.3.393.

Costello, J. L. *et al.* (2017a) ‘ACBD5 and VAPB mediate membrane associations between peroxisomes and the ER.’, *The Journal of cell biology*. Rockefeller University Press, 216(2), pp. 331–342. doi: 10.1083/jcb.201607055.

Costello, J. L. *et al.* (2017b) ‘Peroxisomal ACBD4 interacts with VAPB and promotes ER-peroxisome associations.’, *Cell cycle (Georgetown, Tex.)*. Taylor & Francis, 16(11), pp. 1039–1045. doi: 10.1080/15384101.2017.1314422.

Costello, J. L. *et al.* (2017c) ‘Predicting the targeting of tail-anchored proteins to subcellular compartments in mammalian cells.’, *Journal of cell science*. Company of Biologists, 130(9), pp. 1675–1687. doi: 10.1242/jcs.200204.

Costello, J. L. and Schrader, M. (2018) ‘Unloosing the Gordian knot of peroxisome formation’, *Current Opinion in Cell Biology*. Elsevier Current Trends, 50, pp. 50–56. doi: 10.1016/J.CEB.2018.02.002.

Crameri, A. *et al.* (1996) ‘Improved Green Fluorescent Protein by Molecular Evolution Using DNA Shuffling’, *Nature Biotechnology*. Nature Publishing Group, 14(3), pp. 315–319. doi: 10.1038/nbt0396-315.

Csordás, G. *et al.* (2006) ‘Structural and functional features and significance of the physical linkage between ER and mitochondria.’, *The Journal of cell biology*. Rockefeller University Press, 174(7), pp. 915–21. doi: 10.1083/jcb.200604016.

Csordás, G. *et al.* (2010) ‘Imaging Interorganelle Contacts and Local Calcium Dynamics at the ER-Mitochondrial Interface’, *Molecular Cell*. Cell Press, 39(1), pp. 121–132. doi: 10.1016/J.MOLCEL.2010.06.029.

Datta, S. C. *et al.* (1990) ‘Purification and properties of acyl/alkyl dihydroxyacetone-phosphate reductase from guinea pig liver peroxisomes.’, *The Journal of biological chemistry*, 265(14), pp. 8268–74. Available at:

http://www.ncbi.nlm.nih.gov/pubmed/2335525 (Accessed: 9 August 2018).

David, C. *et al.* (2013) 'A combined approach of quantitative interaction proteomics and live-cell imaging reveals a regulatory role for endoplasmic reticulum (ER) reticulon homology proteins in peroxisome biogenesis.', *Molecular & cellular proteomics : MCP*, 12, pp. 2408–2425. doi: 10.1074/mcp.M112.017830.

Delille, H. K. *et al.* (2006) 'Peroxisomes and Disease-an Overview', *International Journal of biomedical science*, 2(4), pp. 308–314. Available at: http://www.ijbs.org/User/ContentFullText.aspx?VolumeNO=2&StartPage=308.

Delille, H. K. *et al.* (2010) 'Pex11pbeta-mediated growth and division of mammalian peroxisomes follows a maturation pathway.', *Journal of cell science*, 123(Pt 16), pp. 2750–2762. doi: 10.1242/jcs.062109.

Deosaran, E. *et al.* (2013) 'NBR1 acts as an autophagy receptor for peroxisomes.', *Journal of cell science*, 126(Pt 4), pp. 939–952. doi: 10.1242/jcs.114819.

Dirkx, R. *et al.* (2005) 'Absence of peroxisomes in mouse hepatocytes causes mitochondrial and ER abnormalities.', *Hepatology (Baltimore, Md.)*, 41(4), pp. 868–878. doi: 10.1002/hep.20628.

Dresser, M. E. (2001) 'Electron Microscopy', *Encyclopedia of Genetics*. Academic Press, pp. 605–608. doi: 10.1006/RWGN.2001.0398.

Duolink® PLA Technology - Protein Interaction | Sigma-Aldrich (2017). Available at: https://www.sigmaaldrich.com/life-science/molecular-biology/molecular-biology-products.html?TablePage=112232138 (Accessed: 5 September 2018).

De Duve, C. and Baudhuin, P. (1966) 'Peroxisomes (microbodies and related particles).', *Physiological Reviews*. Am Physiological Soc, 46(2), pp. 323–357.

Ebberink, M. S. *et al.* (2012) 'A novel defect of peroxisome division due to a homozygous non-sense mutation in the PEX11$β$ gene.', *Journal of medical genetics*, pp. 307–313. doi: 10.1136/jmedgenet-2012-100778.

Eisenberg-Bord, M. *et al.* (2016) 'A Tether Is a Tether Is a Tether: Tethering at Membrane Contact Sites', *Developmental Cell*. Cell Press, 39(4), pp. 395–409.

doi: 10.1016/J.DEVCEL.2016.10.022.

Elbaz-Alon, Y. *et al.* (2014) 'A Dynamic Interface between Vacuoles and Mitochondria in Yeast', *Developmental Cell*. Cell Press, 30(1), pp. 95–102. doi: 10.1016/J.DEVCEL.2014.06.007.

Van Engelenburg, S. B. and Palmer, A. E. (2010) 'Imaging type-III secretion reveals dynamics and spatial segregation of Salmonella effectors', *Nature Methods*. Nature Publishing Group, 7(4), pp. 325–330. doi: 10.1038/nmeth.1437.

Erdmann, R. and Schliebs, W. (2005) 'Peroxisomal matrix protein import: the transient pore model', *Nature Reviews Molecular Cell Biology*, 6, pp. 738–742. Available at: http://www.nature.com/nrm/journal/v6/n9/abs/nrm1710.html.

Ernster, L. and Schatz, G. (1981) 'Mitochondria: a historical review.', *The Journal of cell biology*, 91(3 Pt 2), p. 227s–255s. Available at: http://www.ncbi.nlm.nih.gov/pubmed/7033239 (Accessed: 24 August 2018).

Fahimi, H. D. (1968) 'Cytochemical localization of peroxidase activity in rat hepatic microbodies (peroxisomes)', *Journal of Histochemistry & Cytochemistry*, 16(8), pp. 547–550. doi: 10.1177/16.8.547.

Fahimi, H. D. and Yokota, S. (1981) 'Ultrastructural and Cytochemical Aspects of Animal Peroxisomes — Some Recent Observations', in *International Cell Biology 1980–1981*. Berlin, Heidelberg: Springer Berlin Heidelberg, pp. 640–650. doi: 10.1007/978-3-642-67916-2_71.

Fan, J. *et al.* (2016) 'ACBD2/ECI2-Mediated Peroxisome-Mitochondria Interactions in Leydig Cell Steroid Biosynthesis.', *Molecular endocrinology (Baltimore, Md.)*. The Endocrine Society, 30(7), pp. 763–82. doi: 10.1210/me.2016-1008.

Fang, Y. *et al.* (2004) 'PEX3 functions as a PEX19 docking factor in the import of class I peroxisomal membrane proteins', *J Cell Biol*. 2004/03/10, 164(6), pp. 863–875. doi: 10.1083/jcb.200311131 jcb.200311131 [pii].

Feinberg, E. H. *et al.* (2008) 'GFP Reconstitution Across Synaptic Partners (GRASP) Defines Cell Contacts and Synapses in Living Nervous Systems', *Neuron*. Cell Press, 57(3), pp. 353–363. doi: 10.1016/J.NEURON.2007.11.030.

Ferdinandusse, S. *et al.* (2000) ‘Mutations in the gene encoding peroxisomal α-methylacyl-CoA racemase cause adult-onset sensory motor neuropathy’, *Nature Genetics*. Nature Publishing Group, 24(2), pp. 188–191. doi: 10.1038/72861.

Ferdinandusse, S. *et al.* (2006) ‘Mutations in the Gene Encoding Peroxisomal Sterol Carrier Protein X (SCPx) Cause Leukencephalopathy with Dystonia and Motor Neuropathy’, *The American Journal of Human Genetics*, 78(6), pp. 1046–1052. doi: 10.1086/503921.

Ferdinandusse, S. *et al.* (2017) ‘ACBD5 deficiency causes a defect in peroxisomal very long-chain fatty acid metabolism.’, *Journal of medical genetics*. BMJ Publishing Group Ltd, 54(5), pp. 330–337. doi: 10.1136/jmedgenet-2016-104132.

Fransen, M. *et al.* (1998) ‘Identification of a human PTS1 receptor docking protein directly required for peroxisomal protein import.’, *Proceedings of the National Academy of Sciences of the United States of America*. National Academy of Sciences, 95(14), pp. 8087–92. Available at: http://www.ncbi.nlm.nih.gov/pubmed/9653144 (Accessed: 2 July 2018).

Fransen, M. *et al.* (2012) ‘Role of peroxisomes in ROS/RNS-metabolism: Implications for human disease’, *Biochimica et biophysica acta*. Elsevier B.V., 1822(9), pp. 1363–1373. doi: 10.1016/j.bbadis.2011.12.001.

Fredriksson, S. *et al.* (2002) ‘Protein detection using proximity-dependent DNA ligation assays’, *Nature Biotechnology*. Nature Publishing Group, 20(5), pp. 473–477. doi: 10.1038/nbt0502-473.

Friedman, J. R. *et al.* (2011) ‘ER tubules mark sites of mitochondrial division.’, *Science (New York, N.Y.)*, 334(6054), pp. 358–362. doi: 10.1126/science.1207385.

Fujiki, Y. *et al.* (2006) ‘Import of peroxisomal membrane proteins: The interplay of Pex3p- and Pex19p-mediated interactions’, *Biochimica et Biophysica Acta - Molecular Cell Research*, 1763(12), pp. 1639–1646. doi: 10.1016/j.bbamcr.2006.09.030.

Gärtner, J. *et al.* (2002) ‘Functional characterization of the adrenoleukodystrophy protein (ALDP) and disease pathogenesis.’, *Endocrine*

research, 28(4), pp. 741–8. Available at: http://www.ncbi.nlm.nih.gov/pubmed/12530690 (Accessed: 2 July 2018).

Gatta, A. T. and Levine, T. P. (2017) 'Piecing Together the Patchwork of Contact Sites', *Trends in Cell Biology*. Elsevier Current Trends, 27(3), pp. 214–229. doi: 10.1016/J.TCB.2016.08.010.

Geillon, F. *et al.* (2017) 'Peroxisomal ATP-binding cassette transporters form mainly tetramers.', *The Journal of biological chemistry*. American Society for Biochemistry and Molecular Biology, 292(17), pp. 6965–6977. doi: 10.1074/jbc.M116.772806.

Ghosh, I. *et al.* (2000) 'Antiparallel Leucine Zipper-Directed Protein Reassembly: Application to the Green Fluorescent Protein'. American Chemical Society. doi: 10.1021/JA994421W.

Ghosh, M. K. and Hajra, A. K. (1986) 'Subcellular distribution and properties of acyl/alkyl dihydroxyacetone phosphate reductase in rodent livers', *Archives of Biochemistry and Biophysics*. Academic Press, 245(2), pp. 523–530. doi: 10.1016/0003-9861(86)90245-6.

Goldberg, M. W. and Fiserova, J. (2010) 'Immunogold Labelling for Scanning Electron Microscopy', in. Humana Press, Totowa, NJ, pp. 297–313. doi: 10.1007/978-1-60761-783-9_24.

Goldfischer, S. *et al.* (1973) 'Peroxisomal and mitochondrial defects in the cerebro-hepato-renal syndrome.', *Science (New York, N.Y.)*, 182(4107), pp. 62–4. Available at: http://www.ncbi.nlm.nih.gov/pubmed/4730055 (Accessed: 24 July 2018).

Gomez-Suaga, P. *et al.* (2017) 'The ER-Mitochondria Tethering Complex VAPB-PTPIP51 Regulates Autophagy.', *Current biology : CB*. Elsevier, 27(3), pp. 371–385. doi: 10.1016/j.cub.2016.12.038.

Gordon, J. A. *et al.* (1994) 'Formation and release of a peroxisome-dependent arachidonic acid metabolite by human skin fibroblasts.', *The Journal of biological chemistry*, 269(6), pp. 4103–9. Available at: http://www.ncbi.nlm.nih.gov/pubmed/8307970 (Accessed: 7 September 2018).

Gould, S. G. *et al.* (1987) 'Identification of a peroxisomal targeting signal at the

carboxy terminus of firefly luciferase.', *The Journal of cell biology*. The Rockefeller University Press, 105(6 Pt 2), pp. 2923–31. Available at: http://www.ncbi.nlm.nih.gov/pubmed/3480287 (Accessed: 22 June 2018).

Gould, S. B. *et al.* (2016) 'Bacterial vesicle secretion and the evolutionary origin of the 1 eukaryotic endomembrane system 2 3 4', *Trends in Microbiology*. Elsevier Ltd, pp. 1–10. doi: 10.1016/j.tim.2016.03.005.

Gould, S. J. and Valle, D. (2000) 'Peroxisome biogenesis disorders: genetics and cell biology.', *Trends in genetics : TIG*, 16(8), pp. 340–345. Available at: http://www.ncbi.nlm.nih.gov/pubmed/10904262.

Grabenbauer, M. *et al.* (2000) 'Three-dimensional ultrastructural analysis of peroxisomes in HepG2 cells. Absence of peroxisomal reticulum but evidence of close spatial association with the endoplasmic reticulum.', *Cell biochemistry and biophysics*, 32 Spring, pp. 37–49. Available at: http://www.ncbi.nlm.nih.gov/pubmed/11330069 (Accessed: 15 August 2018).

Gray, E. G. (1963) 'Electron microscopy of presynaptic organelles of the spinal cord.', *Journal of anatomy*. Wiley-Blackwell, 97(Pt 1), pp. 101–6. Available at: http://www.ncbi.nlm.nih.gov/pubmed/13949972 (Accessed: 10 August 2018).

Gullberg, M. and Andersson, A.-C. (2010) 'Visualization and quantification of protein-protein interactions in cells and tissues', *Nature Methods*. Nature Publishing Group, 7(6), pp. v–vi. doi: 10.1038/nmeth.f.306.

Haan, G.-J. *et al.* (2006) 'Reassembly of peroxisomes in Hansenula polymorpha pex3 cells on reintroduction of Pex3p involves the nuclear envelope.', *FEMS yeast research*, 6(2), pp. 186–194. doi: 10.1111/j.1567-1364.2006.00037.x.

Hajra, A. K. (1997) 'Dihydroxyacetone phosphate acyltransferase', *Biochimica et Biophysica Acta (BBA) - Lipids and Lipid Metabolism*. Elsevier, 1348(1–2), pp. 27–34. doi: 10.1016/S0005-2760(97)00120-3.

Halbach, A. *et al.* (2006) 'Targeting of the tail-anchored peroxisomal membrane proteins PEX26 and PEX15 occurs through C-terminal PEX19-binding sites.', *Journal of cell science*, 119(Pt 12), pp. 2508–2517. doi: 10.1242/jcs.02979.

Hara-Kuge, S. and Fujiki, Y. (2008) 'The peroxin Pex14p is involved in LC3-dependent degradation of mammalian peroxisomes', *Experimental Cell*

Research. Academic Press, 314(19), pp. 3531–3541. doi: 10.1016/J.YEXCR.2008.09.015.

Harmon, M. *et al.* (2017) 'A Bi-fluorescence complementation system to detect associations between the Endoplasmic reticulum and mitochondria', *Scientific Reports*. Nature Publishing Group, 7(1), p. 17467. doi: 10.1038/s41598-017-17278-1.

Harris, H. (2000) *The birth of the cell*. Yale University Press. Available at: https://yalebooks.yale.edu/book/9780300082951/birth-cell (Accessed: 24 August 2018).

Hasan, S. *et al.* (2013) 'Import of proteins into the peroxisomal matrix.', *Frontiers in physiology*, 4(September), p. 261. doi: 10.3389/fphys.2013.00261.

Hedskog, L. *et al.* (2013) 'Modulation of the endoplasmic reticulum-mitochondria interface in Alzheimer's disease and related models.', *Proceedings of the National Academy of Sciences of the United States of America*. National Academy of Sciences, 110(19), pp. 7916–21. doi: 10.1073/pnas.1300677110.

Heiland, I. and Erdmann, R. (2005) 'Biogenesis of peroxisomes', *FEBS Journal*. Wiley/Blackwell (10.1111), 272(10), pp. 2362–2372. doi: 10.1111/j.1742-4658.2005.04690.x.

Helle, S. C. J. *et al.* (2013) 'Organization and function of membrane contact sites', *Biochimica et Biophysica Acta (BBA) - Molecular Cell Research*. Elsevier, 1833(11), pp. 2526–2541. doi: 10.1016/J.BBAMCR.2013.01.028.

Henne, W. M. *et al.* (2015) 'Mdm1/Snx13 is a novel ER-endolysosomal interorganelle tethering protein.', *The Journal of cell biology*. Rockefeller University Press, 210(4), pp. 541–51. doi: 10.1083/jcb.201503088.

Henne, W. M. (2016) 'Organelle remodeling at membrane contact sites', *Journal of Structural Biology*. Academic Press, 196(1), pp. 15–19. doi: 10.1016/J.JSB.2016.05.003.

Herzog, K. *et al.* (2018) 'Functional characterisation of peroxisomal β-oxidation disorders in fibroblasts using lipidomics', *Journal of Inherited Metabolic Disease*. Springer Netherlands, 41(3), pp. 479–487. doi: 10.1007/s10545-017-0076-9.

Herzog, V. and Fahimi, H. D. (1976) 'Identification of peroxisomes

(microbodies) in mouse myocardium.', *Journal of molecular and cellular cardiology*. Elsevier, 8(4), pp. 271–81. doi: 10.1016/0022-2828(76)90003-1.

Hettema, E. H. *et al.* (2000) 'Saccharomyces cerevisiae pex3p and pex19p are required for proper localization and stability of peroxisomal membrane proteins.', *The EMBO journal*. European Molecular Biology Organization, 19(2), pp. 223–33. doi: 10.1093/emboj/19.2.223.

Hettema, E. H. *et al.* (2014) 'Evolving models for peroxisome biogenesis', *Current opinion in cell biology*. Elsevier Ltd, 29, pp. 25–30. doi: 10.1016/j.ceb.2014.02.002.

Heymans, H. S. *et al.* (1985) 'Rhizomelic chondrodysplasia punctata: another peroxisomal disorder.', *The New England journal of medicine*, 313(3), pp. 187–8. Available at: http://www.ncbi.nlm.nih.gov/pubmed/4010717 (Accessed: 25 July 2018).

Hicks, L. and Fahimi, H. D. (1977) 'Peroxisomes (microbodies) in the myocardium of rodents and primates', *Cell and Tissue Research*. Springer-Verlag, 175(4), pp. 467–481. doi: 10.1007/BF00222413.

Hoepfner, D. *et al.* (2005) 'Contribution of the endoplasmic reticulum to peroxisome formation.', *Cell*, 122(1), pp. 85–95. doi: 10.1016/j.cell.2005.04.025.

Honsho, M. *et al.* (2002) 'The membrane biogenesis peroxin Pex16p. Topogenesis and functional roles in peroxisomal membrane assembly.', *The Journal of biological chemistry*. American Society for Biochemistry and Molecular Biology, 277(46), pp. 44513–24. doi: 10.1074/jbc.M206139200.

Hruban, Z. *et al.* (1972) 'Microbodies: constituent organelles of animal cells.', *Laboratory investigation; a journal of technical methods and pathology*, 27(2), pp. 184–91. Available at: http://www.ncbi.nlm.nih.gov/pubmed/5055204 (Accessed: 23 July 2018).

Hua, R. *et al.* (2015) 'Multiple Domains in PEX16 Mediate Its Trafficking and Recruitment of Peroxisomal Proteins to the ER', *Traffic*. Wiley/Blackwell (10.1111), 16(8), pp. 832–852. doi: 10.1111/tra.12292.

Hua, R. *et al.* (2017) 'VAPs and ACBD5 tether peroxisomes to the ER for peroxisome maintenance and lipid homeostasis.', *The Journal of cell biology*.

Rockefeller University Press, 216(2), pp. 367–377. doi: 10.1083/jcb.201608128.

Hyun, S.-I. *et al.* (2015) 'Topology of Endoplasmic Reticulum-Associated Cellular and Viral Proteins Determined with Split-GFP', *Traffic*. Wiley/Blackwell (10.1111), 16(7), pp. 787–795. doi: 10.1111/tra.12281.

Jin, Y. *et al.* (2015) 'Close Encounters of the Lysosome-Peroxisome Kind', *Cell*. Elsevier Inc., 161(2), pp. 197–198. doi: 10.1016/j.cell.2015.03.046.

Jonkman, J. and Brown, C. M. (2015) 'Any Way You Slice It-A Comparison of Confocal Microscopy Techniques.', *Journal of biomolecular techniques : JBT*. The Association of Biomolecular Resource Facilities, 26(2), pp. 54–65. doi: 10.7171/jbt.15-2602-003.

Joshi, A. S. *et al.* (2016) 'A family of membrane-shaping proteins at ER subdomains regulates pre-peroxisomal vesicle biogenesis.', *The Journal of cell biology*. The Rockefeller University Press, 215(4), pp. 515–529. doi: 10.1083/jcb.201602064.

Kaddoum, L. *et al.* (2010) 'One-step split GFP staining for sensitive protein detection and localization in mammalian cells', *BioTechniques*. Future Science Ltd London, UK , 49(4), pp. 727–736. doi: 10.2144/000113512.

Kakimoto, Y. *et al.* (2018) 'Visualizing multiple inter-organelle contact sites using the organelle-targeted split-GFP system', *Scientific Reports*. Nature Publishing Group, 8(1), p. 6175. doi: 10.1038/s41598-018-24466-0.

Kamiyama, D. *et al.* (2016) 'Versatile protein tagging in cells with split fluorescent protein.', *Nature communications*. Nature Publishing Group, 7, p. 11046. doi: 10.1038/ncomms11046.

Kawamoto, R. M. *et al.* (1986) 'Isolation, characterization, and localization of the spanning protein from skeletal muscle triads.', *The Journal of cell biology*. Rockefeller University Press, 103(4), pp. 1405–14. doi: 10.1083/JCB.103.4.1405.

Keller, G. A. *et al.* (1987) 'Firefly luciferase is targeted to peroxisomes in mammalian cells.', *Proceedings of the National Academy of Sciences of the United States of America*. National Academy of Sciences, 84(10), pp. 3264–8. Available at: http://www.ncbi.nlm.nih.gov/pubmed/3554235 (Accessed: 22 June

2018).

Kemp, S. *et al.* (2012) ‘X-linked adrenoleukodystrophy: Clinical, metabolic, genetic and pathophysiological aspects’, *Biochimica et Biophysica Acta (BBA) - Molecular Basis of Disease*. Elsevier, 1822(9), pp. 1465–1474. doi: 10.1016/J.BBADIS.2012.03.012.

Kerppola, T. K. (2006) ‘Design and implementation of bimolecular fluorescence complementation (BiFC) assays for the visualization of protein interactions in living cells’, *Nature Protocols*. Nature Publishing Group, 1(3), pp. 1278–1286. doi: 10.1038/nprot.2006.201.

Kim, P. K. *et al.* (2006) ‘The origin and maintenance of mammalian peroxisomes involves a de novo PEX16-dependent pathway from the ER.’, *The Journal of cell biology*, 173(4), pp. 521–532. doi: 10.1083/jcb.200601036.

Kim, P. K. *et al.* (2008) ‘Ubiquitin signals autophagic degradation of cytosolic proteins and peroxisomes.’, *Proceedings of the National Academy of Sciences of the United States of America*, 105(52), pp. 20567–20574. doi: 10.1073/pnas.0810611105.

Knoblach, B. *et al.* (2013) ‘An ER-peroxisome tether exerts peroxisome population control in yeast.’, *The EMBO journal*. Nature Publishing Group, 32(18), pp. 1–15. doi: 10.1038/emboj.2013.170.

Knoops, K. *et al.* (2014) ‘Preperoxisomal vesicles can form in the absence of Pex3’, *The Journal of cell biology*, 204(5), pp. 659–668. doi: 10.1083/jcb.201310148.

Koch, A. *et al.* (2004) ‘Peroxisome elongation and constriction but not fission can occur independently of dynamin-like protein 1.’, *Journal of cell science*, 117(Pt 17), pp. 3995–4006. doi: 10.1242/jcs.01268.

Kornmann, B. *et al.* (2011) ‘The conserved GTPase Gem1 regulates endoplasmic reticulum-mitochondria connections’, *Proceedings of the National Academy of Sciences*, 108(34), pp. 14151–14156. doi: 10.1073/pnas.1111314108.

Kragt, A. *et al.* (2005) ‘Endoplasmic reticulum-directed Pex3p routes to peroxisomes and restores peroxisome formation in a Saccharomyces

cerevisiae pex3Delta strain.', *The Journal of biological chemistry*, 280(40), pp. 34350–34357. doi: 10.1074/jbc.M505432200.

Law, K. B. *et al.* (2017) 'The peroxisomal AAA ATPase complex prevents pexophagy and development of peroxisome biogenesis disorders', *Autophagy*, 13(5), pp. 868–884. doi: 10.1080/15548627.2017.1291470.

Lazarow, P. B. and Fujiki, Y. (1985) 'Biogenesis of Peroxisomes', *Annual Review of Cell Biology*. Annual Reviews 4139 El Camino Way, P.O. Box 10139, Palo Alto, CA 94303-0139, USA , 1(1), pp. 489–530. doi: 10.1146/annurev.cb.01.110185.002421.

Léon, S. *et al.* (2006) 'Uniqueness of the mechanism of protein import into the peroxisome matrix: Transport of folded, co-factor-bound and oligomeric proteins by shuttling receptors', *Biochimica et Biophysica Acta - Molecular Cell Research*, 1763(12), pp. 1552–1564. doi: 10.1016/j.bbamcr.2006.08.037.

Leonetti, M. D. *et al.* (2016) 'A scalable strategy for high-throughput GFP tagging of endogenous human proteins.', *Proceedings of the National Academy of Sciences of the United States of America*. National Academy of Sciences, 113(25), pp. E3501-8. doi: 10.1073/pnas.1606731113.

Leuchowius, K.-J. *et al.* (2009) 'Flow cytometric *in situ* proximity ligation analyses of protein interactions and post-translational modification of the epidermal growth factor receptor family', *Cytometry Part A*, 75A(10), pp. 833–839. doi: 10.1002/cyto.a.20771.

Loewen, C. J. R. *et al.* (2003) 'A conserved ER targeting motif in three families of lipid binding proteins and in Opi1p binds VAP.', *The EMBO journal*. EMBO Press, 22(9), pp. 2025–35. doi: 10.1093/emboj/cdg201.

Magliery, T. J. *et al.* (2005) 'Detecting protein-protein interactions with a green fluorescent protein fragment reassembly trap: scope and mechanism.', *Journal of the American Chemical Society*, 127(1), pp. 146–57. doi: 10.1021/ja046699g.

Mattiazzi Ušaj, M. *et al.* (2015) 'Genome-Wide Localization Study of Yeast Pex11 Identifies Peroxisome-Mitochondria Interactions through the ERMES Complex.', *Journal of molecular biology*. Elsevier, 427(11), pp. 2072–87. doi: 10.1016/j.jmb.2015.03.004.

McNew, J. A. and Goodman, J. M. (1996) ‘The targeting and assembly of peroxisomal proteins: some old rules do not apply.’, *Trends in biochemical sciences*, 21(2), pp. 54–8. Available at: http://www.ncbi.nlm.nih.gov/pubmed/8851661 (Accessed: 25 July 2018).

Mendez, R. and Banerjee, S. (2017) ‘Proximal Ligation Assay (PLA) on Lung Tissue and Cultured Macrophages to Demonstrate Protein-protein Interaction.’, *Bio-protocol*. NIH Public Access, 7(21). doi: 10.21769/BioProtoc.2602.

Mihalik, S. J. *et al.* (2002) ‘Participation of Two Members of the Very Long-chain Acyl-CoA Synthetase Family in Bile Acid Synthesis and Recycling’, *Journal of Biological Chemistry*, 277(27), pp. 24771–24779. doi: 10.1074/jbc.M203295200.

Miller, K. E. *et al.* (2015) ‘Bimolecular Fluorescence Complementation (BiFC) Analysis: Advances and Recent Applications for Genome-Wide Interaction Studies.’, *Journal of molecular biology*. NIH Public Access, 427(11), pp. 2039–2055. doi: 10.1016/j.jmb.2015.03.005.

Mocanu, M.-M. *et al.* (2011) ‘Comparative analysis of fluorescence resonance energy transfer (FRET) and proximity ligation assay (PLA)’, *PROTEOMICS*. Wiley-Blackwell, 11(10), pp. 2063–2070. doi: 10.1002/pmic.201100028.

Mosser, J. *et al.* (1993) ‘Putative X-linked adrenoleukodystrophy gene shares unexpected homology with ABC transporters’, *Nature*, 361(6414), pp. 726–730. doi: 10.1038/361726a0.

Motley, A. M. and Hettema, E. H. (2007) ‘Yeast peroxisomes multiply by growth and division.’, *The Journal of cell biology*, 178(3), pp. 399–410. doi: 10.1083/jcb.200702167.

Muffly, K. (2007) ‘Structure and Function of Organelles and the Cytoskeleton’, *xPharm: The Comprehensive Pharmacology Reference*. Elsevier, pp. 1–6. doi: 10.1016/B978-008055232-3.60051-0.

Murley, A. *et al.* (2013) ‘ER-associated mitochondrial division links the distribution of mitochondria and mitochondrial DNA in yeast.’, *eLife*, 2, p. e00422. doi: 10.7554/eLife.00422.

Murphy, S. E. and Levine, T. P. (2016) ‘VAP, a Versatile Access Point for the Endoplasmic Reticulum: Review and analysis of FFAT-like motifs in the

VAPome', *Biochimica et Biophysica Acta (BBA) - Molecular and Cell Biology of Lipids*. Elsevier, 1861(8), pp. 952–961. doi: 10.1016/J.BBALIP.2016.02.009.

Nagai, T. *et al.* (2002) 'A variant of yellow fluorescent protein with fast and efficient maturation for cell-biological applications', *Nature Biotechnology*, 20(1), pp. 87–90. doi: 10.1038/nbt0102-87.

Naon, D. and Scorrano, L. (2014) 'At the right distance: ER-mitochondria juxtaposition in cell life and death', *Biochimica et Biophysica Acta (BBA) - Molecular Cell Research*. Elsevier, 1843(10), pp. 2184–2194. doi: 10.1016/J.BBAMCR.2014.05.011.

Nazarko, T. Y. *et al.* (2014) 'Peroxisomal Atg37 binds Atg30 or palmitoyl-CoA to regulate phagophore formation during pexophagy.', *The Journal of cell biology*, 204(4), pp. 541–557. doi: 10.1083/jcb.201307050.

Nazarko, T. Y. (2017) 'Pexophagy is responsible for 65% of cases of peroxisome biogenesis disorders', *Autophagy*, 13(5), pp. 991–994. doi: 10.1080/15548627.2017.1291480.

Neuspiel, M. *et al.* (2008) 'Cargo-selected transport from the mitochondria to peroxisomes is mediated by vesicular carriers.', *Current biology : CB*, 18(2), pp. 102–108. doi: 10.1016/j.cub.2007.12.038.

Nguyen, T. *et al.* (2006) 'Failure of microtubule-mediated peroxisome division and trafficking in disorders with reduced peroxisome abundance.', *Journal of cell science*, 119(Pt 4), pp. 636–645. doi: 10.1242/jcs.02776.

Nishimura, A. L. *et al.* (2004) 'A Mutation in the Vesicle-Trafficking Protein VAPB Causes Late-Onset Spinal Muscular Atrophy and Amyotrophic Lateral Sclerosis', *The American Journal of Human Genetics*, 75(5), pp. 822–831. doi: 10.1086/425287.

Novikoff, A. B. *et al.* (1980) 'Organelle relationships in cultured 3T3-L1 preadipocytes.', *The Journal of cell biology*, 87(1), pp. 180–96. Available at: http://www.ncbi.nlm.nih.gov/pubmed/7191426 (Accessed: 20 August 2018).

Novikoff, A. B. and Goldfischer, S. L. (1969) 'Visualization of peroxisomes (microbodies) and mitochondria with diaminobenzidine', *Journal of Histochemistry & Cytochemistry*. SAGE PublicationsSage UK: London,

England, 17(10), pp. 675–680. doi: 10.1177/17.10.675.

Novikoff, A. B. and Shin, W. (1964) ‘The endoplasmic reticulum in the Golgi zone and its relations to microbodies, Golgi apparatus and autophagic vacuoles in rat liver cell’, *J Microscopy*, 3, pp. 187–206.

Novikoff, P. M. and Novikoff, A. B. (1972) ‘Peroxisomes in absorptive cells of mammalian small intestine.’, *The Journal of cell biology*, 53(2), pp. 532–60. Available at: http://www.ncbi.nlm.nih.gov/pubmed/4112543 (Accessed: 15 August 2018).

Odendall, C. and Kagan, J. C. (2013) ‘Peroxisomes and the Antiviral Responses of Mammalian Cells’, in. Springer, Dordrecht, pp. 67–75. doi: 10.1007/978-94-007-6889-5_4.

Ohashi, K. and Mizuno, K. (2014) ‘A Novel Pair of Split Venus Fragments to Detect Protein–Protein Interactions by In Vitro and In Vivo Bimolecular Fluorescence Complementation Assays’, in *Methods in molecular biology (Clifton, N.J.)*, pp. 247–262. doi: 10.1007/978-1-4939-0944-5_17.

Olink bioscience | *AntibodyChain* (2009). Available at: http://www.antibodychain.com/content/olink-bioscience (Accessed: 17 July 2018).

Paillusson, S. *et al.* (2016) ‘There’s Something Wrong with my MAM; the ER-Mitochondria Axis and Neurodegenerative Diseases.’, *Trends in neurosciences*. Elsevier, 39(3), pp. 146–157. doi: 10.1016/j.tins.2016.01.008.

Patterson, G. H. *et al.* (1997) ‘Use of the green fluorescent protein and its mutants in quantitative fluorescence microscopy.’, *Biophysical journal*. The Biophysical Society, 73(5), pp. 2782–90. doi: 10.1016/S0006-3495(97)78307-3.

Pédelacq, J.-D. *et al.* (2006) ‘Engineering and characterization of a superfolder green fluorescent protein’, *Nature Biotechnology*. Nature Publishing Group, 24(1), pp. 79–88. doi: 10.1038/nbt1172.

Phillips, M. J. and Voeltz, G. K. (2016) ‘Structure and function of ER membrane contact sites with other organelles’, *Nature Reviews Molecular Cell Biology*. Nature Publishing Group, 17(2), pp. 69–82. doi: 10.1038/nrm.2015.8.

Pillardy, J. *et al.* (2001) ‘Recent improvements in prediction of protein structure

by global optimization of a potential energy function'. Available at: http://www.pnas.org/content/pnas/98/5/2329.full.pdf (Accessed: 7 February 2018).

Poll-the, B. T. *et al.* (1988) 'A New Peroxisomal Disorder with Enlarged Peroxisomes and a Specific Deficiency of Acyl-CoA Oxidase', *American journal of human genetics*, 42, pp. 422–434.

Porter, K. R. and Palade, G. E. (1957) 'Studies on the endoplasmic reticulum. III. Its form and distribution in striated muscle cells.', *The Journal of biophysical and biochemical cytology*. Rockefeller University Press, 3(2), pp. 269–300. doi: 10.1083/JCB.3.2.269.

Prinz, W. A. (2010) 'Lipid trafficking sans vesicles: Where, why, how?', *Cell*. Elsevier Inc., 143(6), pp. 870–874. doi: 10.1016/j.cell.2010.11.031.

Prinz, W. A. (2014) 'Bridging the gap: membrane contact sites in signaling, metabolism, and organelle dynamics.', *The Journal of cell biology*. Rockefeller University Press, 205(6), pp. 759–69. doi: 10.1083/jcb.201401126.

Pu, J. *et al.* (2011) 'Interactomic study on interaction between lipid droplets and mitochondria.', *Protein & cell*, 2(6), pp. 487–496. doi: 10.1007/s13238-011-1061-y.

Rao, V. S. *et al.* (2014) 'Protein-protein interaction detection: methods and analysis.', *International journal of proteomics*. Hindawi, 2014, p. 147648. doi: 10.1155/2014/147648.

Raychaudhuri, S. and Prinz, W. A. (2008) 'Nonvesicular phospholipid transfer between peroxisomes and the endoplasmic reticulum.', *Proceedings of the National Academy of Sciences of the United States of America*. National Academy of Sciences, 105(41), pp. 15785–90. doi: 10.1073/pnas.0808321105.

Reddy, J. K. and Mannaerts, G. P. (1994) 'Peroxisomal Lipid Metabolism', *Annual Review of Nutrition*, 14(1), pp. 343–370. doi: 10.1146/annurev.nu.14.070194.002015.

Ren, Y. and Schulz, H. (2003) 'Metabolic functions of the two pathways of oleate beta-oxidation double bond metabolism during the beta-oxidation of oleic acid in rat heart mitochondria.', *The Journal of biological chemistry*. American

Society for Biochemistry and Molecular Biology, 278(1), pp. 111–6. doi: 10.1074/jbc.M209261200.

Reuber, B. E. *et al.* (1997) 'Mutations in PEX1 are the most common cause of peroxisome biogenesis disorders', *Nature genetics*, 17, pp. 445–448. Available at: http://www.nature.com/ng/journal/v17/n4/abs/ng1297-445.html.

Rhodin, J. (1954) *Correlation of ultrastructural organization and function in normal and experimentally changed proximal convoluted tubule cells of the mouse kidney*. Aktiebolaget Godvil.

Rosenbluth, J. (1962) 'Subsurface cisterns and their relationship to the neuronal plasma membrane.', *The Journal of cell biology*. Rockefeller University Press, 13(3), pp. 405–21. doi: 10.1083/JCB.13.3.405.

Rosewich *et al.* (2005) 'Genetic and clinical aspects of Zellweger spectrum patients with PEX1 mutations.', *Journal of medical genetics*. BMJ Publishing Group Ltd, 42(9), p. e58. doi: 10.1136/jmg.2005.033324.

Sargent, G. *et al.* (2016) 'PEX2 is the E3 ubiquitin ligase required for pexophagy during starvation.', *The Journal of cell biology*. The Rockefeller University Press, 214(6), pp. 677–90. doi: 10.1083/jcb.201511034.

Satori, C. P. *et al.* (2013) 'Bioanalysis of eukaryotic organelles.', *Chemical reviews*. NIH Public Access, 113(4), pp. 2733–811. doi: 10.1021/cr300354g.

Schrader, M. *et al.* (1998) 'Tubular peroxisomes in HepG2 cells: Selective induction by growth factors and arachidonic acid', *European Journal of Cell Biology*. Gustav Fischer Verlag GmbH & Co. KG, 75(2), pp. 87–96. doi: 10.1016/S0171-9335(98)80051-4.

Schrader, M. (2001) 'Tubulo – Reticular Clusters of Peroxisomes in Living COS-7 Cells: Dynamic Behavior and Association with Lipid Droplets', *The Journal of Histochemistry and Cytochemistry*, 49(11), pp. 1421–1429.

Schrader, M. *et al.* (2012) 'Fission and proliferation of peroxisomes.', *Biochimica et biophysica acta*. Elsevier B.V., 1822(9), pp. 1343–1357. doi: 10.1016/j.bbadis.2011.12.014.

Schrader, M. *et al.* (2013) 'Peroxisome interactions and cross-talk with other subcellular compartments in animal cells'. Edited by L. A. del Río. Dordrecht:

Springer Netherlands (Subcellular Biochemistry), 69, pp. 1–22. doi: 10.1007/978-94-007-6889-5.

Schrader, M. *et al.* (2015) 'Peroxisome-mitochondria interplay and disease', *Journal of Inherited Metabolic Disease*, 38(4), pp. 681–702. doi: 10.1007/s10545-015-9819-7.

Schrader, M. *et al.* (2016) 'Proliferation and fission of peroxisomes - An update', *Biochimica et Biophysica Acta - Molecular Cell Research*, 1863, pp. 971–983. doi: 10.1016/j.bbamcr.2015.09.024.

Schrader, M. and Fahimi, H. D. (2006) 'Peroxisomes and oxidative stress', *Biochimica et biophysica acta*, 1763, pp. 1755–1766. doi: 10.1016/j.bbamcr.2006.09.006.

Schrader, M. and Fahimi, H. D. (2008) 'The peroxisome: still a mysterious organelle', *Histochemistry and Cell Biology*, 129, pp. 421–440. doi: 10.1007/s00418-008-0396-9.

Schrader, M. and Yoon, Y. (2007) 'Mitochondria and peroxisomes: are the "Big Brother" and the "Little Sister" closer than assumed?', *BioEssays*, 29(11), pp. 1105–1114. doi: 10.1002/bies.20659.

Shai, N. *et al.* (2016) 'No peroxisome is an island — Peroxisome contact sites', *Biochimica et Biophysica Acta (BBA) - Molecular Cell Research*. Elsevier, 1863(5), pp. 1061–1069. doi: 10.1016/J.BBAMCR.2015.09.016.

Shai, N. *et al.* (2018) 'Systematic mapping of contact sites reveals tethers and a function for the peroxisome-mitochondria contact', *Nature Communications*. Nature Publishing Group, 9(1), p. 1761. doi: 10.1038/s41467-018-03957-8.

Shimomura, O. *et al.* (1962) 'Extraction, Purification and Properties of Aequorin, a Bioluminescent Protein from the Luminous Hydromedusan,Aequorea', *Journal of Cellular and Comparative Physiology*. Wiley-Blackwell, 59(3), pp. 223–239. doi: 10.1002/jcp.1030590302.

Shyu, Y. J. *et al.* (2006) 'Identification of new fluorescent protein fragments for bimolecular fluorescence complementation analysis under physiological conditions', *BioTechniques*. Future Science Ltd London, UK , 40(1), pp. 61–66. doi: 10.2144/000112036.

Singh, H. *et al.* (1993) ‘Exclusive localization in peroxisomes of dihydroxyacetone phosphate acyltransferase and alkyl-dihydroxyacetone phosphate synthase in rat liver.’, *Journal of lipid research*, 34(3), pp. 467–77. Available at: http://www.ncbi.nlm.nih.gov/pubmed/8468530 (Accessed: 9 August 2018).

Söderberg, O. *et al.* (2006) ‘Direct observation of individual endogenous protein complexes in situ by proximity ligation’, *Nature Methods*. Nature Publishing Group, 3(12), pp. 995–1000. doi: 10.1038/nmeth947.

Söderberg, O. *et al.* (2008) ‘Characterizing proteins and their interactions in cells and tissues using the in situ proximity ligation assay’, *Methods*. Academic Press, 45(3), pp. 227–232. doi: 10.1016/J.YMETH.2008.06.014.

South, S. T. and Gould, S. J. (1999) ‘Peroxisome Synthesis in the Absence of Preexisting Peroxisomes’, *The Journal of cell biology*, 144(2), pp. 255–266.

Sprecher, H. and Chen, Q. (1999) ‘Polyunsaturated fatty acid biosynthesis: a microsomal-peroxisomal process.’, *Prostaglandins, leukotrienes, and essential fatty acids*, 60(5–6), pp. 317–21. Available at: http://www.ncbi.nlm.nih.gov/pubmed/10471115 (Accessed: 15 August 2018).

Stier, H. *et al.* (1998) ‘Maturation of peroxisomes in differentiating human hepatoblastoma cells (HepG2): possible involvement of the peroxisome proliferator-activated receptor α (PPARα)’, *Differentiation*, 64(1), pp. 55–66. doi: 10.1046/j.1432-0436.1998.6410055.x.

Stoica, R. *et al.* (2016) ‘ALS/FTD-associated FUS activates GSK-3β to disrupt the VAPB-PTPIP51 interaction and ER-mitochondria associations.’, *EMBO reports*. European Molecular Biology Organization, 17(9), pp. 1326–42. doi: 10.15252/embr.201541726.

Su, H. M. *et al.* (2001) ‘Peroxisomal straight-chain Acyl-CoA oxidase and D-bifunctional protein are essential for the retroconversion step in docosahexaenoic acid synthesis.’, *The Journal of biological chemistry*, 276(41), pp. 38115–20. doi: 10.1074/jbc.M106326200.

Sugiura, A. *et al.* (2017) ‘Newly born peroxisomes are a hybrid of mitochondrial and ER-derived pre-peroxisomes’, *Nature*. Nature Publishing Group, 542(7640), pp. 251–254. doi: 10.1038/nature21375.

Suzuki, Y. *et al.* (1997) ‘d-3-Hydroxyacyl-CoA Dehydratase/d-3-Hydroxyacyl-CoA Dehydrogenase Bifunctional Protein Deficiency: A Newly Identified Peroxisomal Disorder’, *The American Journal of Human Genetics*. Cell Press, 61(5), pp. 1153–1162. doi: 10.1086/301599.

Szabadkai, G. *et al.* (2006) ‘Chaperone-mediated coupling of endoplasmic reticulum and mitochondrial Ca2+ channels.’, *The Journal of cell biology*. Rockefeller University Press, 175(6), pp. 901–11. doi: 10.1083/jcb.200608073.

Taylor, R. L. *et al.* (2017) ‘Novel *PEX11B* Mutations Extend the Peroxisome Biogenesis Disorder 14B Phenotypic Spectrum and Underscore Congenital Cataract as an Early Feature’, *Investigative Opthalmology & Visual Science*. The Association for Research in Vision and Ophthalmology, 58(1), p. 594. doi: 10.1167/iovs.16-21026.

Tocheva, E. I. *et al.* (2010) ‘Electron cryotomography.’, *Cold Spring Harbor perspectives in biology*. Cold Spring Harbor Laboratory Press, 2(6), p. a003442. doi: 10.1101/cshperspect.a003442.

Tsien, R. Y. (1998) ‘The Green Fluorescent Protein’, *Annual Review of Biochemistry*. Annual Reviews 4139 El Camino Way, P.O. Box 10139, Palo Alto, CA 94303-0139, USA , 67(1), pp. 509–544. doi: 10.1146/annurev.biochem.67.1.509.

Tubbs, E. *et al.* (2014) ‘Mitochondria-associated endoplasmic reticulum membrane (MAM) integrity is required for insulin signaling and is implicated in hepatic insulin resistance.’, *Diabetes*. American Diabetes Association, 63(10), pp. 3279–94. doi: 10.2337/db13-1751.

Valm, A. M. *et al.* (2017) ‘Applying systems-level spectral imaging and analysis to reveal the organelle interactome.’, *Nature*. Howard Hughes Medical Institute, 546(7656), pp. 162–167. doi: 10.1038/nature22369.

Vasko, R. (2016) ‘Peroxisomes and Kidney Injury.’, *Antioxidants & redox signaling*. Mary Ann Liebert, Inc., 25(4), pp. 217–31. doi: 10.1089/ars.2016.6666.

De Vos, K. J. *et al.* (2012) ‘VAPB interacts with the mitochondrial protein PTPIP51 to regulate calcium homeostasis.’, *Human molecular genetics*. Oxford University Press, 21(6), pp. 1299–311. doi: 10.1093/hmg/ddr559.

Wanders, R. J. *et al.* (2001a) ‘Peroxisomal fatty acid alpha- and beta-oxidation in humans: enzymology, peroxisomal metabolite transporters and peroxisomal diseases.’, *Biochemical Society transactions*. Portland Press Limited, 29(Pt 2), pp. 250–67. doi: 10.1042/BST0290250.

Wanders, R. J. *et al.* (2001b) ‘Refsum disease, peroxisomes and phytanic acid oxidation: a review.’, *Journal of neuropathology and experimental neurology*, 60(11), pp. 1021–31. Available at: http://www.ncbi.nlm.nih.gov/pubmed/11706932 (Accessed: 9 August 2018).

Wanders, R. J. A. (2004) ‘Metabolic and Molecular Basis of Peroxisomal Disorders : A Review’, *American Journal of Medical Genetics*, 126A, pp. 355–375. doi: 10.1002/ajmg.a.20661.

Wanders, R. J. A. *et al.* (2016) ‘Metabolic Interplay between Peroxisomes and Other Subcellular Organelles Including Mitochondria and the Endoplasmic Reticulum’, *Frontiers in Cell and Developmental Biology Front. Cell Dev. Biol*, 3(3), pp. 833383–833389. doi: 10.3389/fcell.2015.00083.

Wanders, R. J. A. and Poll-The, B. T. (2017) ‘“Role of peroxisomes in human lipid metabolism and its importance for neurological development”’, *Neuroscience Letters*. Elsevier, 637, pp. 11–17. doi: 10.1016/J.NEULET.2015.06.018.

Wanders, R. and Waterham, H. (2004) ‘Peroxisomal disorders I: biochemistry and genetics of peroxisome biogenesis disorders’, *Clinical Genetics*. Wiley/Blackwell (10.1111), 67(2), pp. 107–133. doi: 10.1111/j.1399-0004.2004.00329.x.

Wanders, R. J. A. and Waterham, H. R. (2006) ‘Peroxisomal disorders: the single peroxisomal enzyme deficiencies.’, *Biochimica et biophysica acta*, 1763(12), pp. 1707–1720. doi: 10.1016/j.bbamcr.2006.08.010.

Waterham, H. R. *et al.* (2016) ‘Human disorders of peroxisome metabolism and biogenesis’, *Biochimica et Biophysica Acta - Molecular Cell Research*. Elsevier B.V., 1863(5), pp. 922–933. doi: 10.1016/j.bbamcr.2015.11.015.

Weibrecht, I. *et al.* (2010) ‘Proximity ligation assays: a recent addition to the proteomics toolbox’, *Expert Review of Proteomics*. Taylor & Francis, 7(3), pp. 401–409. doi: 10.1586/epr.10.10.

Williams, C. *et al.* (2015) ‘The membrane remodeling protein Pex11p activates the GTPase Dnm1p during peroxisomal fission.’, *Proceedings of the National Academy of Sciences of the United States of America*, 112(20), pp. 6377–6382. doi: 10.1073/pnas.1418736112.

Wu, Y. *et al.* (2017) ‘Contacts between the endoplasmic reticulum and other membranes in neurons.’, *Proceedings of the National Academy of Sciences of the United States of America*. National Academy of Sciences, 114(24), pp. E4859–E4867. doi: 10.1073/pnas.1701078114.

Wyles, J. P. and Ridgway, N. D. (2004) ‘VAMP-associated protein-A regulates partitioning of oxysterol-binding protein-related protein-9 between the endoplasmic reticulum and Golgi apparatus’, *Experimental Cell Research*, 297(2), pp. 533–547. doi: 10.1016/j.yexcr.2004.03.052.

Xu, Y. *et al.* (1999) ‘A bioluminescence resonance energy transfer (BRET) system: application to interacting circadian clock proteins.’, *Proceedings of the National Academy of Sciences of the United States of America*. National Academy of Sciences, 96(1), pp. 151–6. Available at: http://www.ncbi.nlm.nih.gov/pubmed/9874787 (Accessed: 22 August 2018).

Yagita, Y. *et al.* (2017) ‘Deficiency of a Retinal Dystrophy Protein, Acyl-CoA Binding Domain-containing 5 (ACBD5), Impairs Peroxisomal β-Oxidation of Very-long-chain Fatty Acids.’, *The Journal of biological chemistry*. American Society for Biochemistry and Molecular Biology, 292(2), pp. 691–705. doi: 10.1074/jbc.M116.760090.

Yamashita, S. *et al.* (2014) ‘The membrane peroxin PEX3 induces peroxisome-ubiquitination-linked pexophagy’, 3(September), pp. 1549–1564.

Yang, I. S. *et al.* (2016) ‘ISOexpresso: a web-based platform for isoform-level expression analysis in human cancer’, *BMC Genomics*, 17(1), p. 631. doi: 10.1186/s12864-016-2852-6.

Yang, Z. *et al.* (2018) ‘A novel fluorescent reporter detects plastic remodeling of mitochondria-ER contact sites.’, *Journal of cell science*. The Company of Biologists Ltd, 131(1), p. jcs.208686. doi: 10.1242/jcs.208686.

Yorimitsu, T. and Klionsky, D. J. (2005) ‘Autophagy: molecular machinery for self-eating’, *Cell Death & Differentiation*. Nature Publishing Group, 12, pp.

1542–1552. doi: 10.1038/sj.cdd.4401765.

Zaar, K. *et al.* (1984) ‘Peroxisomal aggregates forming large stacks in the lipid segment of the canine kidney.’, *Acta histochemica. Supplementband*, 29, pp. 165–8. Available at: http://www.ncbi.nlm.nih.gov/pubmed/6425923 (Accessed: 20 August 2018).

Zaar, K. *et al.* (1987) ‘Association of isolated bovine kidney cortex peroxisomes with endoplasmic reticulum.’, *Biochimica et biophysica acta*, 897(1), pp. 135–42. Available at: http://www.ncbi.nlm.nih.gov/pubmed/3801475 (Accessed: 15 August 2018).

van der Zand, A. *et al.* (2010) ‘Peroxisomal membrane proteins insert into the endoplasmic reticulum’, *Molecular biology of the cell*, 21, pp. 2057–2065. doi: 10.1091/mbc.E10.

van der Zand, A. *et al.* (2012) ‘Biochemically distinct vesicles from the endoplasmic reticulum fuse to form peroxisomes’, *Cell*, 149(2), pp. 397–409. doi: 10.1016/j.cell.2012.01.054.

Zhang, S. O. *et al.* (2010) ‘Lipid droplets as ubiquitous fat storage organelles in C. elegans’, *BMC Cell Biology*, 11(1), p. 96. doi: 10.1186/1471-2121-11-96.

Zhao, Y. G. *et al.* (2018) ‘The ER Contact Proteins VAPA/B Interact with Multiple Autophagy Proteins to Modulate Autophagosome Biogenesis’, *Current Biology*, 28(8), p. 1234–1245.e4. doi: 10.1016/j.cub.2018.03.002.